

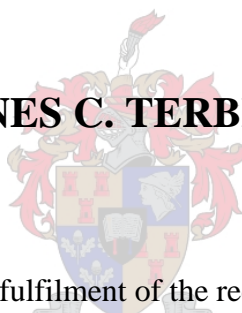


UNIVERSITEIT • STELLENBOSCH • UNIVERSITY
jou kennisvennoot • your knowledge partner

THE DEVELOPMENT OF VESICULATED BEADS

by

JOHANNES C. TERBLANCHE



This thesis submitted in partial fulfilment of the requirements for the degree of
Masters of Science in Engineering (Chemical Engineering)
in the Department of Chemical Engineering
at the University of Stellenbosch

Supervisor:

Prof. J.H. Knoetze

Department of Chemical Engineering

Stellenbosch

April 2003

Declaration

I declare that this thesis is my own work, except where specifically acknowledged in the text. Neither this thesis nor any part thereof, has been submitted to any company or other academic institution.

.....
J.C. Terblanche



Abstract

Vesiculated beads consist of aerated microvoids encapsulated in a solid spherical continuous polymeric shell. The difference in refractive index between the voids and polymer granules causes effective scattering of incident light on the particles, presenting it with a white appearance. The size of these beads generally range in the region of 0.5 – 40 μm , making it suitable for use as pigment extender in the surface coatings or paint industry.

Currently, titanium dioxide pigment is predominantly used as opacifying agent in paint formulations, but due to the high cost associated in purchasing this pigment, as well as fluctuation in import prices, paint manufacturers are looking for alternative products to replace or at least partially replace this pigment. As an alternative, opaque vesiculated polymer particles can be produced locally at a cheaper price and in existing vessels available in the paint industry.

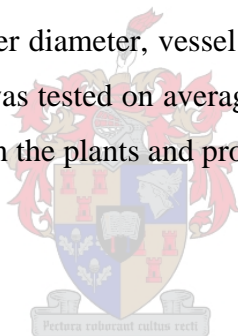
Approximately five years ago a paint company in Mexico and member of the Nova Club, started research in developing vesiculated beads for production in their factories. However, it was found extremely difficult to scale-up the production to industrial size, since the system was very sensitive to process variables. A local paint company and member of the Nova Club acquired this technology and continued further research in developing vesiculated beads on large scale in existing Cowles disperser systems found in the paint industry.

The beads consist mainly of an organic phase comprising of unsaturated carboxylated polyester and styrene. A polyamine is also added to assist the formation of vesicles in the organic phase. This phase is slowly added under agitation to an aqueous phase consisting of deionised water, a thickener and colloid stabilisers to form an oil-in-water emulsion. Agitation is continued for a specified period of time, also known as the emulsification period, to allow sufficient time for the organic globules to break-up to smaller particle sizes. These globules are subsequently catalysed with a free-radical initiator and redox activator and left static overnight to allow formation of the solid beads.

To determine the most important process parameters during production of vesiculated beads, a fully integrated laboratory scale Cowles reactor system was designed and constructed, geometrically analogous to the vessels found in the paint industry.

The system measures and controls production temperature, mixing speed and component addition rates. Production runs were performed where various process parameters were varied to investigate the effect on properties, which include average particle size and particle size distribution, pH, viscosity and opacity. The most important process parameters that were found to play a significant role include production temperature, organic phase addition rate, emulsification time, the Cowles impeller diameter and mixing speed.

Production runs were performed in geometrically similar 5ℓ and 20ℓ vessels on the laboratory-scale system to investigate the effect of scale-up. A model presented by Klein et al. (1996) was used as basis for describing the average particle size as a function of mixing speed, impeller diameter, vessel diameter and emulsification time. The applicability of this model was tested on average particle size data obtained from industrial scale runs performed on the plants and proved to be reasonably accurate.



Opsomming

Sferiese polimeerpartikels met klein lugholtes vasgevang in 'n harde omhulsel word al jare in die verf industrie aangewend as pigment. Weens die verskil in brekingsindeks tussen die soliede polimeerpartikel en die vasgevang lugholtes, word invallende lig versprei op so 'n manier dat die partikels ondeursigtig (of wit) voorkom. Hierdie partikels kan geproduseer word met deursneë wat strek van 0.5 – 40 μm , wat dit geskik maak vir gebruik in verf formulasies.

Tans word titaandioksied poeier hoofsaaklik gebruik in verf as pigment, maar weens die hoë koste van die invoer en aankoop van hierdie produk, het verfmaatskappye begin soek na goedkoper alternatiewe. Aangesien hierdie ondeursigtige polimeerpartikels plaaslik goedkoper vervaardig kan word in bestaande mengvate beskikbaar in verf aanlegte, dien dit as moontlike plaasvervanger.

Ongeveer vyf jaar gelede het 'n Mexikaanse verfmaatskappy, wat lid is van die Nova Klub, navorsing begin doen om hierdie polimeerpartikels in hul fabriek te produseer. Dit was egter vir hulle onmoontlik om die produksie op te skaal na industriële vervaardiging aangesien die proses baie sensitief was vir produksieveranderlikes. Sekere eienskappe soos die gemiddelde partikelgrootte, partikelverspreiding, pH, viskositeit en deursigtigheid van die partikels kon nie van lot tot lot herhaal word nie en verdere navorsing is gestaak. 'n Plaaslike verfmaatskappy (ook lid van die Nova Klub) het die tegnologie oorgeneem en die proses verder ontwikkel. Die proses is aangepas sodat "Cowles" mengers, wat wydverspreid in die verf industrie beskikbaar is, gebruik kan word om dit te vervaardig.

Die partikels bestaan hoofsaaklik uit 'n organiese fase wat 'n onversadigde gekarboksileerde poliëster en stireen insluit. 'n Poli-amien word ook bygevoeg en is verantwoordelik vir die vorming van die lugholtes in die partikels. Hierdie fase word stadig onder menging by 'n tweede water fase, bestaande uit gedeïoniseerde water, 'n verdikker en kolloïdale stabiliseerders gevoeg om 'n olie-in-water emulsie te vorm. Menging word voortgesit vir 'n bepaalde emulsifiseringsperiode om die oliedruppels verder op te breek. Gevolglik word hierdie druppels gekataliseer met 'n vry-radikaal

inisieerder en redoksaktiveerder en oornag staties gelos om vorming van die soliede partikels toe te laat.

Aangesien eienskappe van die polimeerpartikels so sensitief is vir prosesveranderlikes, is besluit om aanvanklik 'n ten volle geïntegreerde laboratorium skaal "Cowles" reaktorsisteem te ontwerp en bou. Hierdie sisteem is geometries gelykvormig aan die mengvate wat in verffabrieke gevind word. Die produksietemperatuur, stuwergrootte, mengspoed en materiaal toevoertempo kan effektief gemeet, verstel en beheer word. Eksperimentele lopies is gedoen en die effek van verskeie produksieveranderlikes op eienskappe is ondersoek. Die belangrikste veranderlikes wat die proses beïnvloed, is die emulsifiseringstemperatuur, die toevoertempo van die organiese fase, emulsifiseringsperiode, stuwendeursnit en mengspoed.

Eksperimentele lopies is gedoen op twee geometriese gelykvormige mengvate (5ℓ en 20ℓ kapasiteit) om die effek van opskaling op eienskappe te ondersoek. 'n Model wat deur Klein et al. (1996) voorgestel is, is as basis gebruik om die gemiddelde partikelgrootte te bepaal as 'n funksie van mengspoed, stuwendeursnit, mengvat deursnit en emulsifiseringstyd. Hierdie model is getoets op partikelgrootte data wat verkry is van groot industriële skaal lopies uitgevoer in die fabriek onder bekende produksie kondisies en daar is gevind dat hierdie model bevredigend gebruik kan word om die gemiddelde partikelgrootte te voorspel.

Acknowledgements

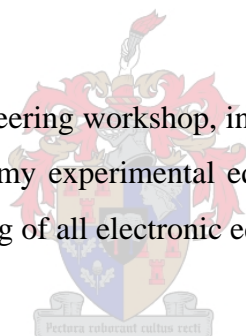
I would especially like to thank the following people:

Prof. J.H. Knoetze, for his guidance, support and intuitive knowledge as my study leader throughout the years.

Plascon (Pty.) Ltd, for their financial support and in particular **Dr. B. Cooray** for accepting me as part of this company.

Members of the Plascon Research Institute, in particular **Mr. J. Engelbrecht**, **Dr. D. de Wet-Roos**, **Mr. A.C. Smit** and **Mr. D. Reyskens** for their help, guidance and support.

Members of the Chemical Engineering workshop, including **Mr. J. Barnard** and **Mr. A. Cordier** for construction of my experimental equipment and **Mr. F.P.J. Muller** for assisting in the commissioning of all electronic equipment.



List of Contents

Abstract	iii
Opsomming	v
Acknowledgements	vii
List of Contents	viii
List of Figures	xiii
List of Tables	xviii
Nomenclature	xx

Chapter 1: Introduction **1**

1.1 Background	1
1.2 What are Vesiculated Beads?	2
1.3 The Need for Synthetic Opacifiers	3
1.4 Objectives of this Study	4

Chapter 2: Development of Vesiculated Beads as Pigment **6**

2.1 Introduction	6
2.2 Multi-Vesiculated Beads (Spindrift)	6
2.2.1 Previously Patented Multi-Vesiculated Beads	6
2.2.2 Spindrift Bead Slurry	16
2.3 Single Vesicle (Opaque) Beads	17
2.3.1 Previously Patented Single-Vesiculated Beads	17
2.3.2 Ropaque Opaque Polymer	20
2.4 Vesiculated Bead Development of Companies within the Nova Club	21
2.4.1 Background	21
2.4.2 Cowles vs. Emulsion Reactor Vessels	22
2.4.3 Current Production Procedure of Vesiculated Beads	24
2.5 Vesiculated Beads in the Coatings Industry: Advantages and Disadvantages	31

<u>Chapter 3: Set-up, Materials and Analysis</u>	33
3.1 Reactor Set-up	33
3.1.1 Reactor Design	33
3.1.2 Electronic Design	38
3.1.2.1 The Interface Board	39
3.1.2.2 Electric Motors and Speed Controllers	39
3.1.2.3 Viscosity Measurements	41
3.1.2.4 Temperature Measurement and Control	43
3.1.2.5 Pumps	44
3.2 Vesicated Bead Production Procedure	45
3.3 Analytical Test Methods	48
3.3.1 Viscosity Analysis	48
3.3.2 pH Analysis	49
3.3.3 Solid Content Analysis	50
3.3.4 Opacity Analysis	50
3.3.5 Average Particle Size Analysis	51
3.3.6 Degree of Vesication	57
3.3.6.1 Method of Average Granule Density	57
3.3.6.2 Microtoming	59
3.3.6.3 Analytical Centrifuge	63
<u>Chapter 4: Transient Properties during Production of Vesicated</u>	
Beads	66
4.1 Average Particle Size Development During Emulsification	66
4.2 Viscosity Development	74
4.2.1 Viscosity Development during Production	74
4.2.2 Rheological Behaviour of Vesicated Beads after Production	76
4.3 Temperature Development During and After Production	80
4.4 Particle Formation after Catalysis	82
<u>Chapter 5: Effect of Processing Parameters</u>	85
5.1 Emulsification Time	85

5.1.1 Standard Formulation	85
5.1.1.1 Effect on Number Average Particle Size	86
5.1.1.2 Effect on pH	87
5.1.1.3 Effect on Final Viscosity	87
5.1.1.4 Effect on Opacity	93
5.1.2 Formulation Excluding Titanium Dioxide	95
5.1.2.1 Effect on Number Average Particle Size	96
5.1.2.2 Effect on pH	97
5.1.2.3 Effect on Viscosity	98
5.1.2.3(a) Final Viscosity	98
5.1.2.3(b) Production Viscosity	101
5.1.2.4 Effect on Opacity	102
5.2 Emulsification Time	103
5.2.1 Effect on Number Average Particle Size	103
5.2.2 Effect on Final Viscosity	105
5.2.3 Effect on Opacity	106
5.3 Organic Phase Addition Rate	106
5.3.1 Effect on Number Average Particle Size	107
5.3.2 Effect on Final Viscosity	108
5.3.3 Effect on pH	109
5.3.4 Effect on Opacity	110
5.4 Impeller Size	110
5.4.1 Effect on Number Average Particle Size	111
5.5 Mixing Speed	112
5.5.1 Effect on Number Average Particle Size	113
5.6 Fluid Height to Vessel Diameter Ratio	114
<u>Chapter 6: Effect of Variations in Chemical Composition</u>	116
6.1 Pre-Addition of Post Treatment Water	116
6.1.1 Effect on Number Average Particle Size	116
6.1.2 Effect on pH	118
6.1.3 Effect on Final Viscosity	119
6.1.4 Effect on Opacity	120

6.2 Polyvinyl Alcohol/Cellulose Thickener Weight Ratios	121
6.2.1 Effect on Number Average Particle Size	121
6.2.2 Effect on pH	122
6.2.3 Effect on Final Viscosity	123
6.2.4 Effect on Opacity	124
6.3 Addition of Surfactant to Organic Phase	124
6.3.1 Effect on Number Average Particle Size	125
6.3.2 Effect on Final Viscosity	126
6.3.3 Effect on Opacity	127
6.4 Effect of Post Additions on Final Viscosity	128

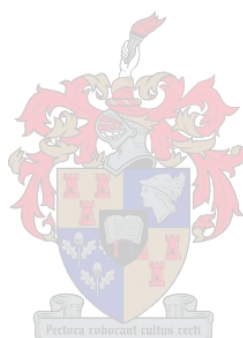
Chapter 7: Scale-up and Average Particle Size Model Development

	134
7.1 Scale-up Parameter Variations	134
7.1.1 Impeller Size	135
7.1.1.1 Effect on Number Average Particle Size	135
7.1.2 Mixing Speed	136
7.1.2.1 Effect on Number Average Particle Size	137
7.2 Average Particle Size Model	137
7.2.1 Average Particle Size (Standard Emulsification Time)	138
7.2.2 Average Particle Size (Reduced Emulsification Time)	141
7.2.3 Average Particle Size (Effect of Temperature)	144
7.2.4 Average Particle Size Comparison of Industrial Scale Runs	145
7.2.4.1 Effect of Mixing Speed	145
7.2.4.2 Effect of Impeller Size	146
7.2.4.3 Effect of Additional Surfactant	148
7.2.5 Average Particle Size (Effect of Additional Surfactant)	149
7.2.6 Specification Range and Limitations of Average Particle Size Models	152

Chapter 8: Conclusions and Recommendations

8.1 Introduction	154
-------------------------	------------

8.2 Transient Properties During Production of Vesiculated Beads	154
8.3 Effect of Processing Parameters	155
8.3.1 Production Temperature	155
8.3.2 Emulsification Time	156
8.3.3 Organic Phase Addition Rate	156
8.3.4 Impeller Size and Mixing Speed	157
8.4 Effect of Variations in Chemical Composition	157
8.5 Average Particle Size Model	158
8.6 Recommendations and Future Work	159
References	161
Appendix A	163
Appendix B	173
Appendix C	180
Appendix D	191
Appendix E	194



List of Figures

Chapter 1:

Fig. 1.1 Cross-section of a Vesiculated Bead ($\times 770$)

Fig. 1.2 Worldwide Titanium Dioxide Capacity/Demand Curve

Chapter 2:

Fig. 2.1 A) Example of an Flat Disc Impeller

B) Fluid Motion caused by Flat Disc Impeller in Cowles Reactors

Fig. 2.2 A) Example of an Axial Flow Turbine

B) Fluid Motion caused by Axial Flow Turbine in Emulsion Reactors

Fig. 2.3 The Production of Carboxylated Unsaturated Polyester

Fig. 2.4 Micelle Formation of Polyamine and Polyester Chains

Fig. 2.5 Typical Polymerisation Reaction Between Unsaturated Polyester and Styrene

Fig. 2.6 Aggregation of Vesiculated Beads due to Cellulose Thickener Chain
Degradation

Chapter 3:

Fig. 3.1 Reactor Vessel Dimension Ratios

Fig. 3.2 Design of Primary and Secondary Reactor Vessels

Fig. 3.3 Diagram of Reactor Set-up

Fig. 3.4 Design of Reactor Lid Including Shaft Bush and Lovejoy Coupling

Fig. 3.5 Photograph of the Cowles Set-up in the Laboratory

Fig. 3.6 Electronic Layout of Reactor System

Fig. 3.7 Strain Gauge Design

Fig. 3.8 Strain Gauge Network Design

Fig. 3.9 Example of a SEM Photograph Taken of the Vesiculated Beads ($\times 2,300$)

Fig. 3.10 Scion Image Analyses of Particle Size

Fig. 3.11 Fast-rotating Centrifuge

Fig. 3.12 Microtomed Sample A

Fig. 3.13 Microtomed Sample B

Fig. 3.14 Microtomed Sample C

Fig. 3.15 Analytical Ultracentrifugation

Fig. 3.16 Zonal Centrifugation Technique

Chapter 4:

Fig. 4.1 Number Average Particle Size Development During the Emulsification Period of Geometrically Similar Reactors

Fig. 4.2 Number Average Particle Size Development During Emulsification Using Various Diameter Impellers in the 20ℓ Vessel

Fig. 4.3 Particle Size Distribution During Emulsification Using Various Diameter Blades in the 20ℓ Vessel

Fig. 4.4 Particle Size Development during an Extended Emulsification Period using a 7 inch Diameter Blade in a 20ℓ Reactor vessel at Different Mixing Speed

Fig. 4.5 Particle Size Distribution Calculated from APS Results using a 7” Diameter Blade in a 20ℓ Reactor Vessel at Different Mixing Speed

Fig. 4.6 Torque Variation During Vesiculated Bead Production at Various Production Conditions in the 20ℓ Reactor Vessel

Fig. 4.7 Viscosity Development During Vesiculated Bead Production at Various Production Conditions in the 20ℓ Reactor Vessel

Fig. 4.8 Shear-time Dependence of Vesiculated Beads' Viscosity Observed at Constant Shear Rate

Fig. 4.9 Shear-Stress Dependence on Shear-Rate of Vesiculated Beads' Viscosity

Fig. 4.10 Logarithmic Plot of Strain against Shear Rate

Fig. 4.11 Temperature Development During and After Production

Fig. 4.12 Vesiculated Bead Development over a Period of 1 Hour after Catalysis

Fig. 4.13 Free Monomer Analysis over Time of Vesiculated Bead Samples taken after Catalysis

Chapter 5:

Fig. 5.1 Effect of Temperature on Number Average Particle Size (Standard Formulation)

Fig. 5.2 Effect of Temperature on pH (Standard Formulation)

- Fig. 5.3** Effect of Temperature on Final Viscosity (Standard Formulation)
- Fig. 5.4** Comparison between Experimental Viscosity Variation with Production Temperature and Modelled Values using the Souheng Wu Model
- Fig. 5.5** Effect of Temperature on Opacity (Standard Formulation)
- Fig. 5.6** Comparison of Temperature Effect on Average Particle Size with and without Titanium Dioxide Addition
- Fig. 5.7** Comparison of Temperature Effect on pH with and without Titanium Dioxide Addition
- Fig. 5.8** Comparison of Temperature Effect on Viscosity with and without Titanium Dioxide Addition
- Fig. 5.9** Viscosity Comparison between Soeheng Wu Model and Experimental Data from Runs Performed Without Titanium Dioxide
- Fig. 5.10** Viscosity Comparison between Soeheng Wu Model and Experimental Data from Runs Performed with and without Titanium Dioxide
- Fig. 5.11** Torque Development during the Emulsification Period as a Function of Temperature
- Fig. 5.12** Comparison of Temperature Effect on Opacity with and without Titanium Dioxide Addition
- Fig. 5.13** Comparison of the Average Particle Size Development using Emulsification Time Reduction and Sample Extraction Method
- Fig. 5.14** Effect of Emulsification Time on the Final Batch Viscosity
- Fig. 5.15** Effect of Organic Phase Addition Time on Particle Size Distribution
- Fig. 5.16** Effect of Organic Phase Addition Rate on Skewness
- Fig. 5.17** Effect of Polyester Addition Rate on pH
- Fig. 5.18** Effect of Organic Phase Addition Rate on Final Batch Viscosity
- Fig. 5.19** Effect of Impeller Diameter Variation on Number Average Particle Size (5ℓ Vessel, Mixing Speed = 400 rpm)
- Fig. 5.20** Effect of Impeller Diameter Variation on Particle Size Distribution (5ℓ Vessel, Mixing Speed = 400 rpm)
- Fig. 5.21** Effect of Mixing Speed on Number Average Particle Size (5ℓ Vessel, 4" Diameter Impeller)
- Fig. 5.22** Effect of Mixing Speed on Number Average Particle Size (5ℓ Vessel, 4" Diameter Impeller)

Chapter 6:

- Fig. 6.1** Effect of Pre-addition of Post Treatment Water on the Number Average Particle Size
- Fig. 6.2** Effect of Pre-addition of Post Treatment Water on the pH
- Fig. 6.3** Effect of Pre-addition of Post Treatment Water on the Final Batch Viscosity
- Fig. 6.4** Effect of Pre-addition of Post Treatment Water on the Luminosity on Black and White Surfaces
- Fig. 6.5** Effect of Cellulose Thickener Concentration on Number Average Particle Size
- Fig. 6.6** Effect of Cellulose Thickener Concentration on pH
- Fig. 6.7** Effect of Cellulose Thickener Concentration on Final Batch Viscosity
- Fig. 6.8** Effect of Cellulose Thickener Concentration on Luminosity
- Fig. 6.9** Effect of Additional Surfactant in Pre-dispersion on Number Average Particle Size at Various Mixing Speed
- Fig. 6.10** Effect of Additional Surfactant in Pre-dispersion on Final Batch Viscosity at Various Mixing Speed
- Fig. 6.11** Effect of Additional Surfactant in Pre-dispersion on Luminosity at Various Mixing Speed
- Fig. 6.12** Pie Plot Indicating the Effect of Variations in Post Addition Constituents on the Final Viscosity for Run 1 (5" Impeller, 400 rpm, 20ℓ Vessel)
- Fig. 6.13** Pie Plot Indicating the Effect of Variations in Post Addition Constituents on the Final Viscosity for Run 2 (4" Impeller, 400 rpm, 20ℓ Vessel)

Chapter 7:

- Fig. 7.1** Effect of Impeller Diameter Variation on Number Average Particle Size (20ℓ Vessel, Mixing Speed = 400 rpm)
- Fig. 7.2** Effect of Mixing Speed on Number Average Particle Size (20ℓ Vessel, 6" Impeller Diameter)
- Fig. 7.3** Comparison of Experimental Number Average Particle Size Data with Modelled Values at Various Mixing Speeds
- Fig. 7.4** Comparison of Experimental Number Average Particle Size Data and Modelled Values at Various Impeller Diameters
- Fig. 7.5** Comparison of Experimental APS and Modelled Values of Runs Performed

in 5ℓ and 20ℓ Vessels at Various Emulsification Times

Fig. 7.6 Number Average Particle Sizes of Runs Performed on 150kg Scale at Various Mixing Speed and Comparison with Modelled Values

Fig. 7.7 Number Average Particle Sizes of Runs Performed on 150kg Scale (Including and Excluding Surfactant) and Comparison with Modelled Values

Fig. 7.8 Number Average Particle Sizes of Runs Performed on 600kg Scale using Additional Surfactant and Comparison with Modelled Values

Fig. 7.9 Comparison of Experimental Number Average Particle Size Data and Modelled Values of Vesiculated Beads Produced with Additional Surfactant



List of Tables

Chapter 2:

Table 2.1 Nova Club Formulation for Producing Multi-Vesiculated Beads

Table 2.2 Comparison of Polyester Parameter Values for KZN and Cray Valley Resins

Chapter 3:

Table 3.1 Laboratory Reactor Vessel Dimensions

Table 3.2 Blade Geometry Values for Blade Impellers used in Cowles Reactors

Table 3.3 Reproducibility of Vesiculated Bead Particle Size Analysis

Table 3.4 Average Degree of Vesiculation Based on Area

Table 3.5 Property Analysis Results of Microtomed Samples

Chapter 4:

Table 4.1 Number Average Particle Size Development during Emulsification Using Different Impeller Diameters

Table 4.2 Particle Size Distribution during Emulsification at Various Impeller Diameters

Table 4.3 Number Average Particle Size and Distribution Development During Extended Emulsification Time using 7" Impeller in 20ℓ

Chapter 5:

Table 5.1 Effect of Emulsification Temperature on Properties (Standard Formulation)

Table 5.2 Effect of Emulsification Temperature on Properties (Formulation Excluding TiO₂)

Table 5.3 Effect of Emulsification Time on Properties

Table 5.4 Effect of Organic Addition Time on Properties

Table 5.5 Effect of Impeller Size on Properties (5ℓ Vessel, 400 rpm)

Table 5.6 Effect of Mixing Speed on Properties (5ℓ Vessel, 4" Impeller Diameter)

Table 5.7 Effect of Fluid Height to Vessel Diameter Ratio on Properties

Chapter 6:

Table 6.1 Effect of Pre-addition of Post-treatment Water on Properties

Table 6.2 Effect of Polyvinyl Alcohol/ Cellulose Thickener Weight Ratios on Properties

Table 6.3 Effect of Additional Surfactant Addition on Properties at Various Mixing Speed

Table 6.4 Analysis of Post-treatment Constituents that Affect Final Viscosity – Run 1

Table 6.5 Analysis of Post-treatment Constituents that Affect Final Viscosity – Run 2

Chapter 7:

Table 7.1 Effect of Impeller Size on Properties (20ℓ Vessel, 400 rpm)

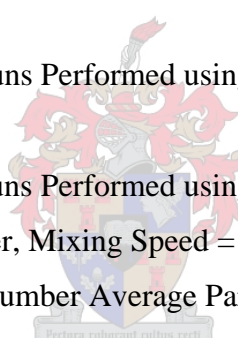
Table 7.2 Effect of Mixing Speed on Properties (20ℓ Vessel, 6” Impeller Diameter)

Table 7.3 Industrial Scale-up Runs Performed at Various Mixing Speed (150kg, 20cm Impeller)

Table 7.4 Industrial Scale-up Runs Performed using Larger Impeller (150kg, 30cm Impeller)

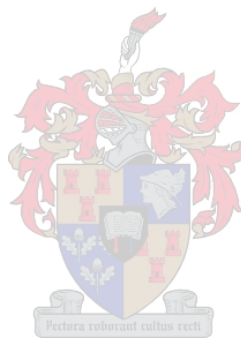
Table 7.5 Industrial Scale-up Runs Performed using Additional Surfactant (630kg, 46cm Impeller, Mixing Speed = 160rpm)

Table 7.6 Data used to Model Number Average Particle Size (incl. Additional Surfactant)



Nomenclature

APS	: Number Average Particle Size	[μm]
b	: Regression Coefficient	[]
D	: Diameter	[m]
g	: Gravitational Constant	[m/s^2]
h	: Distance of Impeller from Bottom of Vessel	[m]
K	: Consistency Index	[]
N	: Rotational Speed	[rev/s]
n	: Power Law Index	[]
PSD	: Particle Size Distribution	[]
RRF	: Relative Response Factor	[]
Skew	: Skewness	[]
SSE	: Sum of Squared Errors	[]
T	: Temperature	[$^{\circ}\text{C}$]
t_e	: Emulsification Time	[s]
X	: Independent Variable	[]
x	: Regression Coefficient	[]
Y	: Dependent Variable	[]
y	: Regression Coefficient	[]
z	: Regression Coefficient	[]



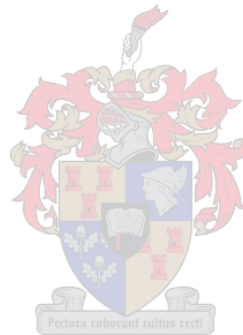
Greek Symbols

α	: Average Particle Size	[μm]
ρ	: Density	[kg/m^3]
σ	: Interfacial Tension	[mN/m]
θ	: Opacity ($=\theta_b/\theta_w$)	[]
γ	: Shear Rate	[1/s]
τ	: Shear Stress	[Pa]
η	: Viscosity	[mPa.s]
ϕ	: Volume Fraction	[m^3/m^3]
$\Delta\rho$: Fluid Density Difference between Monomer and Cont. Phase	[kg/m^3]

θ_b	: Luminosity on Black Surface	[%]
θ_w	: Luminosity on White Surface	[%]

Subscripts

a	: Ambient Temperature
c	: Continuous
d	: Dispersed Drop
f	: Final
i	: Point Number
ISTD	: Internal Standard
m	: Matrix
n	: Number
n	: Number of Points in Data Series
p	: Production
STY	: Styrene
v	: Volume



Chapter 1

Introduction

1.1 Background

The main components of surface coatings are the binder and pigment^[1]. The binder, after application and drying/curing of the coating, forms the final paint film. It is further responsible for the mechanical adhesion of the film to the painted substrate and other factors like weather stability and water sensitivity. The pigment (and extender) component is primarily to colour the paint film and provide opacity. In addition, coatings contain other materials which are present in relatively small quantities (typically about 1 percent or less) and is known as additives. Some examples of typical additives used include rheology modifiers, defoamers and preservatives.

Rheology modifiers are used to provide a good balance of container viscosity, application viscosity, antisetling properties, spatter resistance and anti-sagging when applied to a substrate.

Foam bubbles on paint film cause surface defects, while intact foam in the film can impair its mechanical and protective properties. Defoamers are used as additives to reduce foam formation.

Preservatives are an additive used to inhibit rapid biodeterioration of surface coatings caused by bacteria, fungi or algae.

Paint manufacturers require the use of titanium dioxide pigment aside from other pigments and extenders to achieve whiteness of the paint with good hiding power and obliteration. However, this is currently also the most expensive component in the formulations, increasing the production cost of paint.

A local member of the Nova Club, the latter comprising an association of paint companies around the world, is currently investigating the possibility of manufacturing less expensive synthetic opacifiers that can be used to partially replace titanium dioxide and extenders, the latter being constituents which increase the bulk volume of the paint, while retaining its binding and opacifying power. This will

decrease the formulation cost, thereby increasing profitability. Vesiculated beads have been used with success in the past to accomplish this.

1.2 What are Vesiculated Beads?

Vesiculated beads can be described as synthetic, opaque insoluble polymeric beads containing a plurality of micro-voids, and optionally a small amount of pigment, such as titanium dioxide, dispersed within the beads. These beads are held stable within a continuous aqueous phase and contain water encapsulated in the vesicles.

Upon drying, the vesicles empty and develop micro-void hiding power due to the difference in refractive index between the entrapped air and polymeric beads. This causes an increased scattering efficiency of incident light, presenting it with a white appearance. This is also found in naturally white products, such as snow and sea foam where the whiteness arises from the interaction of light with a multiplicity of interfaces and microvoids.

In the production of paint coatings, vesiculated beads can be used as opacifying agent with conventional paint additives such as binders, rheology modifiers, solvents, wetting agents, defoamers and other materials well known in the art.

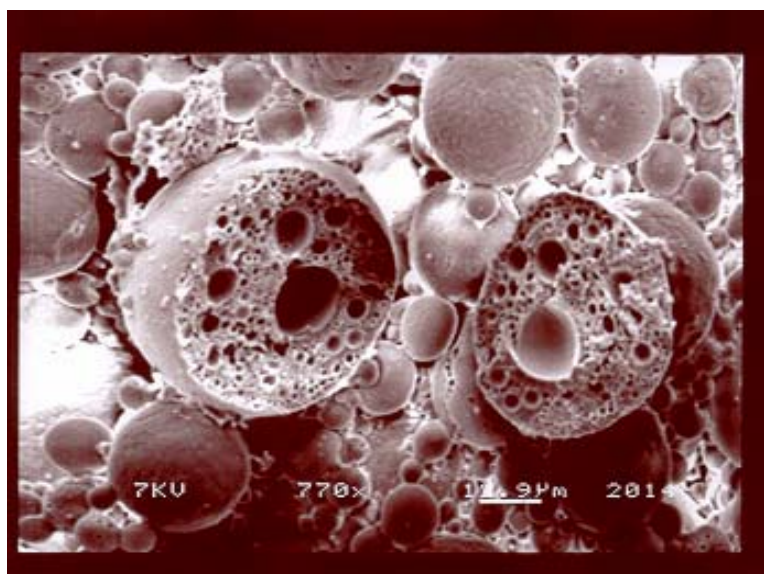


Fig. 1.1 Cross-section of a Vesiculated Bead (×770)

Vesiculated beads produced for incorporation into paint compositions generally range from 1.5 – 40 micrometers in size with vesicles preferably occupying 10 to 50%, by volume of the beads. Figure 1.1 presents a microscopic view ($\times 770$) of a dried vesiculated bead film showing a cross section of a typical bead. The vesicles are clearly visible.

1.3 The Need for Synthetic Opacifiers

To date, the primary pigment used in the manufacturing of surface coatings is titanium dioxide powder, which is also the most expensive component in paint and comprises a significant part of the formulation. Presently, the price of imported titanium dioxide range in the region of R28-29 per kilogram.

The annual cost of titanium dioxide also fluctuates significantly due to factors such as changes in product availability and mineral demand. Figure 1.2 presents a global capacity/demand curve^[2] indicating a steady increase in the demand of titanium dioxide, exceeding the production capacity by the year 2000. According to the Roskill Reports on Metals and Minerals^[3], the increased demand will cause a significant shortage of titanium dioxide by the year 2005. This implies that manufacturers will have to expand and upgrade their plants in an attempt to satisfy demand, driving up the cost of this mineral even further.

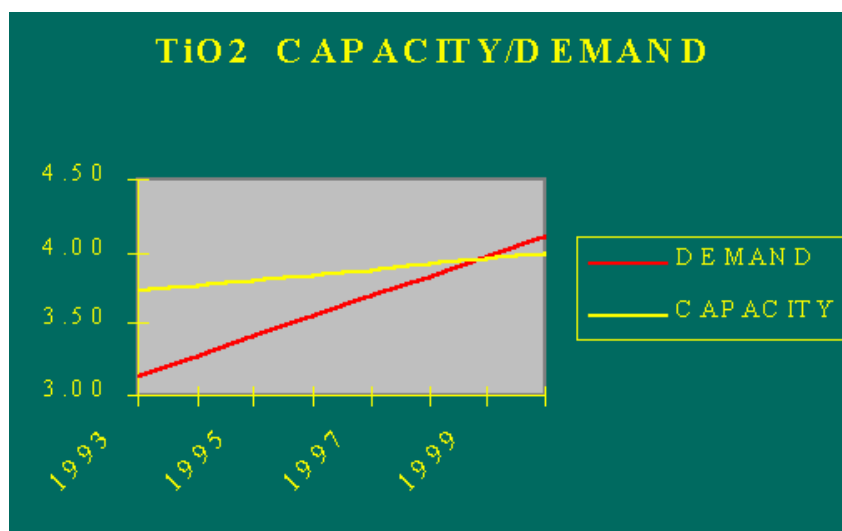


Fig. 1.2 Worldwide Titanium Dioxide Capacity/Demand Curve (in million tonnes per annum) for years 1993 – 2001.^[2]

In order to minimise the effect of high cost and price fluctuations on paint production cost, a less expensive commercially available mono-vesicle bead, marketed by Rohm & Haas under the tradename “Ropaque”, can be used to partially replace titanium dioxide. This can be obtained at about half the price of titanium dioxide. However, almost 80% of this pigment consists of water, resulting in the fact that the major expenditure goes to waste.

This formed the basis for companies within the Nova club to start developing and producing vesiculated beads in their own factories. Currently, this can be achieved at a production cost of about R3.70 per kilogram.

Exactly the same, if not better, opacifying properties can be obtained with the introduction of vesiculated beads into paint compositions, while maintaining its film integrity.

1.3 Objectives of this Study

It was decided to ultimately produce vesiculated beads in existing mixing vessels found in paint factories within the Nova Club, thereby eliminating unnecessary expenditure for the construction of new ones. Cowles vessels are commonly found in the paint industry and mainly used for dispersing pigment powder agglomerates in suspension and blending paint constituents to form the final product. These vessels serve as a possible production medium for the beads.

To date, success has been achieved in producing vesiculated beads on laboratory scale Cowles reactors. However, the system is extremely sensitive to processing variables and reproducibility of properties, including average particle size, stability and opacity is difficult to obtain. This becomes more pronounced when the system is scaled up to industrial size production. It is therefore necessary to identify important production parameters and investigate why and to what extent this will influence these properties. This will give a better understanding of the process and assist in gathering information in order to appropriately exercise control on production on any scale and under any processing conditions.

This also needs to be done on smaller scale under accurately controlled processing conditions. Performing a study on larger robust scale will not only be increasingly difficult to control, but will also result in higher cost due to the higher demand for raw materials.

The objectives of this study was therefore:

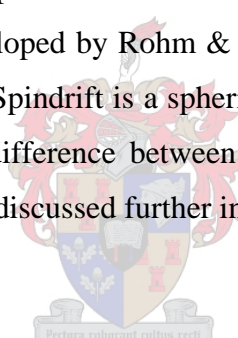
- Design of a laboratory scale Cowles reactor system, a downscaled version of the reactor vessels found in the paint factories. Different, geometrically similar vessels must be constructed to enable an investigation into the effect of scale-up. The system must be integrated to accurately control process conditions such as temperature, constituent addition rates and impeller speed as well as effectively monitor potential viscosity changes.
- Construction and installation of the reactor and electronic network system.
- Performing vesiculated bead production runs focussing on the effect of single variable changes of different process parameters such as impeller speed, addition rate, reaction temperature, etc.
- Performing, to a lesser extent, production runs where the effect of selected chemical composition variations is studied.
- Determine what variables have a significant effect on the final properties namely pH, viscosity, average bead size, etc. and identify possible reasons for this.
- Repeat production runs on a larger scale vessel where physical variations, which were found to be influential on final properties on small scale, are repeated, thereby enabling a study into the effect of scale-up
- By taking all the important variables into consideration, derive suitable models describing the final properties of the vesiculated beads.
- To test the accuracy of the models in describing properties recorded from production runs performed on much larger industrial scale.

Chapter 2

The Development of Vesiculated Beads as Pigment

2.1 Introduction

Microvoids have been used for many years as very cost-effective opacifying agents in a variety of coatings^[1]. It has also received considerable recognition as opacifiers in the plastic mouldings and paper industry^[4]. Recently new uses for pigmented vesiculated beads have been established, most notably in aerospace coatings. However, because the amount of light scattered by microvoids and therefore the opacity per unit volume is low, they are more widely used in the surface coatings sector in conjunction with titanium dioxide pigment in order to achieve the required level of opacity. Two main products have been incorporated into the market. Ropaque Opaque Polymer, developed by Rohm & Haas, is a spherical polymer bead containing a single void, whilst Spindrift is a spherical polymer containing a multiple of irregular sized voids. The difference between the two as far as properties and production is concerned, will be discussed further in this chapter.



2.2 Multi-Vesiculated Beads (Spindrift)

2.2.1 Previously Patented Multi-Vesicle Beads

There are numerous published patents commercially available. Only a few of these will be discussed in this section.

Gunning, et al.^[4] filed a patent, which explains the process of preparing aqueous slurries of multi-vesiculated beads with granule sizes varying from 0.5 to 500 micrometers, and can be used in paints as matting or texturing agent.

In order for the slurry to effectively act as an opacifying agent in paints, it has been proposed that each vesicle encapsulated in a bead, be at least 5 times smaller than the mean granule diameter.

The polymer phase is known to consist primarily of an unsaturated polymer resin that is cross-linked with polymerisable unsaturated monomer(s). The polymer resin is “carboxylated”, which refers to the unreacted free carboxyl groups found on the organic structure. A measure of the concentration of these groups is commonly known as the acid value of the resin and is given as milligram KOH per gram resin, which is the amount of KOH base needed to neutralise all the acid groups found on the polyester chains.

When these groups cross-link with unsaturated monomer(s), a solid granule is created which is insoluble in organic fluids, thus explaining its importance in paint manufacture. When allowed to dry in a paint film, the granules may in some cases shrink significantly, causing cracks in the dry film. The granules are then referred to as “dimensionally unstable”. The process of this invention to produce dimensionally stable vesiculated beads can briefly be summarised as follows^[4]:

- (a). Water is dispersed by means of agitation into the carboxylated unsaturated resin (acid value ranging from 10 to 45 milligram KOH per gram polyester) in conjunction with the monomer (with less than 5 wt% solubility in water at 20°C) in the presence of polyamine (with at least 3 amine groups per molecule). If it is desired to include additional titanium dioxide pigment to the beads, it can be done by pre-dispersion in either the water or polyester phase above.
- (b). The water-in-oil phase is then dispersed by means of agitation to form stable globules in water. Dispersion stabilisers should be present in the latter. The most satisfactory stabiliser is water-soluble partially hydrolysed polyvinyl acetate.
- (c). Polymerisation is initiated and cross-linking of the polyester with the monomer takes place to create the solid polyester granules.

A water-in-oil-in-water system is formed.

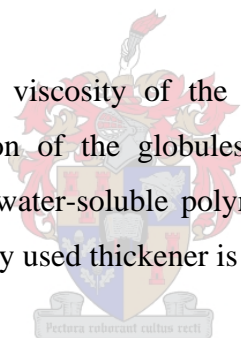
Alternatively, the primary water phase, i.e. the phase used to create the water vesicles, can be excluded from the process and the polyester resin, monomer and polyamine added to the secondary continuous water phase under agitation. A stable oil-in-water

suspension is thus created. Simultaneously, water vesicles form spontaneously inside the polymer globules.

After catalysis, cross-linking occurs and polymerisation initiated with the water vesicles intact in the solid granules.

It has been found that the polymer beads can be stabilised in the continuous (secondary) water phase by the addition of partially hydrolysed water-soluble polyvinyl acetate with a molecular weight of about 100,000. The degree of hydrolysis, i.e. the percentage of acetate groups replaced by alcohol groups to form polyvinyl alcohol, should be in the region of 85-90%. It has also been found that a concentration of 0.1-1.0 wt% polyvinyl acetate in the aqueous phase offers satisfactory results. Adding excess stabiliser causes comprehensive emulsification resulting in a loss of discreteness of the suspended globules. On the other hand, insufficient amounts of stabiliser can cause instability.

It has further been found that viscosity of the continuous water phase plays a significant role during formation of the globules. Higher viscosity is generally favoured and in obtaining this, water-soluble polymeric thickeners are added to the water phase. The most commonly used thickener is hydroxyethyl cellulose.



The polyester resin used, should consist of the condensation products of polybasic acids (or the corresponding anhydrides) and dihydric alcohols.

A combination of saturated and unsaturated polybasic acids can be used and suitable acids are among the following:

Unsaturated aliphatic acids, e.g. maleic-, fumaric-, itaconic acid;

Saturated aliphatic acids, e.g. malonic-, succinic-, glutaric acid;

Saturated aromatic acids, e.g. phthalic, isophthalic, trimesic acid

The unsaturated monomer used in conjunction with the polymer resin will generally contain one polymerisable double bond. Polyfunctional group monomers are sometimes also used, but are normally only present as minor constituents in a monomer mixture.

Preferred monomers that are used in this invention are selected from styrene, vinyl toluene and methyl methacrylate. These monomers copolymerise easily with the

polymer resin. Generally, at least 50 wt% of the monomer used consists of styrene to obtain optimal results.

Aside from the monomers mentioned, typical co-monomers that may be used are ethyl acrylate, n-butyl methacrylate, and acrylonitrile. These co-monomers should, however, never exceed 10 wt% of the total monomer. Excessive amounts cause the final paint to be either too brittle or too rubbery.

The water-soluble polyamine used must contain at least 3 amine groups and can either be primary, secondary, or tertiary amine groups. Typical polyamines used are diethylene triamine, triethylene tetramine and oligomers of vinyl pyridine.

Polymerisation in the organic droplets is started by free radical initiation, either using organic peroxide or direct exposure to a radiation source such as radioactive cobalt or ultra-violet radiation. When using organic peroxide, addition of a free radical activator is required. As an example benzoyl peroxide can be used in conjunction with diethylaniline as activator.

By using this invention, vesiculated beads with diameters ranging from 0.1-500 micrometers (microns) can be prepared and with microvoids ranging between 0.01-5 microns. These beads are very suitable for use as opacifiers and matting agents for aqueous emulsion (latex) paints. The granules produced have shown to possess extremely high dimensional stability.

Example of Preparation (Gunning, et al.^[4])

A polyester resin is made from phthalic anhydride, fumaric acid, and propylene glycol (mole ratios 1: 3: 4.4) and dissolved in styrene to a concentration of 70 wt%. The acid value of the resin is 22.0 mg KOH/gram.

A colloid solution A is prepared by dissolving 1.8 parts of hydroxyethyl cellulose in 326.2 parts of water and a colloid solution B is prepared by dissolving 7.5 parts of polyvinyl acetate/polyvinyl alcohol (molecular weight of 125,000 and 87-89% hydrolysed) in 92.5 parts of water.

The following ingredients are mixed together:

Polyester resin (as above)	91.0 parts
Styrene (monomer)	45.5 parts
Diethylenetriamine (polyamine)	0.9 parts
Benzoyl peroxide (organic peroxide)	7.5 parts

This homogenous liquid is added, with constant mechanical agitation, to a mixture of the following:

Colloid B solution	90.0 parts
Colloid A solution	328.0 parts
Diethylenetriamine (polyamine)	0.3 parts

Globules of dispersed resin solution forms and the mixture is stirred vigorously until the globule size is 30 micrometers (maximum). The stirring rate is then reduced and the following added:

Water	100.0 parts
Diethylaniline (catalyst)	1.5 parts

The resulting polymerisation reaction, leading to cross-linking of the polyester resin, is detected by the resultant exotherm (i.e. temperature increase).

Goldsbrough and Hodge^[5] suggested an invention for producing multi-vesiculated beads where the oil phase comprises a cross-linkable water-insoluble carboxyl-containing polyester resin, which is in solution with a copolymerisable monomer. The resin used must be unsaturated and capable of reaction with the unsaturated organic monomer at a temperature below 100°C.

It is preferable that the resin be formed from the condensation products of a dihydric alcohol (or its corresponding oxide) with proportions of an aliphatic dicarboxylic and an aromatic dicarboxylic acid. These components must be mixed in a proportion such that the resulting resin's acid value fall between 5-100 milligram KOH per gram resin (or more specifically between 10-35 milligram KOH/gram resin).

The pure polyester resin is modified by the addition of polyethylene oxide chains, which assist in providing stable emulsions. The resin is essentially dissolved in the unsaturated monomer. At least 30 wt% of the resin should consist of monomer to permit the necessary cross-linking to take place. It is, however, preferable to use monomer levels between 40 and 70 wt%. The monomer used should be substantially insoluble in water and usually is an unsaturated aromatic hydrocarbon or more preferably a vinyl aromatic hydrocarbon like styrene, divinyl benzene, alpha-methyl styrene and vinyl toluene.

A typical co-monomer that can also be used, if desired, in conjunction with the unsaturated monomer is usually an ester of acrylic or methacrylic acids, like methyl acrylate, ethyl acrylate, methyl methacrylate and n-butyl acrylate or even acrylonitrile, vinyl acetate and ethylene glycol dimethacrylate.

Pigment can be blended in with the oil phase and may either be an organic or inorganic pigment. Typical inorganic pigments that are used, are iron oxide, magnesium titanate or preferably titanium dioxide. In the case of the latter pigment, either anatase or rutile titanium dioxide may be used, but rutile titanium dioxide is more suitable, since it has a coating of one or multiple hydrous oxides, which improves the opacifying effect of the pigment.

The first aqueous phase consists of water, a selected base consisting of alkali metal hydroxides, alkali metal salts of weak acids, ammonium hydroxide and ammonium salts of weak acids (e.g. ammonium carbonate) and a water-soluble inorganic salt. The function of the latter is to increase the surface tension between the aqueous phase and the oil-phase. The amount of base added depends mainly on the amount of carboxyl groups found in the resin. Normally about 0.3-2 equivalents of base should be used per carboxyl group.

A water-in-oil emulsion is prepared by mixing the first aqueous phase with the oil phase, generally at an accelerated speed. The second aqueous phase consists of water and an emulsifying agent. The emulsifying agent assists in stabilising the oil globules. The preferable emulsifying agent used is a partially hydrolysed polyvinyl acetate with 85%-95% of its hydrolysable groups hydrolysed.

The second aqueous phase can also contain a thickener to assist in the formation of the globules and a typical thickener is hydroxyethyl cellulose.

Mixing the emulsion formed by addition of the first aqueous phase with the oil phase to the second aqueous phase produces the water-in-oil-in-water emulsion. This is also referred to as double emulsification.

The required dimensionally stable beads are formed after addition of a polymerisation initiator, which initiates cross-linking of the polyester resin with the copolymerisable monomer. The most generally used initiator is an organic peroxide like cumene hydroperoxide, together with an accelerator if desired. A typical accelerator that can be used, is an aqueous solution of ferrous sulphate.

Allowing the suspension to cure at a temperature anywhere between 45°C and 70°C for an appropriate time allows beads to form with the required degree of opacity. Beads created by the use of this invention have diameters ranging from 1 to 25 micrometers and larger.

Polyamines are generally believed to cause yellowing of the vesiculated beads. The use of any polyamines (e.g. diethylene triamine) to stabilise the first emulsion is avoided in this invention.

Example of Preparation (Goldsbrough and Hodge^[51])

An unsaturated polyester resin is prepared by condensation polymerisation of maleic anhydride, phthalic acid, and propylene glycol in molar proportions of 3: 1: 4.5. The product has an acid value of 24 mg KOH/gram and a viscosity of 2,500 mPa.s as a 70 wt% solution in styrene (at 25°C).

An organic phase is prepared by dispersing 178 parts of rutile titanium dioxide pigment in 166 parts of a 50 wt% solution of the polyester resin in styrene solution. 41 parts of additional styrene is then added to the pigmented resin dispersion.

An aqueous phase is prepared, consisting of 0.60 parts sodium hydroxide (base), 0.12 parts sodium chloride (inorganic salt) and 129 parts water. Adding this aqueous

phase, at high-speed agitation, to 385 parts of organic phase forms a water-in-oil emulsion and 192 parts of this emulsion are added, with stirring, to a second aqueous phase. The latter consists of 0.45 parts hydroxyethyl cellulose (thickener), 2.25 parts of 90% hydrolysed polyvinyl acetate (stabiliser) and 0.5 parts of a sodium dihexyl sulfosuccinate in 180 parts of water. This forms a water-in-oil-in-water emulsion.

The organic globules are exposed to further agitation until the average particle diameter reduces to 12 microns. The emulsion is then diluted by adding 177 parts of hot water to give a temperature of 50°C in the total mixture. Polymerisation is then initiated by adding 1.25 parts of cumene hydroperoxide, 10 parts of a 2 wt% aqueous solution of diethylene triamine and 2 parts of a 0.90 wt% aqueous solution of ferrous sulphate. The vesiculated bead slurry of 25 wt% solids is then left overnight for the polymerisation reaction to complete.

Karickhoff ^[6] developed a process for manufacturing vesiculated beads possessing improved scattering efficiency and resistance to shrinkage.

The process involves the formation, in the presence of a polyamine, of a water-in-oil emulsion, consisting of a stable dispersion of water droplets in a solution of carboxylic acid functional unsaturated polyester resin. The resin should also contain at least one ethylenically unsaturated monomer copolymerisable with the polyester and have an acid value between 8 and 20 milligram KOH per gram resin.

The water-in-oil emulsion is added to an additional aqueous solution, forming a stable water-in-oil-in-water emulsion. By polymerising the polyester and copolymerisable monomer through free radical addition granules of opaque, cross-linked vesiculated beads are created that remain stable in solution.

A polyamine is added to the system and acts as neutralising agent, since it is a strong base. The polyamine contains at least 3 amine groups per molecule, which may either be primary, secondary or tertiary. Suitable polyamine compounds are, for example, diethylene triamine, triethylene tetramine and oligomers of vinyl pyridine or dimethyl aminoethyl methacrylate with polyethylene glycol methacrylate. In order to obtain

beads possessing improved scattering efficiency and sufficient dimensional stability, the amine must be present during the formation of the water-in-oil emulsion at a concentration such that there are at least about 2 amine groups per polyester carboxylic acid group, but preferably between 2 and 10 groups per acid group. In general, higher ratios of amine- to acid groups provide beads with greater scattering efficiency and the higher the scattering efficiency, the greater the opacity of the bead.

The polyester should have a number average molecular weight between 1,000 and 100,000. It is preferable that the polyester consists of the condensation reaction product of propylene glycol, fumaric acid and phthalic anhydride.

Optionally, additional inorganic pigment can be added to the first aqueous phase (i.e. water phase in the polyester). Examples of pigment that can be used include titanium dioxide, clays, zinc oxide, carbon black, mica, silica and calcium carbonate.

The ethylenically unsaturated copolymerisable monomer in which the unsaturated polyester resin is dissolved and cross-linked, must essentially be water-insoluble. Monomers that have a solubility of less than 5 wt% at 20°C in water are considered to be suitable for this purpose. A single monomer or a mixture of monomers may be used and, in general, the monomer should contain only a single polymerisable double bond. Styrene, vinyl toluene and methyl methacrylate may be used, because of the ease with which they can be copolymerised with the polyester. For the best results, the monomer used should comprise at least 50 wt% of styrene, and it is usually preferred to exclusively use styrene. A few weight percentage of a non-polymerising organic liquid, e.g. n-butanol or toluene, may be mixed with the monomer to increase the solubility of the monomer in the polyester resin.

The second step in the formulation of the beads involves addition of the water-in-oil emulsion to another aqueous solution, typically containing stabilisers such as polyvinyl alcohol or hydroxyethyl cellulose to maintain the formed water-in-oil-in-water double emulsion at the required bead size.

The third basic step in the preparation of the beads of this invention involves polymerising the polyester and copolymerisable monomer by free radical addition

polymerisation. This is done through the use of a free radical initiator, which can either involve the use of inorganic peroxide (e.g. cumene hydroperoxide) or exposure to a radiation source such as ultraviolet radiation. When an organic source of free radicals is used, it is conveniently introduced into the reactants by dissolving it in the monomer or polyester solution before the globule suspension is prepared. The free radical source can be activated by heating it to its decomposition temperature. Alternatively, a redox process can be used using, for example, diethylaniline as an activator.

Example of Preparation (Karickhoff ^[6])

An aqueous phase is prepared by mixing, at high speed, 10 parts (by weight) ice, 11.08 parts water, 2.20 parts of a 75 wt% solution of sodium dioctyl succinate in butanol, 0.32 parts ethanol and 0.79 parts defoamer. This is done using a Cowles disperser to obtain a homogenous solution. Titanium dioxide (53.2 parts) is added over 3 minutes and dispersed at high speed for a further 15 minutes. At low speed 1.04 parts water is added and mixed for 2 minutes.

In a separate vessel 49.0 parts unsaturated polyester resin (58 wt% solution in styrene) and 18.52 parts styrene are mixed at low speed. With the agitator remaining at low speed, the aqueous dispersion is added over a period of 2 minutes. The agitator speed is increased for about 3 minutes and then reduced and maintained for about 15 minutes.

An aqueous solution consisting of 43.23 parts hydroxyethyl cellulose (1.5 wt% solution in water), 47.97 parts polyvinyl alcohol (7.5 wt% solution in water) and 110.27 parts water is prepared separately and mixed at low speed. The water-in-oil emulsion is added over a 4-minute period. The agitation is increased and held for 20 minutes. At low speed, 102.57 parts hot (52°C) water is added followed by 0.921 cumene hydroperoxide. After a few minutes, 0.159 parts diethylene triamine (10 wt% solution in water) and 1.05 parts ferrous sulphate (1 wt% solution in water) are added. Agitation is stopped after 2 minutes and the batch left overnight for polymerisation to complete.

2.2.2 Spindrift Bead Slurry

Spindrift pigmented beads ^[1] are produced as a slurry in water, making it convenient for use in aqueous emulsion paints. It consists of spherical polymer beads containing preformed variable sized microvoids and additional encapsulated titanium dioxide. The micro-voids are encapsulated by using a double emulsification or suspension polymerisation process. Titanium dioxide is first dispersed at high speed in an aqueous phase and then emulsified into a solution of unsaturated polyester resin and styrene to form a stable water-in-oil emulsion (first emulsion). This emulsion is then added to water and colloid stabilisers and stirred at moderate speed to form the preformed globules (or second emulsion), containing multiple vesicles formed from the first aqueous phase. Polymerisation is initiated to form the final beads. Alternatively, the first aqueous phase can be omitted and the titanium dioxide can be dispersed in the polyester and styrene solution. In the presence of polyamine in the polyester phase, water droplets form spontaneously inside the polymer globules, thus creating the vesicles.

The solid component of the beads is about 35% by volume of the dry bead and optimally possesses a top diameter of 10-25 μm , with a number average mean of 5-12 μm . Due to this large particle size, the beads act as a matting agent, making it useful in low gloss paint.

The Spindrift process was first developed by Dulux, Australia, during the 1960's and 1970's and fully commercialised under licence in the 1980's ^[1]. Simpler production processes have been developed afterwards with beads possessing additional advantages imparting paint films with increased cleanability and better scour (burnish) resistance.

2.3 Single Vesicle (Opaque) Beads

2.3.1 Previously Patented Single Vesicle Beads

An invention presented by **Adam, et al.**^[7] relates to a process of making a hydrophobic polymer containing at least one void suitable for use in products such as coating compositions, plastics, cosmetics, papers or leather.

This invention provides a process for making hydrophobic particles by dispersing droplets of water in a hydrophobic monomer (containing an essentially hydrophobic surfactant) insoluble in water. The dispersion is further dispersed in another quantity of water containing an essentially hydrophilic surfactant. The stable monomer globules, dispersed in a continuous aqueous phase, now contain a single aqueous vesicle and are subsequently polymerised to form the final particles.

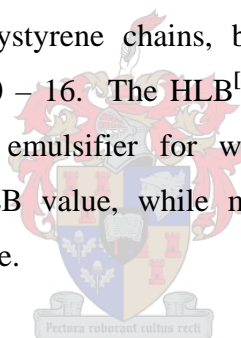
The hydrophobic polymer (i.e. the polymer or copolymer which forms the main part of the particle) may be any polymer or copolymer which is not soluble in or swollen by water to an extent that totally destroys any light scattering ability of the voids. Preferably the hydrophobic polymer should be a cross-linked material. Conveniently the hydrophobic polymer should be obtainable by a free radical initiated polymerisation performed on a dispersion of monomer in water in the presence of hydrophobic and hydrophilic surfactants. Suitable monomers include vinyl aromatics such as styrene or divinyl benzene, vinyl acetate, acrylates such as alkyl esters of acrylic or methacrylic acids and in particular methyl, ethyl or butyl esters. Styrene polymers or copolymers are sometimes preferred because of its high refractive index.

The dispersions used can be made by conventional techniques such as stirring or ultrasonic vibration. Preferably the monomer phase contains from 0.5 to 15 wt% (based on the monomer) hydrophobic surfactant whilst the continuous water phase preferably contains from 0.1 to 10 wt% (based on the water phase) hydrophilic surfactant. The presence of the predominantly hydrophobic surfactant increases the stability of the water and monomer pre-dispersion leading to improved control of void size. Sometimes, this effect can be enhanced by the inclusion of a thickening agent in the first (water in monomer) dispersion. Suitable thickening agents may be pre-

formed polymers (including copolymers) which are soluble or swellable by monomer, for example pre-formed polystyrene.

The system can often be stabilised further by including a thickening agent in the water in which the first dispersion is dispersed. A suitable thickener would be a high molecular weight (20,000 to 400,000) polyoxyethylene.

The hydrophobic surfactant incorporated into the monomer phase should be a block copolymer having a minimum molecular weight of 5,000 and comprising hydrophobic and hydrophilic chains in an amount such that the hydrophobic portion comprises from 55 to 95 wt% of the copolymer. The high molecular weight ensures that the hydrophobic portion of the surfactant anchors firmly into the hydrophobic polymer particle whilst permitting the copolymer to cross a boundary which defines a void so that the hydrophilic chain or chains are exposed to the void. A preferred essentially hydrophobic surfactant will contain hydrophobic polyoxyethylene chains together with hydrophobic polystyrene chains, but with a Hydrophile-Lipophile Balance (HLB) ranging from 10 – 16. The HLB^[8] is an expression of the relative simultaneous attraction of an emulsifier for water and oil. More hydrophilic emulsifiers possess a high HLB value, while more lipophilic (or hydrophobic) emulsifiers have a low HLB value.



The hydrophilic surfactant used in the continuous aqueous phase should possess at least one hydrophilic chain long enough to interact with the water in which the particle is dispersed whilst also comprising a hydrophobic portion which can firmly anchor in the particle. These requirements are achieved if the hydrophilic surfactant has a molecular weight of at least 2,000 and the hydrophilic chain or chains amount to 40 to 90 wt% of the surfactant. In these circumstances, the surfactant can cross the surface of the particle in such a way that the hydrophobic portion is anchored in the particle whilst the hydrophilic chain or chains are exposed and available for interaction. Preferably the hydrophilic surfactant must also contain hydrophilic polyoxyethylene chains and hydrophobic polystyrene chains, but with an HLB in the range of 10 – 16.

Polymerisation of the monomer may be conveniently achieved by adding a free radical initiator to the monomer phase. Suitable initiators include azodi-isobutyronitrile or peroxides such as lauroyl peroxide, benzoyl peroxide or most

preferably an initiator, which does not involve a gas, for example cyclohexyl percarbonate. Polymerisation can easily be initiated by heating the system to a temperature at which the free radical initiator decomposes, generally 30°C to 80°C. Preferably the system should not be stirred during polymerisation and rather left static.

The particles of hydrophobic polymer usually have a number average particle size ranging between 0.5 to 100 microns and generally it is from 1 to 50 micron. Refinement of the invention might allow the production of particles as small as 0.3 micron whereupon the particles will almost certainly only contain one void each. Where the particles are primarily intended for use as opacifying agents, their number average particle size is preferably below 10 micron.

Example of Preparation (Adam, et al.^[7])

A mixture of the following is made (parts by weight):

Styrene monomer	32.5 parts
Divinyl benzene monomer	10.0 parts
Essentially hydrophobic triblock copolymer	2.5 parts
Polystyrene	2.5 parts
Cyclohexyl percarbonate	2.5 parts

The essentially hydrophobic copolymer listed above contains 30 wt% polyoxyethylene and 70 wt% polystyrene chains with an HLB of 6 and a molecular weight of 25,000.

Fifty parts by weight of water is added to the mixture above and then stirred at high speed until a dispersion of water droplets in monomer is obtained. This dispersion is, in turn, dispersed in a further 100 parts of water using high-speed stirring. This water contains 1 wt% of an essentially hydrophilic surfactant, which is a triblock copolymer having a molecular weight of 11,000, comprising of 73 wt% polyoxiethylene and 27 wt% polystyrene chains. This surfactant should possess an HLB value of about 15. A white emulsion of the first dispersion is obtained.

The emulsion is heated to 60°C in a closed pressure vessel and the temperature maintained for 12 hours for polymerisation to complete. A dispersion of styrene/divinyl benzene cross-linked copolymer is obtained with each particle containing a plurality of voids. The dispersion is passed through a 50-micrometer sieve and concentrated by centrifugation. The vesiculated beads produced in this manner possess a number average particle size of about 1.60 micrometer.

The particles can be washed to remove unanchored surfactant and dried to produce a powder which can easily be re-dispersed in water.

2.3.2 Ropaque Opaque Polymer

In the early 1980's, Rohm & Haas successfully developed the technology to manufacture micro-spheres containing only one large void in the centre of the polymer sphere ^[1]. These micro-spheres are industrially known as Ropaque Opaque Polymer. The polymers are produced using water-insoluble particulate heteropolymers made by sequential emulsion polymerisation in dispersed particles of which a "core" of a polymeric acid is encased in a "sheath" or "shell" polymer that is permeable to a volatile base, namely sodium hydroxide. The base is incorporated to hydrolyse the acidic core polymer, causing the core to swell as neutralisation takes place. However, the base does not interact with the shell polymer. The swelling of the core, in return, causes fine cracks in the harder polymeric shell allowing the neutralised poly-acid to migrate through the sheath wall towards the outside of the bead, producing an encapsulated micro-void. This presents the bead with its opacifying qualities. The polymer does not contain any additional inorganic pigment.

Since the opaque particles are made by an emulsion polymerisation process, the particles can be controlled to a very uniform size distribution with a diameter usually in the region of 0.5µm. This is much smaller comparative to Spindrifit, making it useful in the production of gloss and semi-gloss paints.

Earlier inventions other than Ropaque and Spindrifit include Pittment, consisting of polymer granules containing incompatible non-evaporative solvent inside the voids to


provide the substantive difference in refractive index. It is also possible to produce an extender by casting foamed plastics and milling it down to a fine powder. Although the obtained particles are non-spherical, it is equitably effective for use in paint.

Another example of opacifying polymer particles is Microbloc, a non-vesiculate containing and ultra-fine polystyrene sphere aggregate. However, this extender has not received considerable commercial development.

Of all the void-containing polymer granules, discussed above, Ropaque Opaque Polymer, possessing a small and consistent particle size, offering outstanding opacifying power, received by far the most utilisation. However, Spindrifit retains considerable applicability in the market, since its larger vesiculated particle makes it suitable for use as extender in flat and some semi-gloss coatings.

2.4 Vesiculated Bead Development of Companies within the Nova Club

2.4.1 Background



Approximately five years ago, a paint company, Comex, situated in Mexico and member of the Nova Club, started a research project for developing multi-vesiculated beads in the laboratory. However, it was found extremely difficult to perform the process on industrial scale since it is very sensitive to scale-up parameters. The project was terminated, but the technology released to other members of the Nova Club. Recently, Plascon, a local member of the Nova Club decided to continue research into developing vesiculated beads, using this technology.

The process was initially developed for production on Cowles dispersers, since most members of the Nova Club have access to this. However, further investigation is currently undertaken to also produce vesiculated beads in emulsion reactors. The difference between these two reactors will be discussed briefly in this section as well as the formulation that is currently being developed for manufacturing multi-vesiculated beads.

2.4.2 Cowles vs. Emulsion Reactor Vessels

Cowles dispersers are extensively used in paint manufacturing to break down suspensions of powder pigment agglomerates to the desired fineness. The flat disc impeller blade fortified with adjacent slanted teeth (Figure 2.1A) at the edge promotes an intense turbulent motion at high dispersion (or ‘grinding’), ultimately causing a donut-shaped mixing pattern (Figure 2.1B). The geometry of the blade together with the elevated mixing speed imparts a very high velocity to the dispersion at the tip of each tooth, promoting the pigment particle separation process.

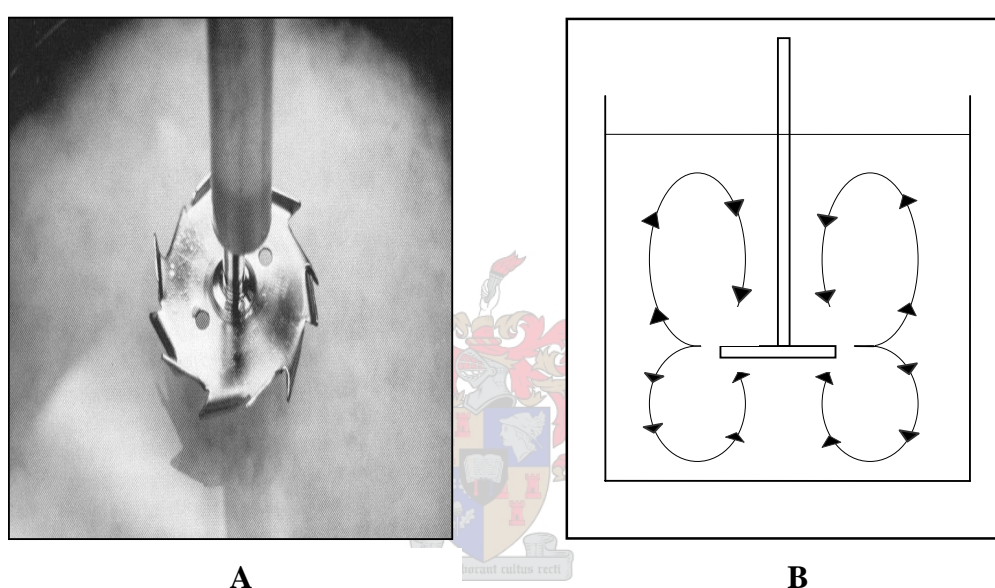


Fig. 2.1 A) Example of an Flat Disc Impeller
B) Fluid Motion caused by Flat Disc Impeller in Cowles Reactors

In the industry pigment grinding is performed at rotational speeds of approximately 1,000 rpm, but is capable of delivering speeds of up to 5,000 rpm^[9]. The impeller to vessel diameter is normally limited to a maximum of about 0.6 and a lower limit of 0.3. Should the vessel diameter substantially exceed three times the blade diameter, movement at the vessel wall will cease. Consequently any material at the vessel periphery will not pass over the blade. Due to the high operating speeds, a very high mechanical energy input is required, which makes it possible to perform dispersion on relatively high viscosity fluids.

Cowles dispersers are also used in the industry for blending the pigment phase with the binder phase together with all post-additions to form the final paint.

Emulsion reactors have been utilised in many paint factories in the past for the production of emulsions used as binders (or film-formers) in surface coatings. Binders are largely responsible for the protective and general mechanical properties of the paint film. Emulsions are produced under controlled moderate stirring of about 35 rpm using a 45° axial-flow turbine (Figure 2.2A) to form a mild axial fluid motion pattern (Figure 2.2B), thereby avoiding destruction or instability of the polymer particles caused by harsh agitation. The impeller to vessel diameter ratio generally ranges between 0.5 and 0.7^[10].

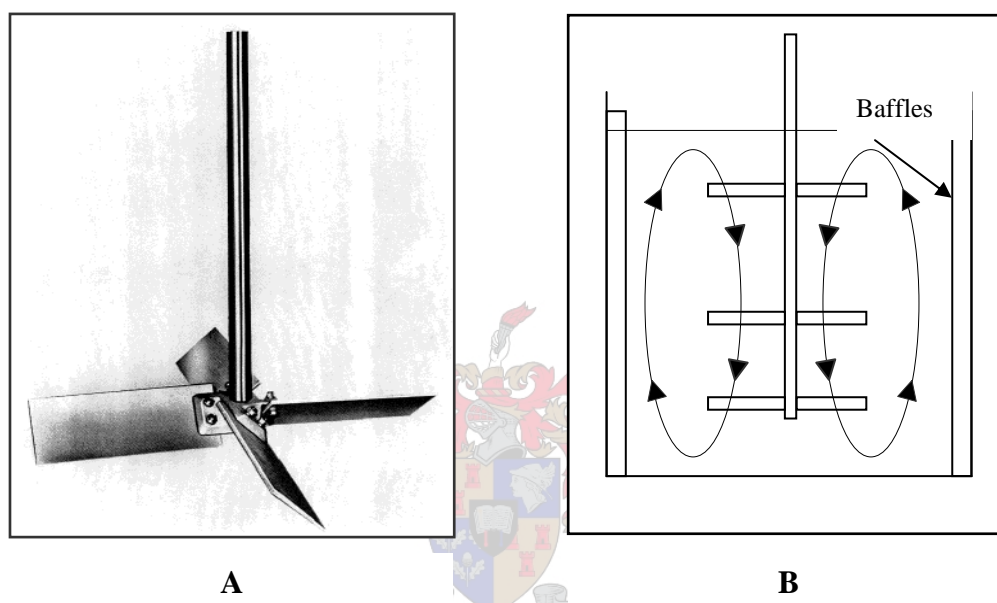


Fig. 2.2 A) Example of an Axial Flow Turbine
B) Fluid Motion caused by Axial Flow Turbine in Emulsion Reactors

The inclusion of fixed baffles on the tank wall increases the efficiency of the turbine agitation considerably. The mechanical energy input to the impeller is relatively low to medium in comparison to other forms of agitation like homogenisers and only capable of effectively blending low to medium viscosity fluids. The maximum obtainable speed of Plascon's emulsion reactor mixers is in the region of 70 rpm.

Plascon, who is responsible for developing vesiculated beads on industrial scale, is currently phasing out their emulsion production in the factories. Emulsions are now obtained from an external production source. Consequently, this will result in the non-utilisation of existing emulsion reactors in the factories. This provides an opportunity for vesiculated beads to be manufactured in these vessels as well. The difference in Cowles and emulsion impeller geometry and dispersion conditions

causes extensive variance in the properties of the final beads, thereby necessitating adaptation of the vesiculated bead production method in both cases.

2.4.3 Current Production Procedure of Vesiculated Beads

Formerly, the double emulsification procedure for manufacturing multi-vesiculated beads (Section 2.2.1) was investigated by the Mexican Nova Club member. However, locally it was found nearly impossible to successfully perform industrial size production since the system was too sensitive to process variables. This forced the local investigators to change the formulation and production procedure using the single emulsification process. This formulation is outlined in Table 2.1 and beads produced using this possess a solid content of 24 wt%.

Table 2.1 Formulation for Producing Multi-Vesiculated Beads (single emulsification)

Material Name	Parts by Weight
<i>Organic Pre-dispersion</i>	
Polyester	15.01%
Titanium Dioxide	0.86%
Styrene	6.54%
Polyamine	0.21%
<i>Aqueous Let-down Phase</i>	
Surface Active Agent (10.7 wt% aq. sol.)	13.30%
Cellulose Thickener (0.5 wt% aq. sol.)	48.47%
Polyamine	0.06%
<i>Post-additions</i>	
De-ionised Water	14.23%
Redox Activator Solution	0.01%
Organic Peroxide	0.12%
Fungicide	0.18%
Surfactant	1.00%
<i>Total</i>	100%

The polyester that is used in the production of vesiculated beads is manufactured by the combination of maleic acid, phthalic acid, and propylene glycol at an elevated temperature of 130°C, as presented in Figure 2.3. This polyester chain must have a molecular mass in the region of 5000 and an acid value in the range of 24-28 mg KOH per gram resin, the latter giving an indication of the concentration of carboxylic acid groups situated at the end of each chain.

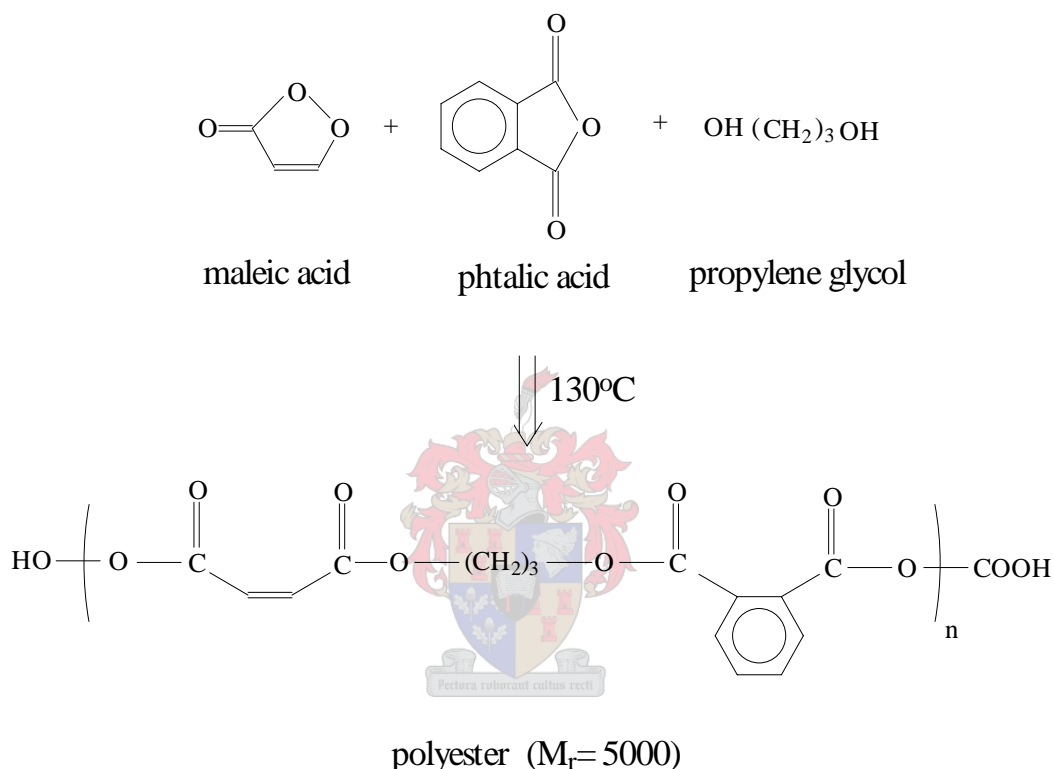


Fig. 2.3 The Production of Carboxylated Unsaturated Polyester

After formation, the polyester will be extremely viscous if left to cool down. For this reason the heated fluid is dissolved in styrene monomer. The final solution should consist of 68 wt% polyester. However, at high temperatures, the styrene monomer will start polymerising, and should be avoided. This can be surmounted with the addition of an inhibitor, usually tertiary butyl catechol, which will allow the styrene to remain unreacted during the polyester cool-off period.

Formerly, a company called KZN Resins supplied the polyester resin, but since about July 2001, resin is obtained from a company called Cray Valley. The production processes of these two companies are not identical, and certain parameters were found

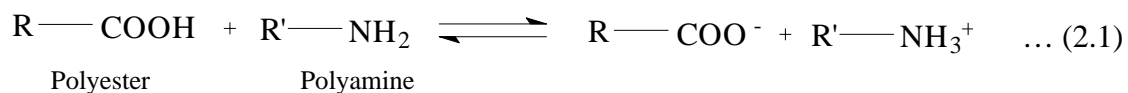
to differ from each other. Table 2.2 presents the specification range for each of these parameters and the estimated value for both the KZN and Cray Valley resins.

Table 2.2 Comparison of Polyester Parameter Values for KZN and Cray Valley Resins

<u>Parameter</u>	<u>Specification</u>	<u>KZN</u>	<u>Cray Valley</u>
Solids (%)	66 - 68	67.8	66.8
Acid No. (mg KOH/g)	24 - 28	26.0	26.5
Gel Time (min)	40 - 55	41.5	42
Curing Time (min)	50 - 65	54	50
Peak Exotherm (°C)	178 - 185	192.8	180

Titanium dioxide is combined with the polyester solution to form a stable pre-dispersion. This is done in order to increase the inherent opacifying effect of the beads while still in its wet state, i.e. before the water in the vesicles have had time to diffuse (or dry) out of the particles. This is done at high speed using a Cowles disperser to break up titanium dioxide powder agglomerates.

Further addition of styrene is performed under mild stirring in order to obtain a final polyester concentration of about 50 wt% in styrene solution. A polyamine is now added, comprising of about 1 wt% of the polyester solution. The polyamine must be a strong base enabling partial ionisation of the free carboxyl groups on the polyester. The ionisation occurs as shown by (2.1) below.



This interaction causes the polyester chains to orientate themselves in the region of the polyamine molecules. Meanwhile, the positively charged amine groups will start grouping together with surrounding negatively charged polyester chains to form a more stable macro-molecular structure. This is also referred to as micelle formation (Figure 2.4).

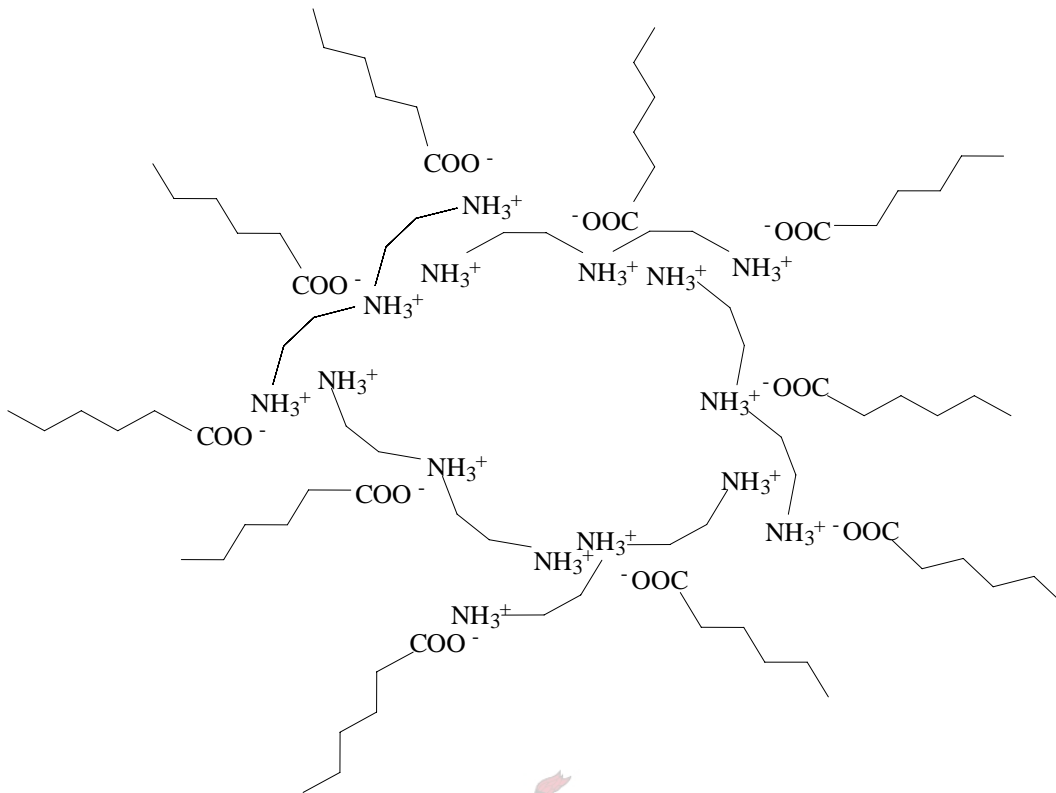


Fig. 2.4 Micelle Formation of Polyamine and Polyester Chains

The resin is then added under dispersion to an aqueous phase consisting of a 10 wt% partially hydrolysed polyvinyl acetate solution (colloid stabiliser) and a cellulose thickener, also acting as a colloid stabiliser. The agitation causes break-up of the oil phase into small globules, evenly dispersed in the continuous aqueous phase to form an oil-in-water emulsion. The partially hydrolysed polyvinyl acetate acts as a surface-active agent and assists in the stabilisation of the produced polyester globules.

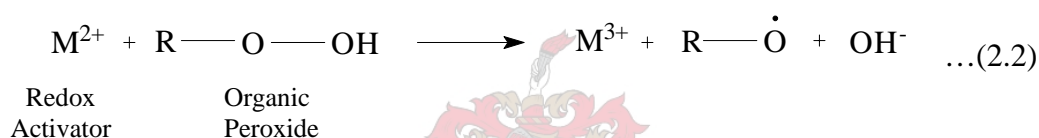
Since the polyamine is a strong base reducing the pH of the resin, it is also added to the aqueous phase to prevent pH shock when the resin is introduced to the relatively neutral aqueous phase.

The exact mechanism(s) with which vesicle encapsulation occurs has not been conclusively established, but experimental investigations conducted in the past, concluded that the polyamine added to the polyester phase, might cause an increase in the solubility of water in the organic phase. Since the formed micelles, discussed above, possess hydrophilic character in the centre, it is possible that water molecules, which have dissolved in the organic phase, diffuse towards these micelle centres to

form a more thermodynamically stable conformity. Agglomeration of these water molecules might be responsible for aqueous voids to form inside the organic globules.

After an emulsification period, allowing time for the globules to break up and vesiculation to occur, post-treatment can be started where, if necessary, de-ionised water is added to reduce the solid content of the batch to the desired level.

The emulsion is now ready for polymerisation. Since free radical formation of the polymer chains will only occur naturally at a temperature of 120°C, a catalyst is required to obtain formation at ambient temperatures. A combination of two initiators is used to do this, namely organic peroxide in combination with a metal redox activator solution. The metal redox activator reduces the peroxide molecule with the formation of an anion and an oxygen-centred radical according to reaction (2.2).



The free radicals made available by this reaction initiate further polymerisation involving styrene and the maleic-anhydride-derived double bonds of the unsaturated polyester. The result is the vitrification of the resin by means of high-density cross-linking to form a thermoset. An example of a typical polymerisation reaction is presented in Figure 2.5.

After addition of the catalyst, agitation is stopped and the batch left to complete polymerisation, which is an exothermic process, resulting in a temperature increase.

First of all, the granules remain stable due to mechanical stabilisation where granules pocket themselves in an entangled network of cellulose thickener chains, preventing it from settling. Furthermore, due to the assembly of partially hydrolysed polyvinyl acetate chains (colloid stabiliser) around the granules, steric hindrance prevents aggregation of the beads.

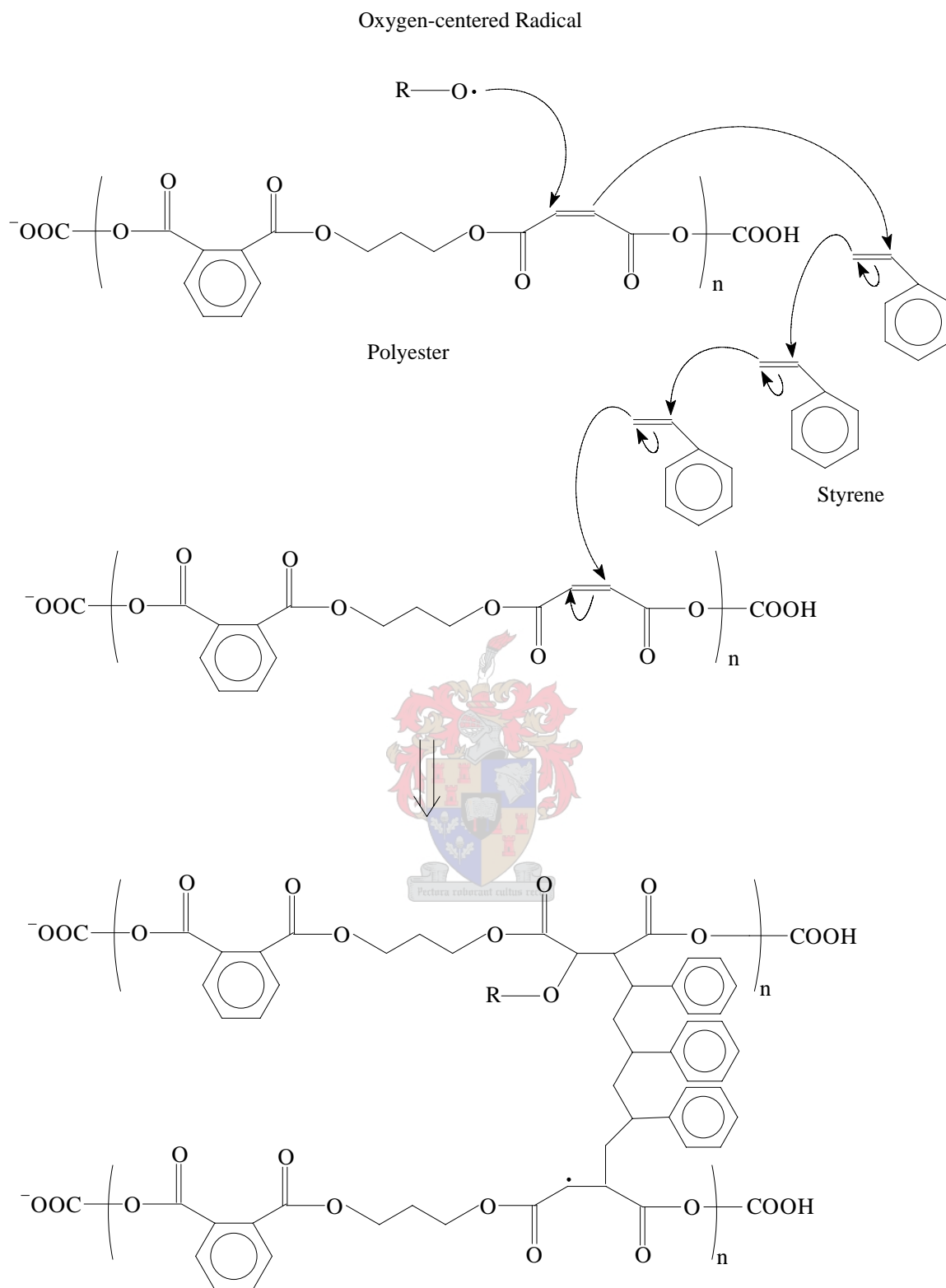


Fig. 2.5 Typical Polymerisation Reaction Between Unsaturated Polyester and Styrene

A completed batch is left static for a period of at least 12 hours (overnight) after which agitation is applied and a fungicide mixed into the system, preventing bacterial degradation.

It is also found that the system's viscosity increases significantly after production. This might be due to the degradation of the cellulose thickener chains caused by the free radicals formed in the beads after catalysis. This occurrence will most probably be concentrated in the vicinity of the vesiculated granules, since free radical propagation takes place in the beads. Theoretically the beads will start congregating closer together (Figure 2.6), resulting in a viscosity increase.

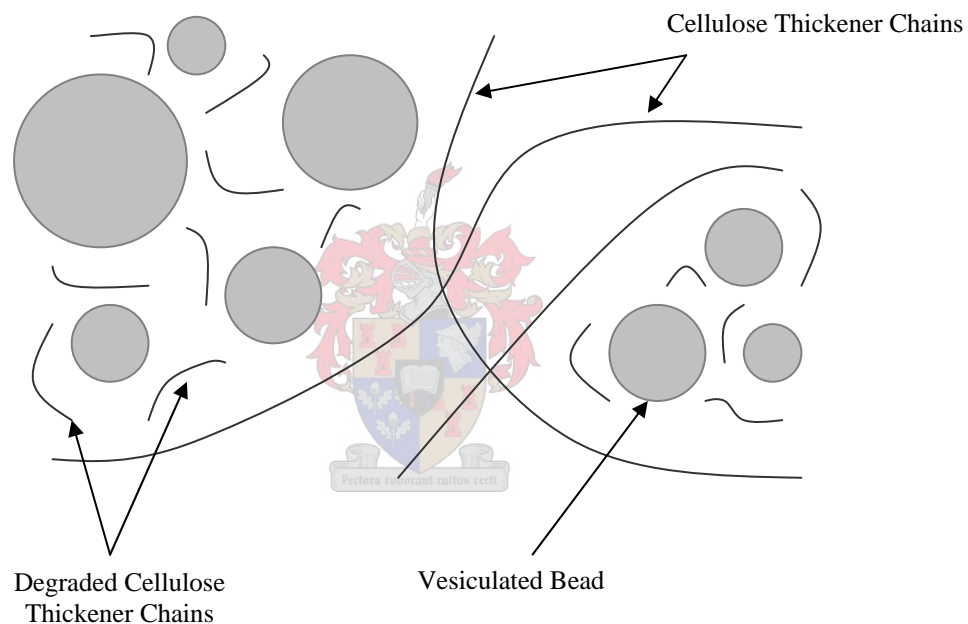


Fig. 2.6 Aggregation of Vesiculated Beads due to Cellulose Thickener Chain Degradation

The high viscosity can be reduced and stabilised by the addition of a surfactant during agitation consisting of hydrophobic and hydrophilic end groups. The chains will orientate themselves around the vesiculated granules in such a manner that the hydrophobic end groups gather close to the surface, while the hydrophilic groups, possessing a negative ionic charge in solution, attenuate towards the continuous aqueous phase. This results in an overall negative charge surrounding each particle, propelling the granules away from each other and consequently causing electrostatic stabilising. Hence, a reduction in viscosity is obtained.

The vesiculated beads can now be used as paint pigment and will remain stable for the remainder of its shelf life which is in the region of about 6 weeks.

2.5 Vesiculated Beads in the Coatings Industry: Advantages and Disadvantages

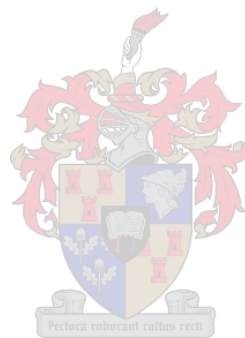
Vesiculated beads are potentially considered to be a practical cost-effective way to at least partially replace very expensive and imported titanium dioxide pigment and extender powders, used in the manufacturing of paint. The process for making these synthetic opacifiers can be adapted, enabling production on existing dispersion vessels found in the paint industry, thus providing a cost-effective method for local acquirement. From a paint production point of view, there is some advantages of using vesiculated beads instead of titanium dioxide exists^[11]. The relatively low viscosity aqueous slurry makes it possible to accurately and effortlessly pump it to the paint finishing tanks. Titanium dioxide and extender powders require manual complexity of handling bulky supply bags. Dust hazards are also associated with handling these fine powders, increasing environmental and health risks.

The paint making process is also simplified by using vesiculated beads, since no high shear grinding and dispersion of pigment powder agglomerates are necessary, before addition to the binder. Preformed beads can be added directly to the binder and blended at low speed.

Development work in this field has also shown that vesiculated beads can enhance the properties of the final coating. These properties include higher opacity, better adhesion and increased exterior durability. Vesiculated beads also possess film-forming abilities. Upon drying, the spherical beads bind together to form a mechanical resistant film. This means that less (expensive) binder is necessary in paint formulations, compared to the case where pigment and extender powder is used.

Currently, the multi-vesiculated beads being developed locally need improvement in certain properties. The beads possess a relatively high affinity for water when present in the dry paint film, which may cause the film to soften and flake. However, this can

be resolved by incorporating a long chain hydrophobic monomer in conjunction with styrene in the formulation resulting in higher water resistance of the beads.



Chapter 3

Set-up, Materials, and Analysis

The first step in investigating the production of vesiculated beads on a Cowles dispersion system was to build a controlled reactor system on laboratory scale geometrically analogous to the industrial size reactors found in paint factories.

3.1 Reactor Set-up

3.1.1 Reactor Design

Prior to the start of this study, vesiculated bead runs were performed in 5ℓ-vessels in the laboratories of a local paint research centre. The vessels were dimensionally analogous to the Cowles reactors found in the factories. Measurements of these vessels were taken in order to design geometrical similar 5ℓ and 20ℓ vessels. The ratio of vessel diameter to vessel height (A/B , Figure 3.1) was found to be 0.72:1. Technical data taken from Cowles dissolvers in one of the paint factories in Mobeni, showed that the impeller should be positioned half the impeller diameter length from the vessel's bottom, i.e. $C = \frac{1}{2} D$ (Figure 3.2). The impeller/vessel diameter (D/A , Figure 3.1) is in the order of 0.55:1. The dimensions of the two vessels appear in Table 3.1.

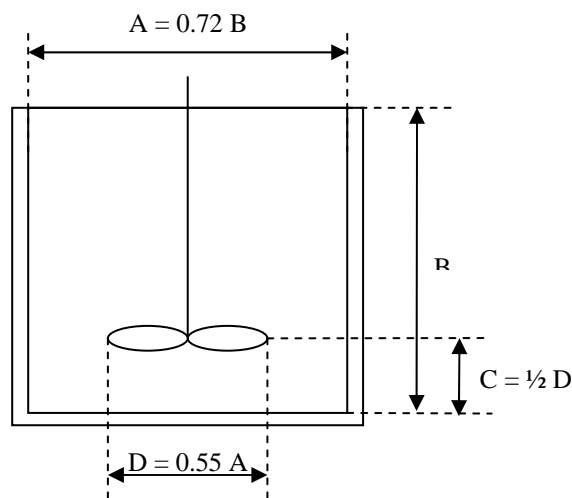


Fig. 3.1 Reactor Vessel Dimension Ratios

Table 3.1 Laboratory Reactor Vessel Dimensions

Dimension	5ℓ Vessel (mm)	20ℓ Vessel (mm)
A	180	285
B	250	400
C	50	80
D	102	153

The reactor system was designed to consist of three identical stainless steel reactor vessels. The primary or main vessel is used for the emulsification stage where the organic phase is added to the aqueous phase. Figure 3.2 shows the design of this vessel.

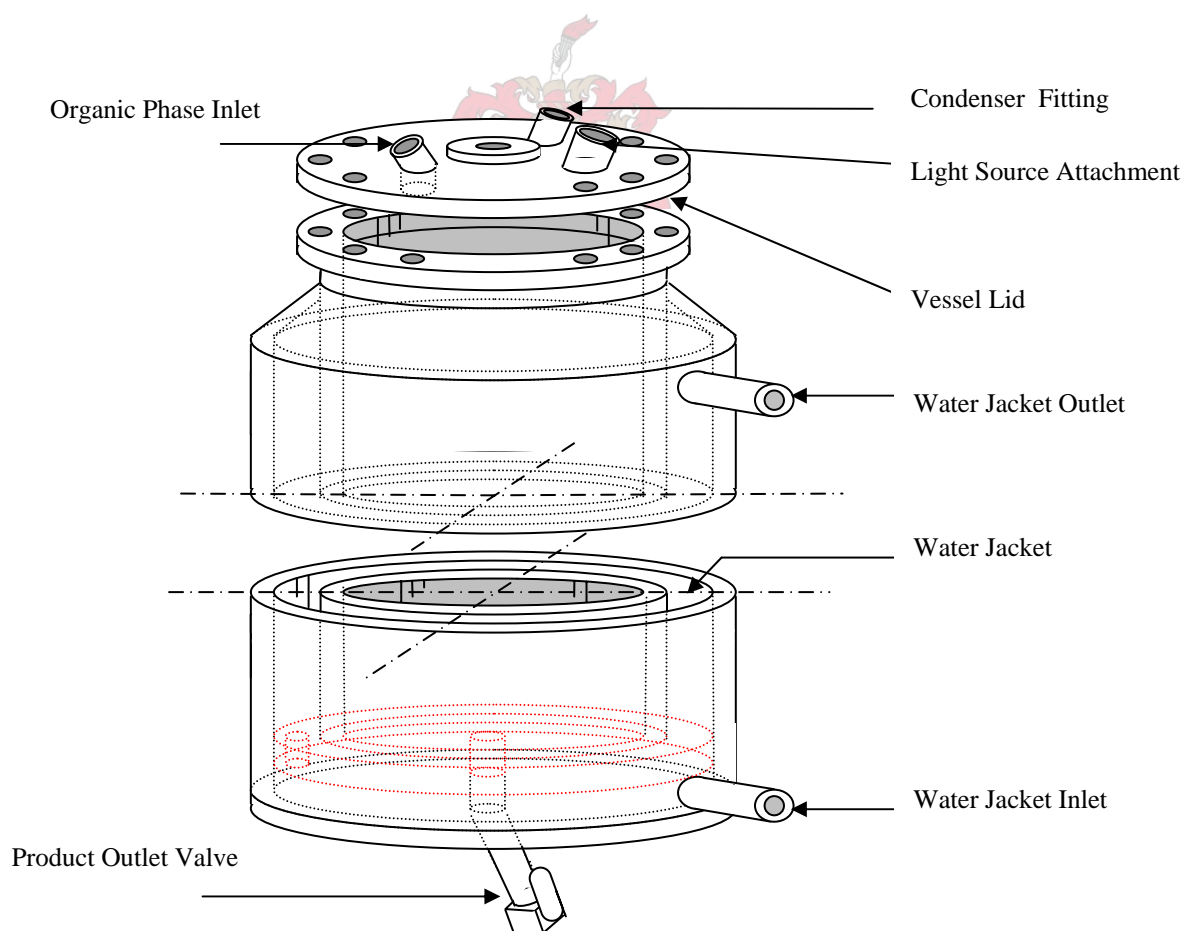


Fig. 3.2 Design of Primary and Secondary Reactor Vessels

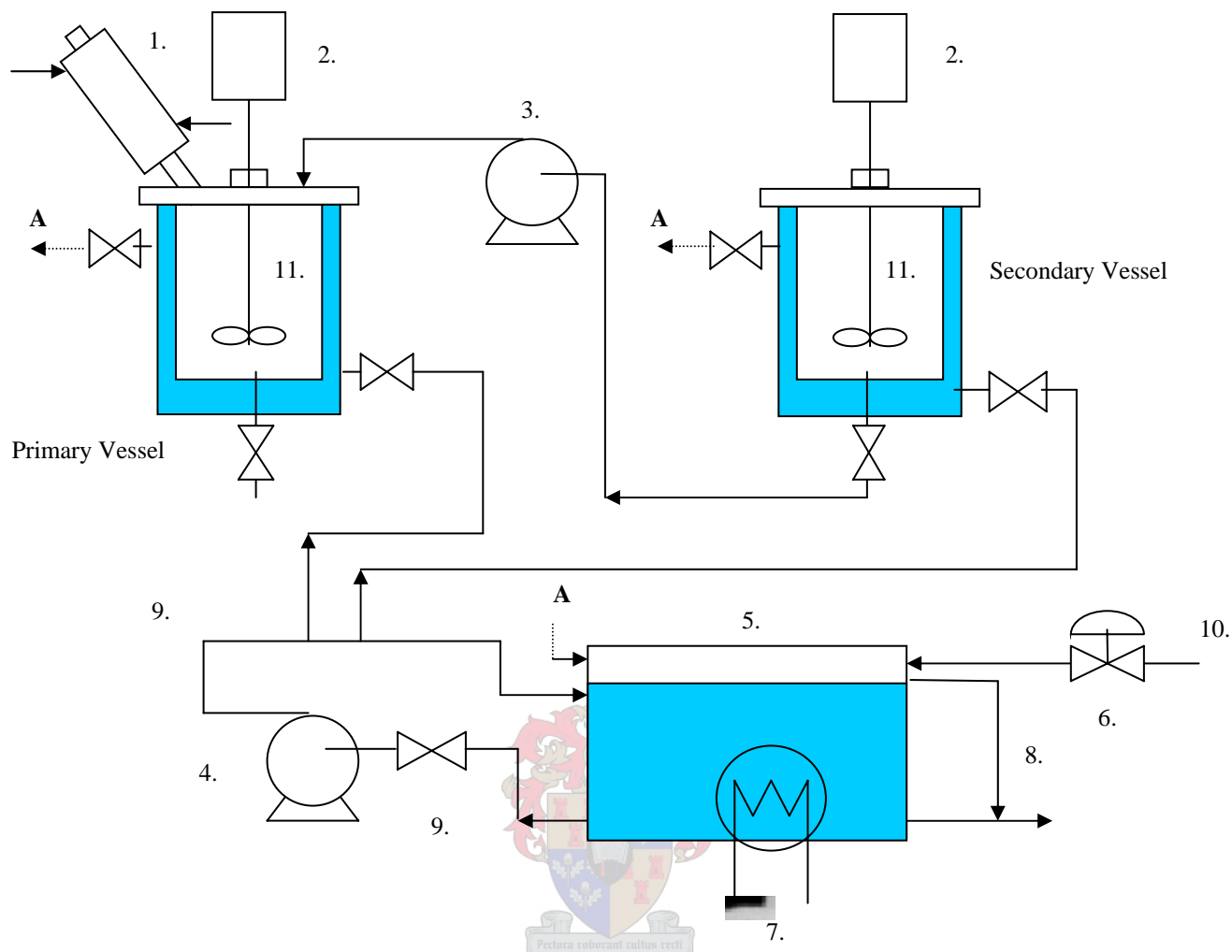
As indicated in Figure 3.2, the primary as well as the secondary reactor vessels is fitted with a water jacket for temperature control purposes. The jackets are also fitted with baffles to ensure more effective water flow through the jacket and hence better heat transfer to the dispersed fluid. These two vessels also contain an opening in the lids to accommodate a light source, ensuring clear visibility of the fluid.

Figure 3.3 shows a diagram of the reactor set-up. A condenser (1, Figure 3.3) is fitted on the primary vessel to prevent evaporation of the monomers in the aqueous vesiculated bead mixture at elevated temperatures. Water is used as cooling medium.

The secondary reactor is used for dispersing the polyester and titanium dioxide slurry before being pumped to the main reactor with a flowrate controlled FMI slurry pump (3, Figure 3.3).

A 100ℓ temperature-controlled waterbath (5, Figure 3.3) is used to prepare the water passing through the reactor jackets. From here, it is pumped by a centrifugal water pump to the primary and secondary reactor vessels. Water not passing through these vessels is circulated back to the waterbath. This also provides sufficient circulating movement in the bath, ensuring effective contact with the 2 kW heating element (7, Figure 3.3). Adjustment of the ball valve situated on the recirculation line (9, Figure 3.3) can be used to vary the flowrate through the jackets. After passing through the jackets, the water is fed back to the waterbath.

Effective temperature control is achieved by means of combined manipulation of the heating element and a fresh water inlet flow (10, Figure 3.3) to the bath. An increase in temperature is accomplished through the element to a desired value after which the element switches off electronically. If the temperature exceeds this level, a solenoid valve (6, Figure 3.3) is opened, letting fresh cooling water into the bath. This interaction keeps temperatures at constant levels. An overflow (8, Figure 3.3) is found on the bath to prevent accumulation of water.



- | | |
|---------------------------|-------------------------|
| 1. Condensor | 7. Heating Element |
| 2. Motors | 8. Waterbath Overflow |
| 3. Slurry Pump | 9. Recirculation Line |
| 4. Centrifugal Water Pump | 10. Cooling Water Inlet |
| 5. Waterbath | 11. Impellers |
| 6. Solenoid Valve | |

Fig. 3.3 Diagram of Reactor Set-up

At the time of the design of the reactor system, a tertiary reactor was also included for the purpose of possible modification of the formulation where titanium dioxide might be dispersed in a separate aqueous phase before being added to the organic polyester phase (double emulsification procedure). In all the reactor vessels, 0.55 kW motors (2, Figure

3.3) are used to propel the mixing impellers (11, Figure 3.3). All three motors are mounted on a stainless steel support framework that can be adjusted to different levels closer or further away from the reactor vessels. The stainless steel shafts of the primary and secondary vessels, connecting the motor to the mixing blade, are broken up into two parts and adjoined with an interlocking “lovejoy” coupling at the top of the reactor lids (Figure 3.4). This coupling can be easily disassembled by removing a screw joining the coupling to the shaft. This allows the reactors to be completely removed from the framework without requiring vertical shifting of either the motor or the vessel. Easy exchange of the 5ℓ and 20ℓ reactors are therefore, possible.

Two bearings are situated in a stainless steel bush on the reactor lid through which the lower shaft passes and this allows free and stable rotation of the shaft. The lower part of the lovejoy coupling also rests on the top bearing rotating without friction while preventing the lower shaft from plunging through the lid.

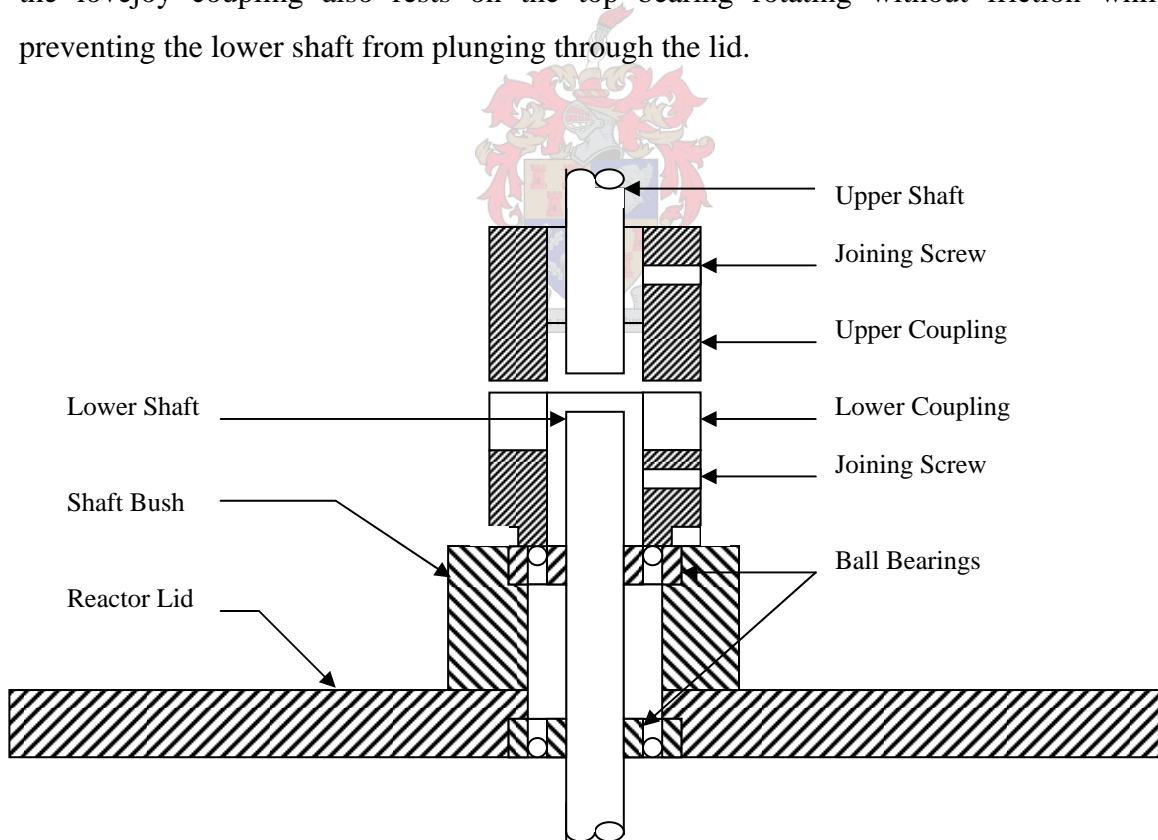


Fig. 3.4 Design of Reactor Lid Including Shaft Bush and Lovejoy Coupling

The Cowles mixing impeller can be easily removed from the lower shaft allowing interchangeability of various size impellers. Five different geometrical similar impeller sizes were used during this study. They were individually 3, 4, 5, 6, and 7 inches in diameter and constructed of 316 stainless steel. The 3 and 4-inch impellers each have 12 teeth, while the 5 and 6-inch blades have 16 teeth and the 7-inch blade 18 teeth. A table of the exact blade sizes in metric units appears in Table 3.2.

Table 3.2 Blade Geometry Values for Blade Impellers used in Cowles Reactors

Impeller Diameter (inches)	Impeller Diameter (mm)*	Teeth Height (mm)	Number of Teeth
3	76	13	12
4	102	13	12
5	127	13	16
6	153	13	16
7	178	13	18

* Measured from one tooth tip across to the other.

The whole set-up including the vessels, framework, waterbath and pipelines were constructed of 316 stainless steel to prevent corrosion or possible chemical deterioration. Where the use of metal piping was intricate, rubber hoses were used. It was, however, important to evade extended use of piping and hoses to avoid excessive heat losses from the waterbath to the jacket. Figure 3.5 shows a picture taken of the reactor system.

3.1.2 Electronic Design

In order to effectively study the process parameters that influence the properties of vesiculated beads, it is vital to accurately measure and control all these parameters during processing. This can effectively be achieved with a well-designed electronic network. Figure 3.6 shows a diagram of the integrated network.



Fig. 3.5 Photograph of the Cowles Set-up in the Laboratory

3.1.2.1 The Interface Board

A PC30G Eagle Technology Analog/Digital interface board installed in an Intel MMX Pentium II processor personal computer with 64 megabyte ram is used to control the network system. The board contains 16 analog inlets and 24 digital input/output lines. The card is supported by DOS and Windows languages. In this case, DOS was used with Turbo Pascal (version 7.0) as programming language. A complete copy of the main program that was used can be found in Section A1, Appendix A.

3.1.2.2 Electric Motors and Speed Controllers

A 240 V AC single-phase power source is connected to 3 Varispeed motor rotation speed controllers – one controller for each motor. The required rotation speed is individually fed to the PC every time the program is initiated and from here transmitted to the controllers through a 0 – 10 V analog output. The controllers subsequently supply the necessary power in 3-phase (0 –240V altogether) output to each motor.

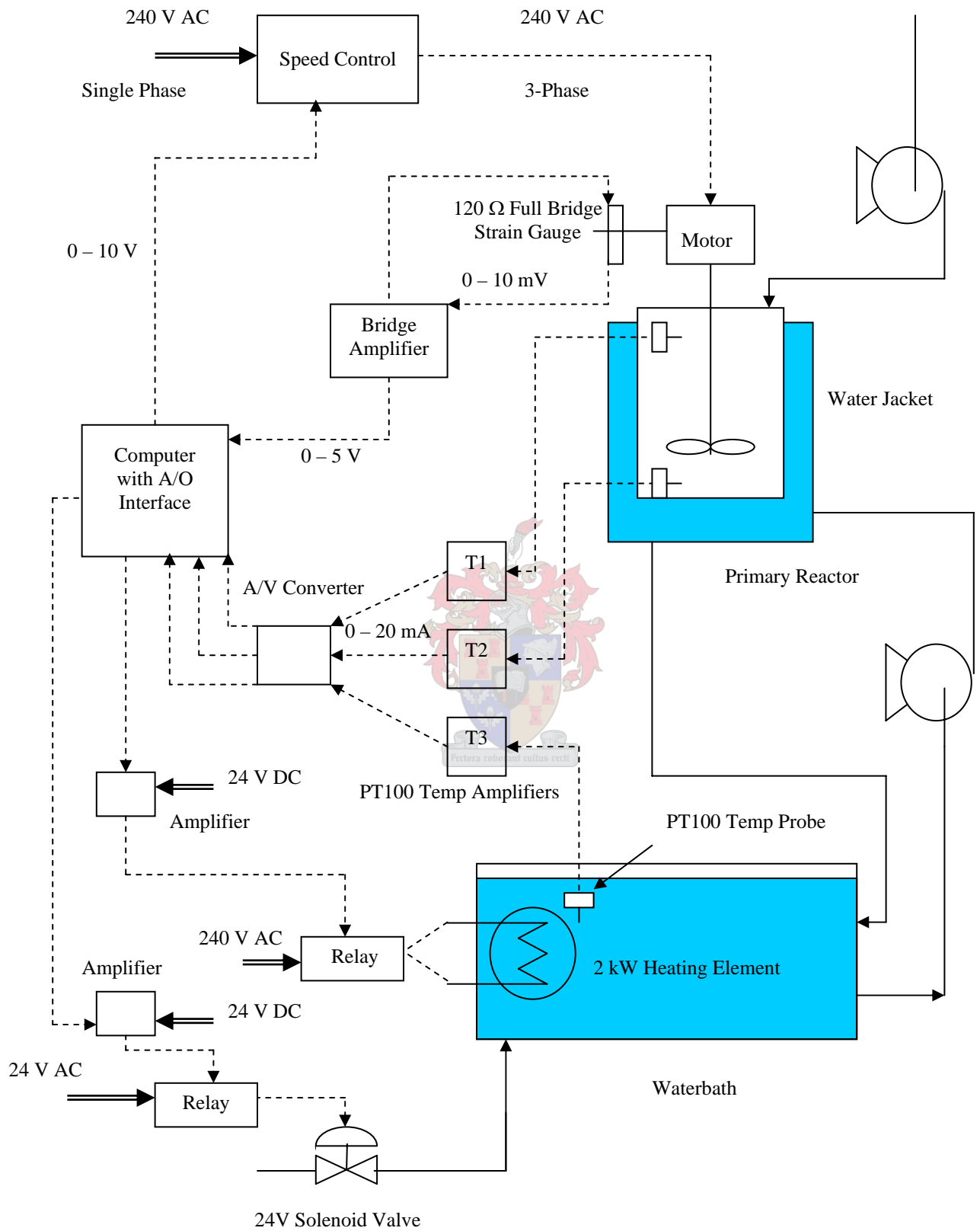


Fig. 3.6 Electronic Layout of Reactor System

The controllers can either be set electronically, as described above, or manually with a speed control knob. The motors can also be stopped manually at any time during operation.

3.1.2.3 Viscosity Measurement

An estimation of the viscosity change of the vesiculated beads can be measured during production with the use of a strain gauge. This is only done in the primary reactor vessel. The motor is mounted on a large bearing, allowing the whole unit to rotate freely on the frame (Figure 3.7).

A small soft stainless steel rod is attached to the motor and supported at the end with an anchor block and two adjustable support pins. Four flexible 120 Ω resistor strain strips are attached onto the neck of the strain rod and electrically connected to each other, as shown in Figure 3.8. When the motor is switched on, the force will be focussed on the end part of the rod where the pins keep it stationary. Strain will be concentrated at the neck of the rod, causing it to deform slightly. Correspondingly, the strips will also deform and as a result cause the resistance to change. A voltage of 5V is placed over two opposing bridge terminals with the help of a bridge amplifier. The voltage measured over the other two terminals will be affected by the change in resistance of the strips and ultimately a weak analog signal is transmitted back to the bridge amplifier where it is amplified to 0 – 5V and sent to the computer. The control card reads these values once every second, and every minute the average voltage over an interval of ten seconds is recorded and saved to a file. This is done to obtain more accurate readings without substantial noise.

The measured voltage can directly be converted to change in torque (N.m) through calibration, which is done by applying a known force at the tip of the soft steel rod, where the support pins are, and recording the measured voltage. By multiplying this force by the distance between the rod tip and the centre of the motor, the corresponding torque can

be calculated. This can be repeated using different known forces to ultimately obtain a calibration curve describing torque as a function of voltage.

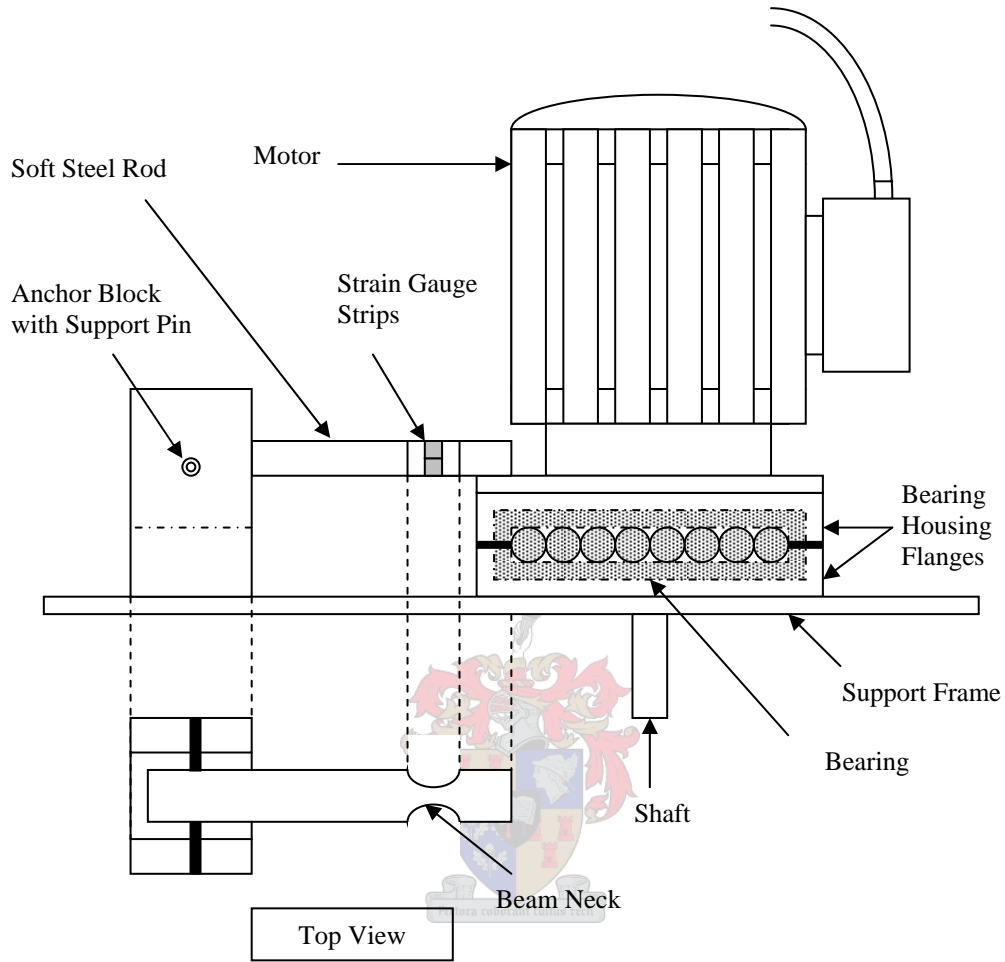


Fig. 3.7 Strain Gauge Design

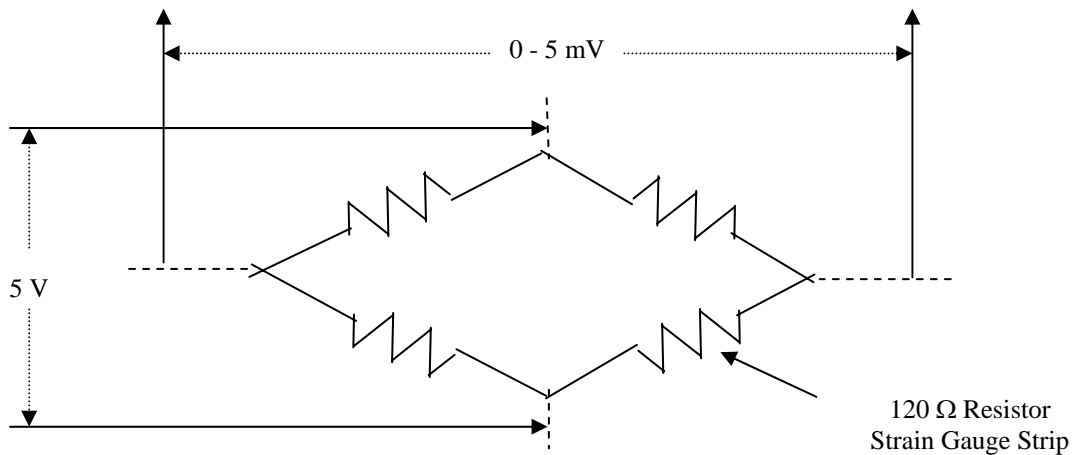


Fig. 3.8 Strain Gauge Network Design

By calculating the gain and offset values of this curve, the input voltage can be directly converted in the computer program to present results as torque measurements. This needs to be converted to viscosity units (mPa.s), which is also done through calibration. The torque is recorded over short time intervals during the emulsification period. At the end of each interval, a sample is extracted and the viscosity immediately measured on a Haake rheometer. Figures A2.1-A2.3, Appendix A, graphically shows the results when the torque is plotted against the measured viscosity for runs where different mixing speeds and impeller diameters were used. It is reasonable to conclude that a very linear relationship exists between the two parameters. By determining the gain as well as the offset values with the help of the graph, the torque can easily be converted to viscosity. As seen from Table A2.1 (Appendix A), each conversion only holds true for consistent process conditions like impeller size and stirring speed. It is also important that the same fluid level in the vessel be maintained, i.e. the impeller must be immersed to the same position on the shaft.

3.1.2.4 Temperature Measurement and Control

Temperature is measured with PT100 temperature probes. There are 3 points where temperature is measured. The first probe measures the temperature of the vapour phase at the top of the primary reactor vessel. The second unit is found at the bottom of the latter vessel and measures the temperature of the liquid phase. This unit is situated below the mixing blade close to the bottom of the vessel where considerable fluid movement is exerted, giving a good indication of the average temperature in the reactor. The last PT100 is placed in the waterbath and is also at a position of good water circulation.

Small metal strips in these probes produce a weak current that gets transmitted to their individual PT100 temperature amplifiers. Here the signal is amplified to values ranging between 0 – 20mA and sent to a current to voltage converter where the current is converted to a 0 – 5V analog voltage signal and transmitted back to the computer.

The voltage signal must now be converted to degrees Celsius. The current output of 0 – 20mV from the temperature amplifiers corresponds to a linear increase in temperature from 0 – 50°C. It is therefore, possible to once again determine the gain value and program the computer to record input values in degrees.

Temperature control is performed by first manually introducing the required reactor temperature to the computer program. The program then compares this value to the temperature measured by the PT100 probe at the base of the reactor. If the value exceeds the probe temperature, heating is necessary. A 5V digital logic signal is sent to an amplifier, which has a 24V DC power supply. Here the signal is amplified to 24V and transmitted to a solid state relay. The relay is connected to a 2kW-heating element situated in the bath and a 240V AC power supply. When the relay receives the signal, the element is switched on and the waterbath heated. When the desired temperature level is reached, the output signal from the computer to the relay is cancelled (0V) and the relay switches the power source to the element off.

If the temperature in the reactor vessel continues to exceed the input temperature by a maximum of 0.5°C, a digital 5V-voltage signal is transmitted to another 24V solid state relay unit. This unit activates a 24V AC power source to a 24V-solenoid valve, which then allows cooling water to be fed to the waterbath. When the temperature falls back within the admissible 0.5°C temperature interval, the output signal is cancelled and the solenoid valve switched off.

Through this continuous reciprocation of heating and cooling, effective temperature control is achieved. As in the case of viscosity measurement, temperature is measured once every second and the average value over 10 seconds saved to file every minute.

3.1.2.5 Pumps

The pump used for transporting the polyester resin from the secondary to the primary vessel consists of a 4-pole high-speed motor pedestal supplying a speed of up to 1725

rpm. This drive can not be controlled by a computer, and is valveless, the latter making it easy for handling slurries, suspensions, emulsions, solvents and viscous concentrates. It is connected to a pump head module possessing a ¼ inch ceramic piston positioned in a 316 stainless steel cylinder with a ceramic liner. The ceramic is inert and corrosion resistant. The pumping action is accomplished through a synchronous rotation and reciprocation action of the piston. By adjusting the pump head position on the motor drives the piston stroke length changes and, in turn the flowrate. Flow is adjustable from 28.8 to 576 ml/min.

The pump used for circulating water through the vessel jackets is a 0.59 kW self-priming centrifugal pump and in operation provides a flowrate of about 37.5 ℓ/min. The pump body and motor support is constructed of cast iron with a technopolymer impeller and diffuser. The 240V single-phase motor provides a synchronous rotating action and is cooled by external ventilation. This pump is exclusively used for pumping solid-free, non-viscous, and chemically neutral fluids.

3.2 Vesiculated Bead Production Procedure

Prior to starting production of a vesiculated bead batch, it is necessary to separately prepare a pre-dispersion consisting of polyester and titanium dioxide pigment powder. The dispersion must be prepared at an elevated mixing speed in the region of 700 – 1,000 rpm over a minimum period of 10 minutes in order to effectively separate and disperse the titanium dioxide powder into the polyester. This pre-dispersion can be kept stable in a closed container and used over a maximum period of two weeks without significant settling occurring. It is for this reason that large 5kg batches of pre-dispersion can be prepared once off and used for more than one vesiculated bead run. It was attempted to use the same pre-dispersion batch in each set of experiments as far as possible. This proved to be advantageous in regard to obtaining good solid content and opacity reproducibility for every set. All the pre-dispersions were prepared using a 5-inch diameter Cowles mixing impeller at a speed of 1,000 rpm in a standard plastic 5ℓ

container and dispersed over a period of 10 minutes. Although never utilised, the tertiary reactor can be used to prepare this phase.

Five-kilogram batches of cellulose thickener solution were prepared separately in the small primary reactor by first charging 97.4 wt% of the vessel with de-ionised water. Under low stirring 2.5 wt% cellulose powder were sprinkled in and dissolved in the water. The mixture was slowly heated to 80°C using the water jacket and held constant for 1 hour. The temperature was gradually brought down and at 35°C or below 0.2 wt% fungicide was added to prevent bacterial degradation of the cellulose chains during shelf life. It was important not to use a high mixing speed to avoid aeration. The colloid stabiliser concentration in the vesiculated bead formulation should, however, be at a concentration of 0.5 wt%. Therefore, it was necessary to dilute it with de-ionised water every time a batch of vesiculated beads was prepared.

A part of the pre-dispersion is weighed off and loaded to the secondary reactor. At this stage, the main control program is initiated, enabling the dispersion procedure to commence in both the primary and secondary reactor vessels. The default mixing speed in both reactors is set at 400 rpm and the temperature maintained at a value of 24°C. The circulation of the water through the jackets is also started by manually switching on the water pump.

Styrene is slowly added to the pre-dispersion and allowed to mix for a minimum period of 2 minutes. Meanwhile, the aqueous phase consisting of the partially hydrolysed polyvinyl acetate and cellulose thickener is loaded to the primary reactor.

Before the 2.5 wt% cellulose thickener and partially hydrolysed polyvinyl acetate is loaded to the primary reactor, de-ionised water, used to dilute the cellulose thickener, is loaded first. This is done to allow water to fill the small section of piping found at the bottom of the reactor leading to the outlet valve. By first loading the thickener and partially hydrolysed polyvinyl acetate into this piece of dead volume, these components will remain undispersed, consequently not participating in the reaction.

The aqueous phase is allowed to mix for at least 2 minutes. When both the organic and aqueous phases are ready, a small amount of polyamine is added to both phases at the same time and allowed to blend in for 5 minutes.

The FMI slurry pump is manually adjusted to the desired flowrate and switched on, allowing the polyester slurry to be pumped to the aqueous phase over a period of 9 – 10 minutes under constant agitation (400 rpm).

After the organic phase is completely added to the primary vessel, mixing is maintained over a timed period of 20 minutes. This period is known as the emulsification stage and during this time the organic dispersion is broken up into small discrete stable globules.

When the emulsification stage is completed, the mixing speed is reduced to 300 rpm. De-ionised water is added and allowed to blend in over a period of 2 minutes. This is done to reduce the total solid content of the final vesiculated bead batch. Meanwhile, an aqueous redox activator solution is prepared and added. After 2 minutes of blending the organic peroxide catalyst is added and mixed for another 2 minutes.

The computer program is terminated, shutting the motors off and the completed batch let down into a 5ℓ plastic container. The batch is sealed and left static for a minimum period of 12 hours (overnight) allowing polymerisation to take place, thereby creating the solid vesiculated granules.

Before the final additions can be made, it is necessary to re-disperse the batch. An adjustable Cowles mixer is lowered into the batch and dispersed at a rotation speed of no more than 500 rpm with a 4-inch diameter impeller. It is important not to exceed this speed to avoid rupturing the beads. Initially the system possesses a very high viscosity, which reduces under continuous agitation (thixotropic behaviour). Therefore, the batch is dispersed for a period of 5 minutes at constant shear rate to ensure complete homogenisation at a low viscosity.

Fungicide is added and mixed for about 2 minutes after which a surfactant is introduced and mixed for another 2 minutes. The vesiculated bead batch is now completed and can be removed from the stirrer. All the batches throughout this study were formulated to have a 24 wt% solid content.

3.3 Analytical Test Methods

Immediately after completion of a vesiculated bead batch, analysis of certain properties can commence. Properties that were investigated include viscosity, pH, solid content, opacity and average particle size.

3.3.1 Viscosity Analysis

Immediately after the vesiculated beads batch is completed and removed from the Cowles mixer, the viscosity is measured using a LV model Brookfield viscometer with a LVT range attachable spindle set.

This viscometer is a rugged, mechanically simple instrument. Its calibration spring is unaffected by long term use or extreme environmental conditions, retaining its calibration indefinitely. Readings from the dial can directly be converted into centipoise (cPs) which is equivalent to mPa.s and is accurate within 1.0% of the range in use.

The viscometer uses rotational viscometry allowing uninterrupted measurements to be made over a long period of time while the spindle is under synchronous rotation. The LV spindle set is suitable for accurately measuring fluids with a relatively low viscosity and is widely used in the paints and coatings industry.

A selection can be made from four cylindrical spindles, each suited for a specific viscosity range. Spindle #1 possesses a large cylinder diameter and is used for measurement of very low viscosity fluids, while cylinder #4 has a very small diameter

and effective for measuring more viscous fluids. The rotation speed of the spindle can also be adjusted from 0.3 – 60 rpm. Selecting the right spindle and rotation speed will ensure maximum sensitivity and accuracy in the viscosity range that is being measured.

In the case of vesiculated beads, the viscosity of the system is quite high, even after removing it from prolonged agitation. It was found that using spindle #3 at a rotation speed of 30 rpm, provides the most accurate readings. The spindle was allowed to rotate for a period of 30 seconds before a reading was taken and the procedure repeated until the results proved to be reproducible.

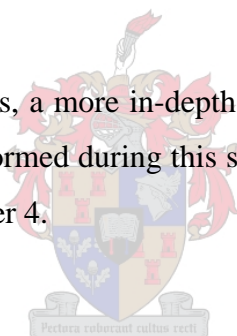
The dial reading is noted and multiplied by a factor, which is unique for every spindle number used at a particular rotation speed. This yields a viscosity value given in centipoise (cP).

Aside from viscosity measurements, a more in-depth study on the rheological behaviour of vesiculated beads was also performed during this study using a Haake Rotoviscometer and this will be discussed in Chapter 4.

3.3.2 pH Analysis

pH measurements are performed with the use of a Metrohm 744 pH meter. A pH glass electrode is inserted into a buffer solution of known pH value and tested for accuracy. If the displayed value does not accurately match the pH of the buffer, calibration is necessary before pH can be measured. This is easily done electronically using two calibration buffer solutions.

The glass probe is rinsed using neutral de-ionised water before being inserted into the vesiculated bead batch along with a Pt100 temperature sensor, which is also connected to the meter. This allows accurate analysis since pH values are temperature dependent. The instrument indicates when the measured pH value has stabilised and is ready to be recorded.



The procedure was repeated to test the reproducibility of the values.

3.3.3 Solid Content Analysis

The solid content of the vesiculated beads is measured using a Metler Toledo HR73 Halogen Moisture Analyser. This unit can be used to determine the moisture content of virtually any substance. The instrument operates on the thermogravimetric principle. At the start of the measurement the Moisture Analyser determines the weight of the sample. The integral halogen dryer unit then quickly heats the sample and the moisture evaporates. During this operation, the instrument continuously determines the weight of the sample and displays the loss of moisture. On completion of drying, the moisture content or dry substance content of the sample is displayed as the final result in weight percentage.

An empty sample pan is placed in the sample pan holder of the unit and the unit closed. The internal balance is set to zero. The unit is opened again and a few drops of the vesiculated bead batch placed on the sample pan and spread out evenly. It is important that the nett weight of the sample not be lower than 1.5 grams. If the amount of sample is too small, the result may not be representative. The sample holder is closed and the halogen dryer activated. A drying temperature of 180°C is used and the unit reaches this temperature within a period of a few seconds. The dry weight of the sample is displayed as a percentage of the wet weight and this value drops continuously as the sample dries. When no more change in weight is measured, indicating that all the moisture has escaped, the instrument automatically switches off and ejects the dry sample.

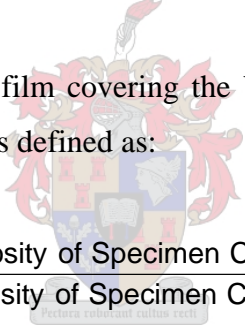
3.3.4 Opacity Analysis

About 15ml sample of a vesiculated beads batch is placed on a Leneta chart, which is widely used in the paint industry to perform opacity measurements. One half of the chart has a white background, while the other half is black. A Sheen metal draw-down bar is then placed next to the sample and a thin 200 micrometer film of the sample drawn over

the chart, covering both backgrounds. This is done with an apparatus that evenly drives the bar horizontally over the chart, providing an even layer. The chart is placed in an oven and left to dry for an hour at 50°C.

Opacity or contrast ratio measurements can now be carried out using a Micropac portable measuring unit, which is used to determine the luminosity of paint. The unit is first placed over the film that covers the white background. This is done at a position containing no imperfections or unevenness on the surface. Light is directed from the unit onto the surface of the specimen at a defined angle of 45°C and the reflected light is measured photoelectrically. The ratio of reflected to directed light, is displayed. Since the luminosity quality does not show constant values over the entire white background surface, measurements are repeated until a constant average luminosity is obtained. The unit automatically calculates this average value.

The procedure is repeated on the film covering the black background and the average luminosity recorded. The opacity is defined as:


$$\text{Opacity} = \frac{\text{Average Luminosity of Specimen Covering the Black Surface}}{\text{Average Luminosity of Specimen Covering the White Surface}}$$

3.3.5 Average Particle Size Analysis

The most effective way of obtaining an estimate of the average particle size is with the use of a Scanning Electron Microscope (SEM). This device presents highly magnified details (10 – 100,000×) of 3 dimensional surface topography. For this reason a flat dry surface of a vesiculated beads film can be used to visualise the microscopic granules.

The SEM operates on the principle of projecting an electron beam, created by a light or electron source, down an enclosed column. These electrons are deflected by scanning coils situated in the column to make a series of closely spaced, parallel, straight-line sweeps across the sample. The electrons penetrate the surface atoms of the sample and

collide with their orbital electrons. These electrons are knocked out from the atom leaving it in an ionised state, surrounding the atoms at the surface with a negative charge. A high concentration of ionised electrons is found on sharp surfaces containing a large surface area, whereas a lower concentration is found on rounded surfaces. These electrons are detected by a positively charged Secondary Electron Detector (SED) and projected to a computer monitor. The light intensity at a point on the computer monitor is directly related to the strength of the electron signal generated from the corresponding point on the sample. Sharp edges will therefore appear brighter than blunt surfaces. In this manner, the image is build up on the screen, point by point, to reflect the changes in topography and composition of the specimen surface.

A 1 cm² sample of the 200-micrometer bead film used for opacity measurements of each batch was taken and put under the electron column. The electron column as well as the sample is placed under vacuum to avoid electron collisions with gaseous atoms or impurities.

Due to the fact that more secondary electrons are scattered to the specimen's surface, where materials with a high atomic weight is used, a thin layer of gold is electrolysed onto the vesiculated bead sample's surface. Gold has a much higher atomic number and therefore, a much clearer view of the surface is obtained. A large area of the sample area is scanned to examine if the particle size range visually appear consistent. When an area is observed where the range is well represented, a picture is first taken at 1,000 times magnification. This was done with all the samples throughout the study for cross-reference purposes. At least one more picture is then taken at a suitable magnification to allow clear observation of at least 100 identifiable particles with a well representative diameter range. An example of a photograph taken by a SEM of a vesiculated beads batch magnified 2,300 times appears in Figure 3.9.

The photograph printed by the SEM can now be scanned onto computer and saved to file. From here the file is loaded onto a software package called Scion Image. This program

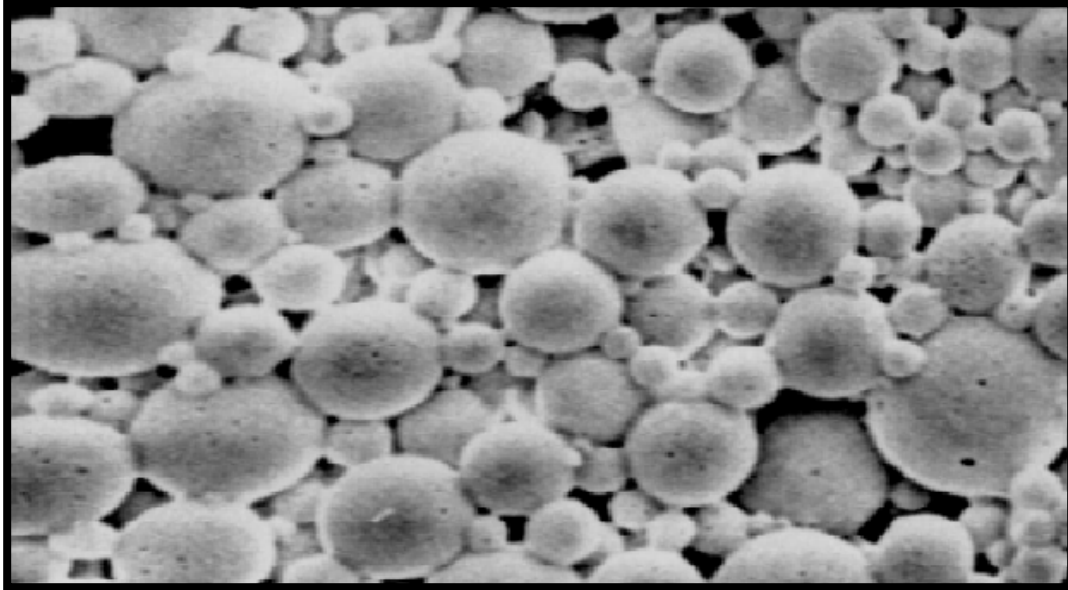


Fig.3.9 Example of a SEM Photograph Taken of the Vesiculated Beads ($\times 2,300$)

allows the user to manually draw diameter lines through each visible particle on the scanned image. The diameters of at least 100 particles are drawn in. This is done to ensure that a reasonably accurate estimate of the average particle size and range is found. Figure 3.10 shows an example of the drafted diameters of 10 particles on a SEM picture. Each diameter is stored separately in the program on a worksheet.

A reference line on the SEM image of known length is used in the program to automatically scale the number of pixels to the distance in micrometer. This line can also be observed at the bottom of Figure 3.10. The distance of the reference line in this case is 5.88 micrometer.

The program contains an option to copy the diameter measurements to other Windows based statistical software worksheets in order to process the measured data further. The calculations that were performed using this data include establishment of the mean arithmetic particle size based on diameter as well as the volume mean diameter particle size.

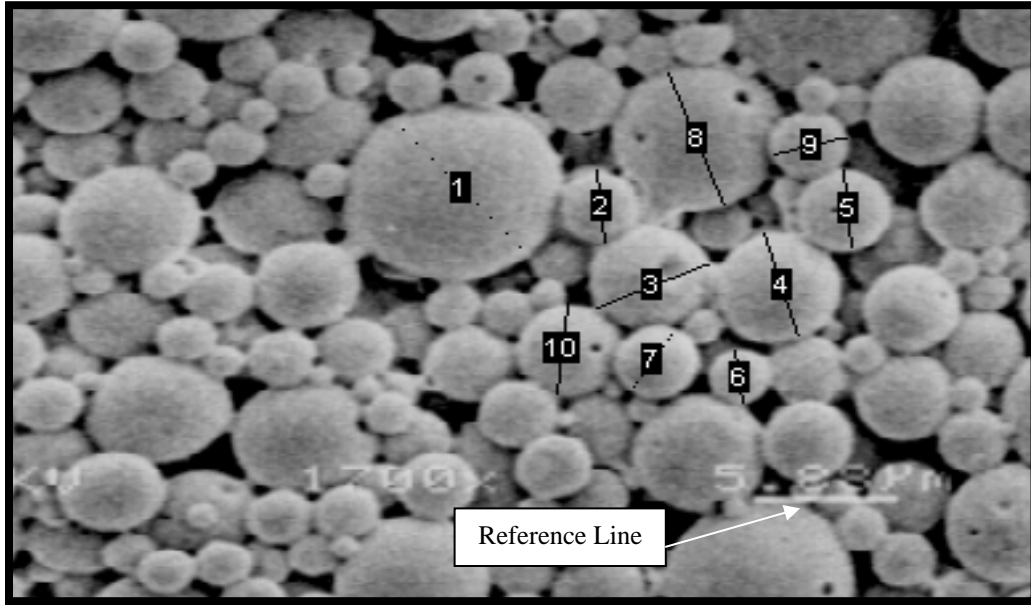


Fig. 3.10 Scion Image Analyses of Particle Size

In this study, the average diameter particle size will predominantly be used for calculations, but for supplementary purposes, it will be investigated how these values compare to the average particle size based on the particle volume. Furthermore the distribution of particle size diameters and the skewness will also be calculated. The particle distribution is a measure of how widely particle size values are distributed around the average value. Skewness characterises the degree of asymmetry of a distribution around its mean. Positive skewness indicates a distribution with an asymmetric tail extending toward more positive values (i.e. values greater than the mean). This means that the distribution of values (or particle sizes) larger than the mean is wider than the distribution of values smaller than the mean. Negative skewness indicates a distribution with an asymmetric tail extending toward more negative values (i.e. values lower than the mean), denoting that the distribution of values (or particle sizes) smaller than the mean is wider than the distribution of values larger than the mean.

The equations used to calculate the number average particle size (α_n), volume average particle size (α_v), particle size distribution (PSD), and skewness (SKEW) are given in Equations 3.1 to 3.4 below.

$$\alpha_n = \frac{\sum_{i=1}^n y_i}{n_y} \quad (\mu\text{m}) \quad \dots(3.1)$$

$$\alpha_v = \sqrt[3]{\frac{\sum_{i=1}^n y_i^3}{n_y}} \quad (\mu\text{m}) \quad \dots(3.2)$$

$$PSD = \sqrt{\frac{\sum_{i=1}^n (y_i - \alpha_n)^2}{(n_y - 1)}} \quad \dots(3.3)$$

$$SKEW = \frac{n_y}{(n_y - 1)(n_y - 2)} \sum_{i=1}^n \left(\frac{y_i - \alpha_n}{PSD} \right)^3 \quad \dots(3.4)$$



where:

- i = point number in diameter series
- n = number of points in data series
- y_i = diameter value at the ith point
- n_y = total number of data values in data series

Note that SKEW > 1 indicates negative skewness and SKEW < 1 denotes positive skewness.

Histograms were also constructed by calculating individual and cumulative frequencies for a cell range of data and data bins. Data was generated for the number of occurrences of a value in a data set, which can be portrayed graphically.

A study was conducted to examine the reproducibility of the technique with which the average particle size is determined, as discussed above. Firstly, three different samples (A, B and C) at different positions on the same draw-down chart of a vesiculated bead batch was viewed under the scanned electron microscope and pictures taken of each one at the same magnification ($\times 2,500$). Furthermore, the reproducibility of the particle size analysis was investigated by repeating diameter measurements on the same SEM picture of sample C three times (C1, C2 and C3). The calculated average particle size based on diameter and volume as well as the particle size distribution and skewness values appears in Table 3.3.

Table 3.3 Reproducibility of Vesiculated Bead Particle Size Analysis

	α_n (μm)	α_v (μm)	α_v / α_n	PSD	SKEW
Sample A	4.14	4.63	1.11	1.53	0.52
Sample B	3.97	4.47	1.13	1.48	0.87
Sample C	3.72	4.19	1.13	1.48	1.06
Sample C1	3.67	4.04	1.10	1.38	0.95
Sample C2	3.81	4.27	1.12	1.47	1.01
Sample C3	3.90	4.36	1.12	1.53	0.83

It is observed that the number average particle diameters (α_n) show a reasonably small variation in both reproducibility studies, with values ranging from 3.67 to 4.14 μm . It can be concluded that, although the method of calculation is somewhat robust, the technique still provides reasonably reproducible estimations of the average particle sizes. There is also very little variation in the particle size distribution. In each case a reasonably wide range of particle sizes are observed ranging from as little as 1.3 μm to as large as 9.5 μm .

Apart from Sample A, the values describing the skewness of distribution are close to unity suggesting an almost symmetrical particle diameter distribution around the average values.

By comparing the volume and number average particle sizes, it is observed that the volume average sizes are consistently about 1.12 times larger than the number average values, ranging from 4.04 to 4.63. This indicates that both calculation methods of the average particle size can be used to give a representation of the change in particle.

3.3.6 Degree of Vesiculation

Degree of vesiculation is a term used that describes the average volume of vesicles inside a bead and mathematically defined as

$$\text{Degree of Vesiculation} = \frac{\text{Total Volume of Vesicles in Bead}}{\text{Total Volume of Bead}} \quad \dots(3.5)$$

Theoretically, the degree of vesiculation may be related to the luminosity and possibly also the opacity of the vesiculated beads. A higher degree of vesiculation possibly suggests that the vesicle volume in a bead is higher in relation to the total bead volume and this may in return suggest that there are a larger number of vesicles present. This may consequently cause an increase in the effective scattering efficiency of incident light, making the bead appear whiter. However, a relatively small number of very large vesicles can also correspond to a high degree of vesiculation, but cause a reduction in the light scattering efficiency. This will allow beads to appear less white, resulting in a low opacity. For this reason it might also be important to accompany degree of vesiculation values with parameters like the number of vesicles, wall thickness between vesicles and average vesicle size, as it will be seen later on in this discussion.

3.3.6.1 Method of Average Granule Density

To date, the techniques used by paint companies within the Nova club to calculate the degree of vesiculation have proven to be quite tedious and time consuming with questionable accuracy. One technique that has been attempted locally involves

determination of the average density of the vesiculated granules^[12]. A wet bead sample is placed in a fast rotating centrifuge (Figure 3.11). The accelerated rotation of this apparatus causes the vesiculated beads to settle at the bottom of the centrifuge container, allowing the remaining aqueous solution to be drained off at the top. This procedure is continued by successively adding de-ionised water to the suspension to gradually dilute and remove all traces of water-soluble constituents, consisting mainly of colloid stabilisers.

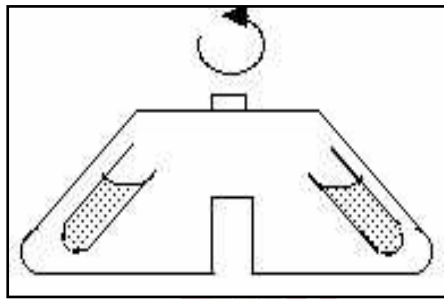


Fig. 3.11 Fast-rotating Centrifuge

The wet granules, now containing almost no impurities effecting granule density, are placed in an oven to dry overnight. The dry powdery granules are suspended in a resin of known density and the new suspension density is measured. The difference in these values presents the dry vesiculated bead density (ρ_b).

The solid bead density (without vesicles), ρ_r , can be obtained by direct catalysis of the polyester resin normally added to the aqueous phase during production. The resulting polymeric mass can be crushed and a weighed sample added to a density bottle to measure fluid displacement. Thus, using the sample weight and displacement volume, the solid bead density can be calculated.

Since the dry vesicles are hollow, the vesicle density, ρ_a , is the same as air. A mass balance can now be performed to calculate the volume fraction of vesicles (see Equation 3.6).

$$\phi_a \rho_a + \phi_r \rho_r = \rho_b \quad \dots(3.6)$$

where:

- ϕ = volume fraction (m^3/m^3)
- ρ = density (kg/m^3)
- a = dry vesicle
- r = solid granule (excluding vesicles)
- b = dry vesiculated bead

With $\phi_r = (1 - \phi_a)$, Equation 3.6 can be simplified to Equation 3.7.

$$\phi_a = \frac{\rho_r - \rho_b}{\rho_r - \rho_a} \quad \dots(3.7)$$

The volume fraction of the vesicles, ϕ_a , obtained from Equation 3.7, is analogous to the degree of vesiculation.



3.3.6.2 Microtoming

Another method used for determining the degree of vesiculation is microtoming. The dry vesiculated granule powder is prepared as above and placed in a casting resin. The resin is solidified through catalysis and a thin layer sliced off using a sharp diamond microtome. These slices are viewed under a scanning electron microscope to locate any possible carved cross-sections of the beads. By determining the average vesicle area per particle cross-section, an approximation of the total vesicle volume in a granule can be obtained as a function of particle size, assuming the average wall thickness remains the same for a single vesiculated bead batch of varying particle sizes. This technique for determining the degree of vesiculation is based on two-dimensional (area) measurement approximations and is not only tedious, but may not be completely accurate, since only a small bead area can be used for analysis. Microtoming does, however, provide a visual sense of the average vesicle size, wall thickness and number of vesicles.

This method can be illustrated by using, as an example, the SEM photographs taken of 3 different microtomed bead samples ^[13]. These samples differ in chemical composition and were prepared in different processing vessels as follows:

Sample A: Standard formulation⁼ used to prepare beads in the emulsion reactor vessel.

Sample B: Standard formulation with 0.5 wt% (by total batch weight) additional surfactant added to the pre-dispersion and prepared in the Cowles vessel.

Sample C: Standard formulation with 0.25 wt% (by total batch weight) additional surfactant added to the pre-dispersion and prepared in the emulsion reactor vessel.

The effect of the additional surfactant used in Samples B and C will be discussed in more detail in Section 6.3, Chapter 6. Examples of the microtomed SEM photographs of these three samples appear in Figures 3.12 to 3.14 below.

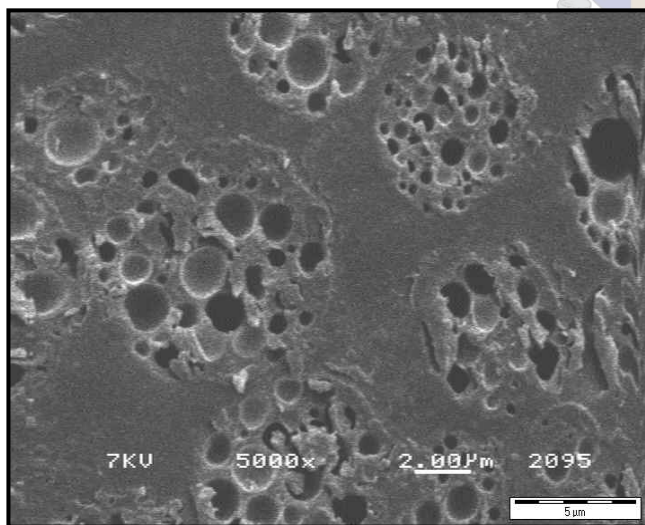


Figure 3.12 Microtomed SEM Photograph of Sample A

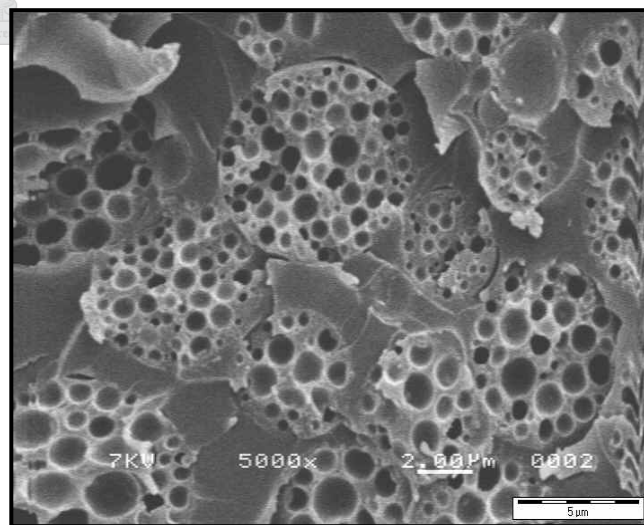


Figure 3.13 Microtomed SEM Photograph of Sample B

⁼ Refer to Section 2.4.3, Chapter 2 for the standard vesiculated bead formulation. The total solid content remained at 24 wt% and Cray Valley polyester batch DV5008 was used.

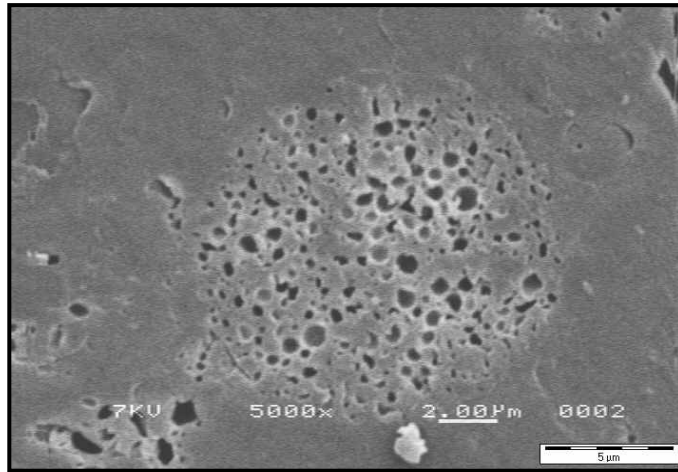


Figure 3.14 Microtomed SEM Photograph of Sample C

By using the Scion Image Analysis software package, the particle diameters of at least 10 individual bead particles per sample were counted and used to determine the bead surface area as well as the total area occupied by vesicles in each particle. The degree of vesiculation (ϕ), based on area, for each particle was then calculated using Equation 3.8 and the results for each particle appear in Table 3.4.

$$(\phi_a)_{\text{area}} = \frac{\text{Area Occupied by Vesicles in Bead Cross - Section}}{\text{Cross - Sectional Area of Bead}} \dots(3.8)$$

Table 3.4 Average Degree of Vesiculation Based on Area for Samples A to C

Particle	Sample A	Sample B	Sample C
1	0.177	0.416	0.085
2	0.188	0.312	0.195
3	0.187	0.414	0.117
4	0.130	0.301	0.186
5	0.144	0.445	0.176
6	0.161	0.347	0.133
7	0.145	0.236	0.126
8	0.169	0.437	0.096
9	0.278	0.324	0.163
10	0.199	0.326	0.132

Average:	0.177	0.362	0.141
-----------------	--------------	--------------	--------------

Table 3.5 contains the degree of vesiculation based on area calculated for each particle as well as each sample's individual average particle size (α_n), viscosity and opacity values.

Table 3.5 Property Analysis Results of Samples A - C

	α_n [μm]	Viscosity [cPs]	Opacity [wt%/wt%]	Average (ϕ_a) _{area}
Sample A	7.40	1600	0.92	0.177
Sample B	1.87	3800	0.91	0.362
Sample C	7.23	1080	0.96	0.141

The results indicate that a higher degree of vesiculation does not necessarily correspond to a higher opacity. On the contrary, it appears that Sample C, which has the lowest degree of vesiculation, also has the highest opacity.

The SEM photograph of Sample C (Figure 3.14) shows a large number of very small vesicles in the bead, possibly causing greater scattering efficiency of light and thus higher opacity. The degree of vesiculation of Sample A (Figure 3.12) does not significantly differ from Sample C, but the opacity is much lower. By comparing Figures 3.12 and 3.14, it is observed that Sample A has fewer vesicles with much larger diameters, possibly causing poorer light-scattering and being the reason for the lower opacity. Sample B has a large number of vesicles with large diameters (Figure 3.13) and even though the degree of vesiculation might be the highest for this sample, the scattering efficiency is the poorest.

It can, therefore, be concluded that opacity should not be a measure of degree of vesiculation, but of the factors that effect the light scattering efficiency, such as the size and number of the vesicles in the beads.

Notice from the viscosity data in Table 3.4 that Sample B, possessing the highest degree of vesiculation, also has the highest viscosity and Sample C, which has the lowest degree

of vesiculation, possesses the lowest viscosity. A reason for this phenomenon will be discussed further in Chapter 5.

3.3.6.3 Analytical Ultracentrifuge

Currently, an investigation is being conducted into using a multi-purpose apparatus called an analytical ultracentrifuge (AUC) to calculate the degree of vesiculation. An AUC is not locally available, but various vesiculated bead samples have been sent to a company in Germany. The selected samples possess different opacity values to study the influence of degree of vesiculation on opacity. The analysis has not been completed and results are being awaited. However, the proposed technique of calculating the degree of vesiculation with this apparatus will be discussed further.

The main characteristic feature of the ultracentrifuge is that it can be used to fractionate particle size, molecular weight and densities of macromolecules or microparticles^[14]. Fractionation means that, not only is it possible to measure average property values, but also complete distributions of particle size, molecular weight and density.

The AUC comprises an electric rotor hanging on a axle in a high vacuum chamber bearing eight sample cells and an analytical optical light path, consisting of a controllable stroboscopic lamp, i.e. modulable laser, vacuum-tight lenses and a digital TV camera, i.e. a photomultiplier, all set up for so-called schlieren optics. The rotation speed of the rotor can be increased in a continuous exponential manner from zero to a maximum of about

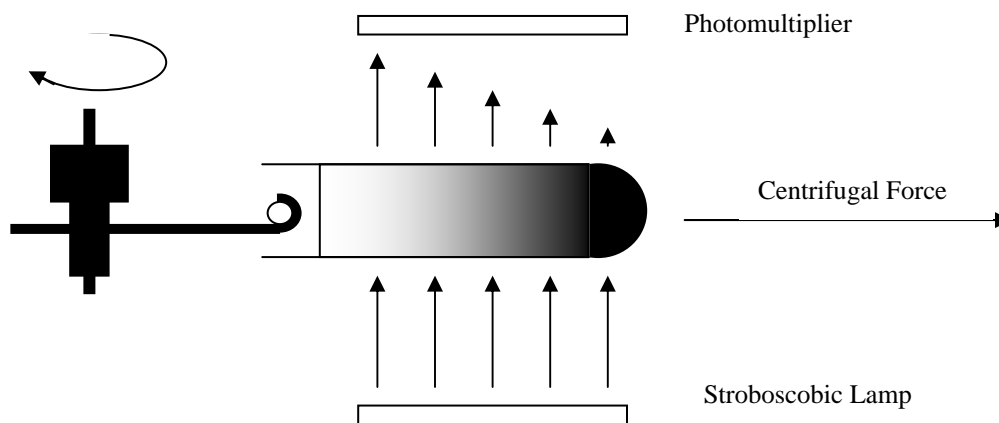


Fig. 3.15 Analytical Ultracentrifugation

60,000 rpm. The sample cells are positioned in the path of the laser and the photomultiplier records the difference in refractive indices (Figure 3.15).

The main objective is to detect the vesiculated particle density. A pure sample of vesiculated beads exposed to extensive centrifugation will cause “pelleting” at the bottom of the sample container, due to gravitational instability. In order to prevent this, a density gradient need to be created. This is also known as zonal centrifugation.

A solution of a water-soluble iodinated sugar or sucrose of very high density, for example metrizamide ($\rho = 2,100 \text{ kg/m}^3$) is added to water at a pre-determined concentration. The sample is left for about 16 hours (overnight) under constant centrifugation. During this time the heavy sugar molecules will be enriched near the cell bottom, causing a radial density gradient across the cell (Figure 3.16). The procedure is repeated, but small concentrations water-insoluble microparticles with known densities are respectively added to the same solution. During the centrifugal period when the density gradient develops, the microparticles sediment and float simultaneously to the position where the gradient density and particle density are identical.

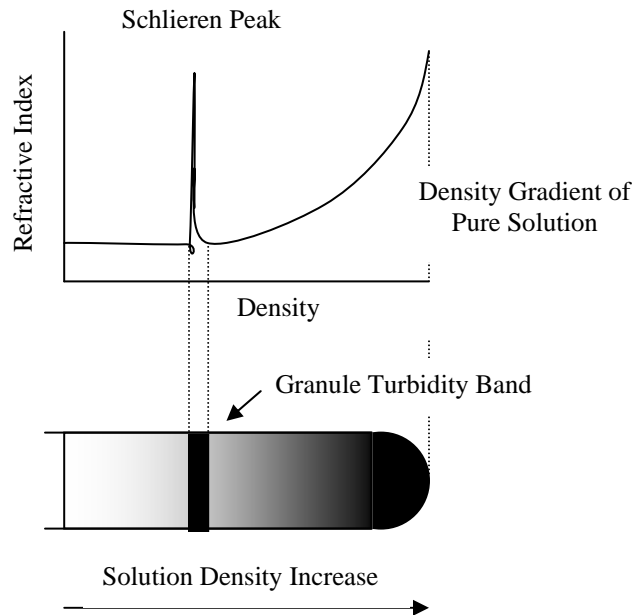


Fig. 3.16 Zonal Centrifugation Technique

There they gather in a very narrow turbidity band, which is detected by the photomultiplier and recorded in the form of a sharp peak, known as the schlieren peak. The position of this peak corresponds to the known density of the particular microparticles used. By using this procedure it is ultimately possible to calculate the density gradient across the solution.

A dispersion of dry vesiculated beads in solution can now be made and centrifuged under the same operating conditions as above to calculate the vesiculated bead density (ρ_b) and density distribution.

It is now possible to use a similar model to Equation 3.7 to calculate the degree of vesiculation. It is important that the selected sucrose molecules do not diffuse into the vesicles with the water molecules, since this may increase the effective granule density and cause the final value to be theoretically equivalent to the solid granule density (ρ_r).

The advantage of using this analytical technique is that particle density can be measured within an error limit of approximately 0.1% and since it is possible to obtain the density distribution, a degree of vesiculation distribution of a batch can ultimately also be obtained.

By using the experimental set-up, vesiculated beads production procedure and analytical test methods to measure properties, discussed in this chapter, experimentation can commence, first looking at the transient properties during production.

Chapter 4

Transient Properties during Production of Vesiculated Beads

This chapter involves a discussion of the development of various properties that occur during the production period and the procedure followed to record this development. Properties that will be focussed on include average particle size (APS), viscosity, temperature and particle formation.

4.1 Average Particle Size Development During Emulsification

As soon as the polyester/titanium dioxide phase is introduced to the aqueous phase, organic droplets immediately start to form. The period after addition of the organic phase, called the emulsification period, is the time allowed for the droplets to complete the break-up process to ultimately form globules approximating uniform particle diameter and a distribution range that is as narrow as possible. In other words, further dispersion under the same conditions will not cause a significant decrease in the average particle size. An investigation was performed where the rate of particle size change was recorded over the emulsification period.

These experiments were conducted by extracting small 100ml samples from each batch over short intervals at 1, 2, 3.5, 5, 7.5, 10, 15, and 20 minutes after the emulsification period started. These samples were immediately post-treated with doses of water and catalyst, proportional to the formulation, to initialise polymerisation. Each sample was prepared for average particle size analysis using the procedure described in Section 3.3.5.

Figure 4.1 indicates the change in the number average particle size of two batches that were prepared in the 5ℓ and 20ℓ reactors, respectively. A table of these results appears in Table 4.1 below. In both batches, the production procedure described in Section 3.2 were

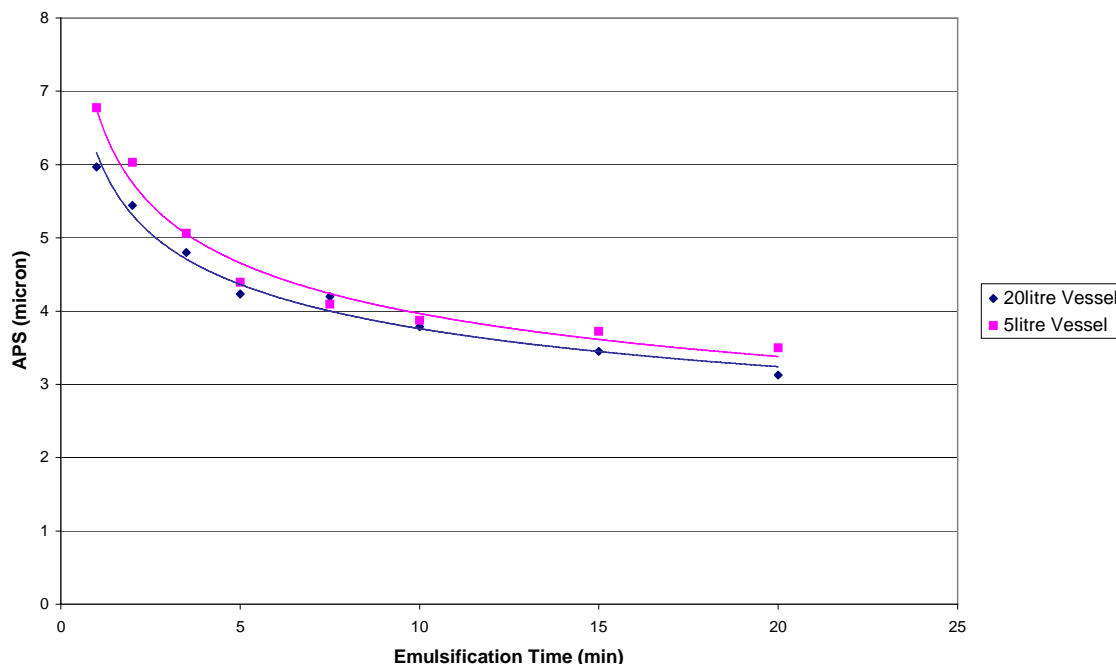


Fig. 4.1 Number Average Particle Size Development During the Emulsification Period of Geometrically Similar Reactors (Mixing Speed = 400rpm, 4" Impeller in 5ℓ Vessel, 6" Impeller in 20ℓ Vessel)

used in the geometrically analogous 5ℓ and 20ℓ reactors. For further geometric similarity it was also required that the 4 inch diameter impeller be used in the 5ℓ reactor whilst the 6 inch impeller was used in the 20ℓ vessel. The rotation speed used was, however, not geometrically similar in the two cases since it was uncertain at the time what the effect of various mixing speeds is on the system. Therefore, it was decided to use a production mixing speed of 400 rpm in both reactors during addition of the organic phase to the aqueous phase and during emulsification. The effect of stirring speed variation will be investigated later in this chapter.

In both runs, it can be clearly observed that a logarithmic trend is followed where the rate of reduction in particle size is high over the first 5 minutes of the emulsification period, subsequently approaching a constant value towards 20 minutes. Extended prolongation of the emulsion period will, therefore, not have a significant influence on the average particle size. This explains the need for an emulsification period of at least 20 minutes.

It is observed that both the average particle size and particle size development over time compare very well with each other. It does appear that the values from the experiment performed in the smaller 5ℓ vessel are somewhat larger. This can be attributed to the difference in tip speed in the two cases. Even though the mixing speed was the same in both cases, the tip speed in the 20ℓ vessel was higher due to the larger diameter impeller used. This caused a higher shear exerted on the fluid resulting in more effective break-up of the oil globules to smaller sizes.

The investigation was continued by varying the size of the mixing impeller and keeping the production mixing speed constant at 400 rpm. This was done on the larger 20ℓ vessel, since it is possible to extract larger samples from the batch without significantly effecting change in batch volume as in the case of the 5ℓ reactor. This ultimately excludes the risk of causing mixing pattern irregularity as the fluid height reduces in the reactor vessel, possibly influencing the average particle size development. Table 4.1 contains the number average particle size (α_n) results and Figure 4.3 graphically shows the reduction during the emulsification period using impeller sizes of 4, 5, 6, and 7 inch diameters, respectively.

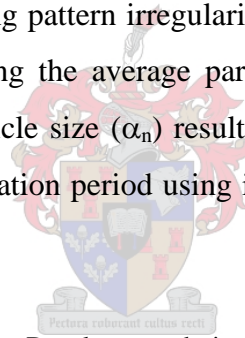


Table 4.1 Number Average Particle Size Development during Emulsification Using Different Impeller Diameters (Mixing Speed = 400 rpm)

Emulsification Time (min)	5ℓ Vessel	20ℓ Vessel			
	α_n (μm) 4" Blade	α_n (μm) 4" Blade	α_n (μm) 5" Blade	α_n (μm) 6" Blade	α_n (μm) 7" Blade
1	6.78	8.81	5.69	5.97	4.35
2	6.03	7.81	4.46	5.44	4.11
3.5	5.06	6.29	3.90	4.80	3.70
5	4.39	5.64	3.73	4.23	3.50
7.5	4.10	5.39	3.28	4.20	3.33
10	3.87	5.07	3.34	3.78	3.21
15	3.72	4.81	3.26	3.45	2.72
20	3.50	4.41	3.17	3.13	2.55

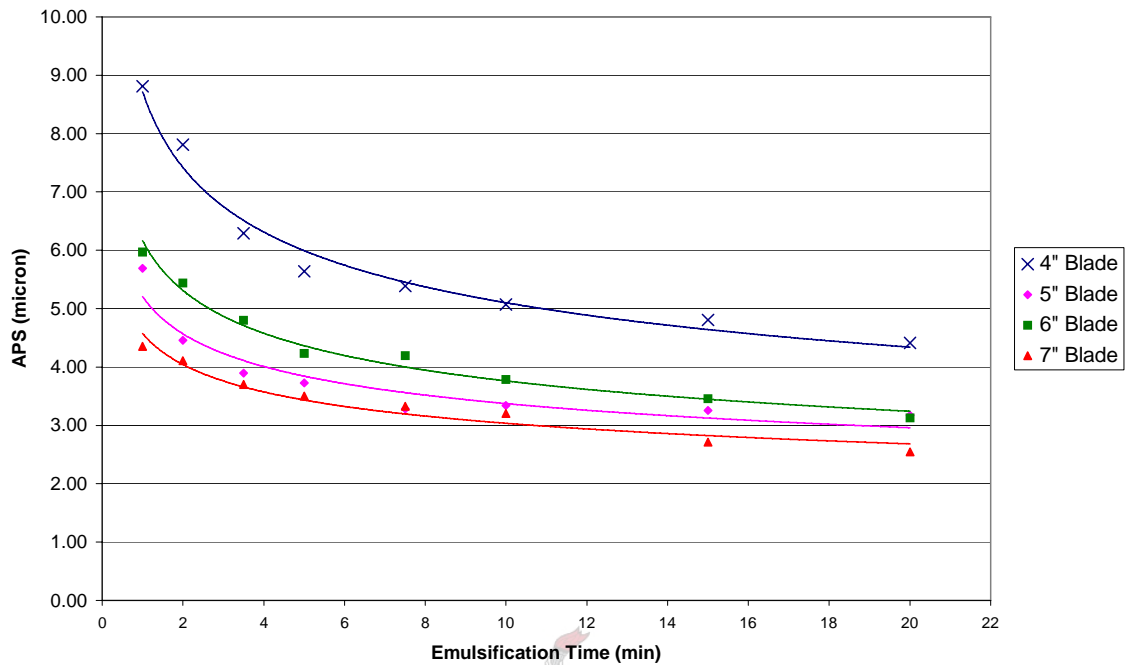


Fig. 4.2 Number Average Particle Size Development During Emulsification Using Various Diameter Impellers in the 20ℓ Vessel (Mixing Speed = 400rpm)

A similar logarithmic trend is observed as in Figure 4.1. Increasing the impeller to vessel diameter the impeller tip speed is increased causing a higher shear rate exerted on the fluid. From this it can be concluded that an increase in impeller diameter at similar process conditions results in a smaller average particle size at corresponding emulsification periods and the break-up to smaller droplets occurs with an increased rate. Hence, if a smaller final average particle size is required, it may be possible to obtain this over a shorter emulsification period if a larger impeller to vessel diameter reactor system is utilised.

It is interesting to observe that almost the exact trend is observed if we plot the particle size distribution curves of each sample presented in Figure 4.2. Table 4.2 contains the distribution range values and Figure 4.3 graphically shows the results obtained. Note that a large distribution value denotes a wide particle size distribution.

Table 4.2 Particle Size Distribution during Emulsification at Various Impeller Diameters
(Mixing Speed = 400 rpm)

Emulsification Time (min)	20ℓ Vessel			
	4" Blade	5" Blade	6" Blade	7" Blade
1	4.82	2.88	3.50	1.96
2	3.57	2.51	2.38	1.75
3.5	2.80	1.88	2.10	1.47
5	2.67	1.74	1.92	1.46
7.5	2.23	1.37	1.71	1.30
10	1.97	1.39	1.46	1.20
15	1.89	1.26	1.59	1.25
20	1.80	1.46	1.52	1.00

The reason for this becomes apparent when we compare the histograms of the samples showing the frequency of different particle sizes over their distribution range. Section B1, Appendix B shows an example of a set of histograms generated from the results taken from the experiment where the 4-inch impeller blade was used in the 20ℓ reactor.

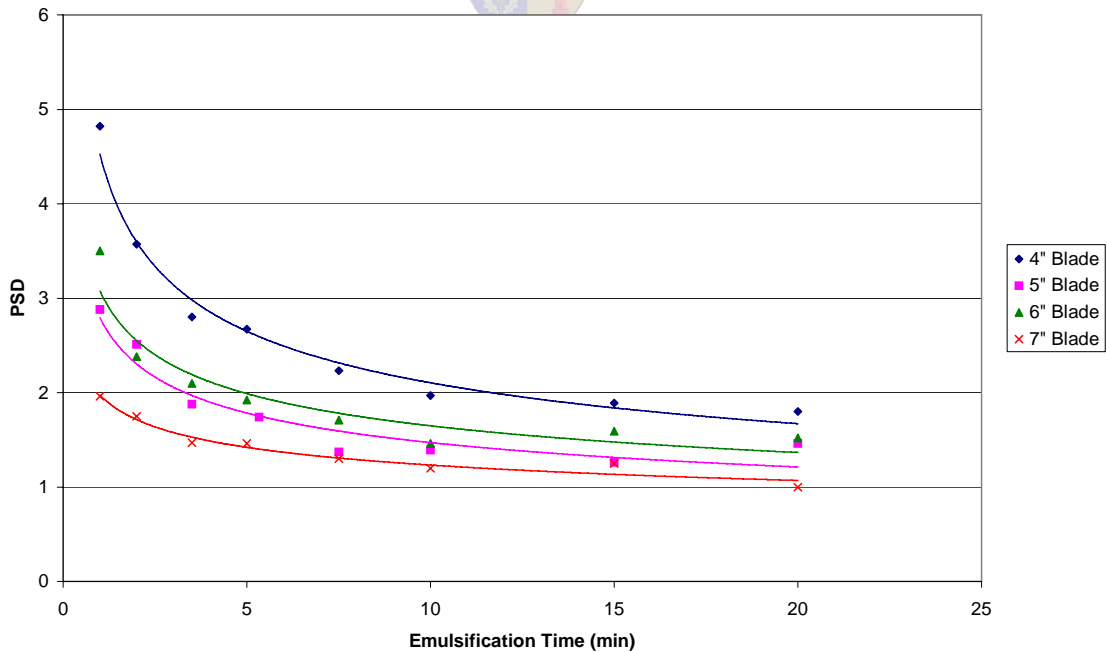


Fig.4.3 Particle Size Distribution During Emulsification Using Various Diameter Blades in the 20ℓ Vessel (Mixing Speed = 400rpm)

The histogram corresponding to the sample extracted at the shortest emulsification period (1 minute) shows a very wide particle size distribution range with a very even frequency of observations over the range. As the emulsification period increases, the distribution range gets narrower with an increase in the number of particles (frequency) possessing diameters close to the average particle size. This observation indicates that at the beginning of the emulsification stage there is already a large number of droplets created that is much smaller than the average diameter value, but there is also particles present with a much larger diameter. As the larger droplets break down over time, the actual droplet diameters approximate the average diameter value.

Next, it was investigated if it might be possible to create a vesiculated bead batch possessing a large average particle size, but with a narrow distribution range by extending the emulsification period. This was experimentally performed using the large 7-inch diameter impeller blade in the 20ℓ reactor and a much lower dispersion speed of 150 rpm. The reason why a large blade was chosen was to ensure that dispersion was sufficient at the low speed. The emulsification period was extended from 20 minutes to 60 minutes and samples were extracted every 10 minutes. Figure 4.4 shows the results of the number average particle size development over this time and the results appear in Table 4.3.

Table 4.3 Number Average Particle Size and Distribution Development During Extended Emulsification Time using 7" Impeller in 20ℓ Vessel (Mixing Speed = 150 rpm)

Emulsification Time (min)	α_n (μm)	PSD
1	11.94	5.63
5	8.09	2.86
10	6.26	2.32
20	5.45	1.99
30	5.20	1.82
40	5.02	1.64
50	4.93	1.63
60	4.89	1.60

It is observed that after about 40 minutes an average particle size is reached that does appear to remain very constant. Also note that the rate at which this reduction occurs, is very low. Comparing these results with those obtained using the 7-inch diameter impeller at 400 rpm in Figure 4.1, it is seen that a much smaller particle size is reached over a shorter emulsification period and at an increased rate.

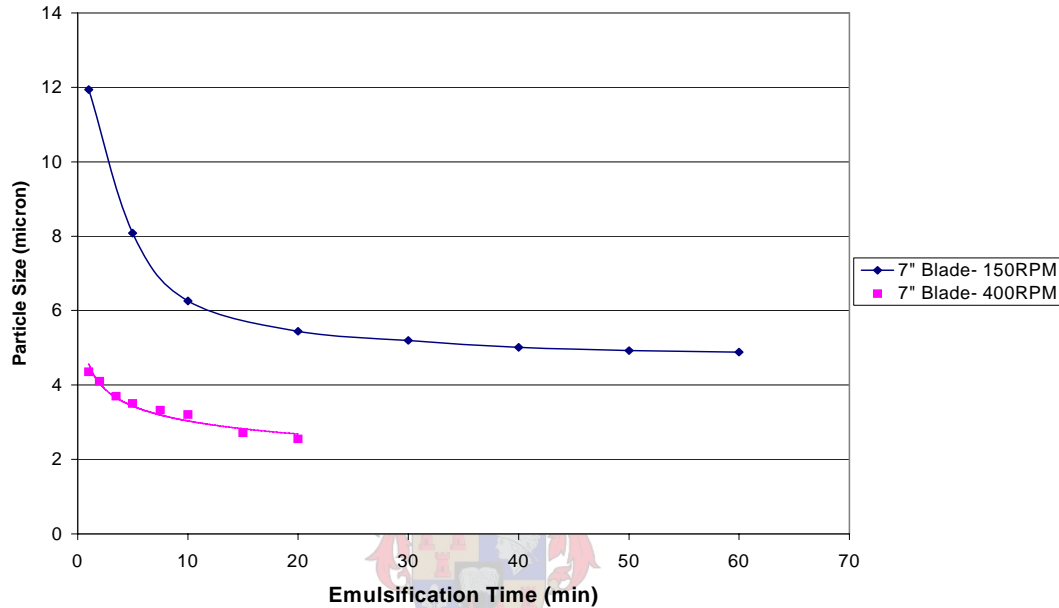


Fig.4.4 Particle Size Development during an Extended Emulsification Period using a 7 inch Diameter Blade in a 20ℓ Reactor vessel at Different Mixing Speed

The distribution of the average particle size data appearing in Table 4.3 was calculated and Figure 4.5 shows these results graphically. The range seems to reach a minimum, but not as narrow as in the case where the mixing speed was higher (400 rpm). However, let us compare the results of the first sample extracted from the batch that was mixed at 400 rpm and the last sample extracted from the batch that was mixed at 150 rpm. From Figure 4.4 (also refer to Tables 4.1 and 4.3) it is seen that the average particle sizes of these two samples are comparable, yet the particle size distribution of the sample mixed at 400 rpm is considerably lower (Figure 4.5).

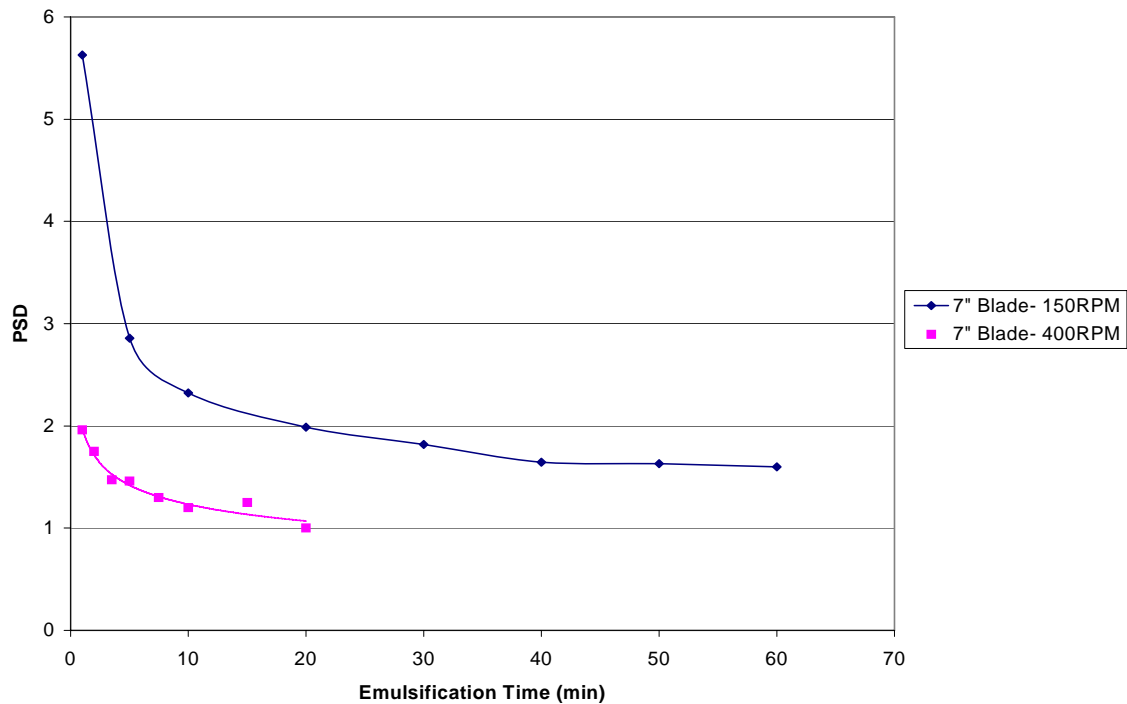


Fig.4.5 Particle Size Distribution Calculated from APS Results using a 7" Diameter Blade in a 20ℓ Reactor Vessel at Different Mixing Speed

From this experiment it can be concluded that a higher mixing speed results in particles possessing a smaller average diameter, with a narrower range of distribution. It may, however, be possible to manufacture vesiculated beads possessing a larger diameter and relatively narrow distribution range by selecting the right impeller diameter to be used at low speed over an extended emulsification period.

The effect of variations in the impeller size, mixing speed and shortened emulsification time on properties will be discussed in more detail in Chapter 5.

4.2 Viscosity Development

4.2.1 Viscosity Development during Production

As described in Section 3.3.1, torque is electronically recorded every minute during production and stored on a data file. By converting this data to viscosity units, the development can be studied as a function of time. As an example, the change in torque was determined for three runs performed in the 20ℓ reactor at different production conditions. In the first experiment, a 7-inch diameter impeller was used at a mixing speed of 400 rpm. In the next, a 5-inch diameter impeller was used at the same speed. The third run was performed by once again using the 7 inch diameter impeller blade, but at a dispersion speed of 150 rpm, the latter being the same run that was used to study particle formation over an extended emulsification period (Section 4.1). The other runs were performed using the standard 30-minute production period. In all three cases the organic phase was added over a period of 10 minutes. The recorded torque measurements are graphically presented in Figure 4.6.

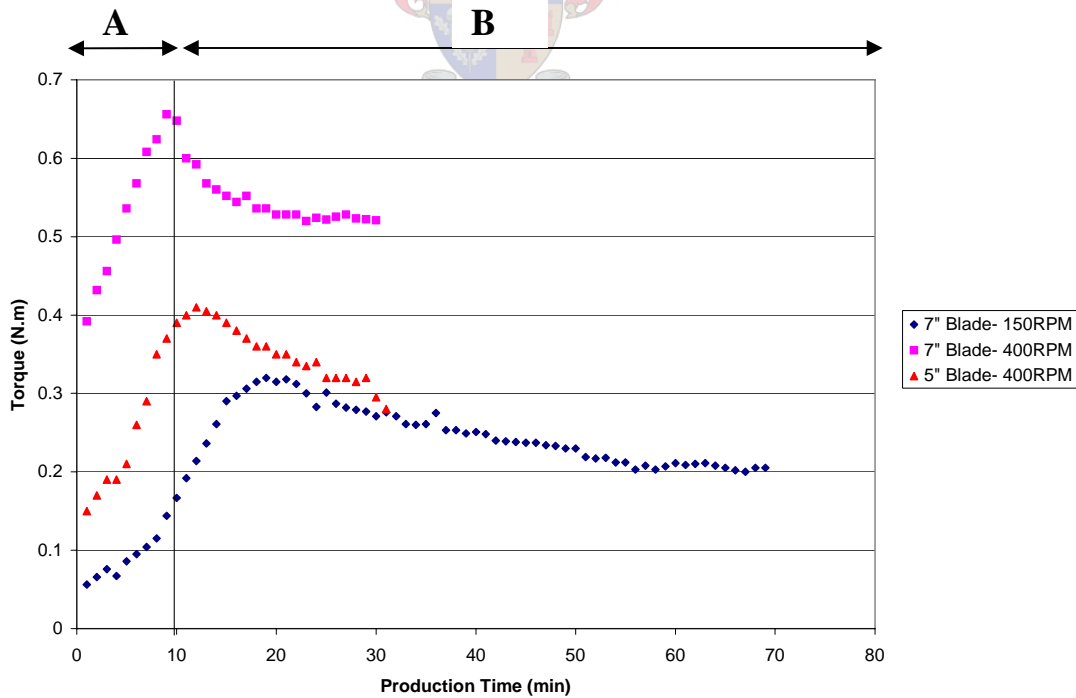


Fig.4.6 Torque Variation During Vesicated Bead Production at Various Production Conditions in the 20ℓ Reactor Vessel
A – Addition Period B – Emulsification Period

From Figure 4.6 it can be seen that the maximum torque was recorded where the large 7 inch impeller was used at the high impeller speed of 400 rpm. A combination of both the high shear rate and area of the impeller blade caused high shear stress on the impeller surface and ultimately increased the torque. The torque measured in the other two runs was mutually more comparable due to the opposing affect of larger impeller size and lower stirring speed, and vice versa, on shear stress.

In all 3 runs, the torque shows a very sharp increase during the addition period of 10 minutes (area A, Figure 4.6). This is due to the relatively viscous polyester being introduced to the aqueous solution. Almost immediately after the addition period is completed, the torque starts to decrease logarithmically towards a minimum during the emulsification period.

The procedure that was followed to experimentally calculate the relationship between viscosity and torque was discussed in Section 3.1.2.3. It was found that a linear dependence existed between the two parameters. This can be seen from the calibration curves illustrated in Figures A2.1-A2.3, Appendix A.

The gain and offset values for converting torque to viscosity were calculated for each of the 3 runs and differed from one to the other due to the different mixing conditions, i.e. impeller diameter and mixing speed. A table of the gain and offset values as well as the recorded torque and calculated viscosity values over production period appear in Table A2.1, Appendix A.

The calculated viscosity of the 3 runs is compared in Figure 4.7 and it is clearly illustrated how the viscosity increases during addition of the organic period and starts reducing toward a minimum value during emulsification (area B, Figure 4.7). Also note the difference in viscosity reduction rate in Figure 4.7. Where the mixing speed is increased using a similar size impeller, the minimum viscosity is reached much quicker. Where the impeller size was changed, it was observed that using a smaller diameter blade decreased the viscosity reduction rate, but didn't affect the final production viscosity that was reached within the 20 minute emulsification period.

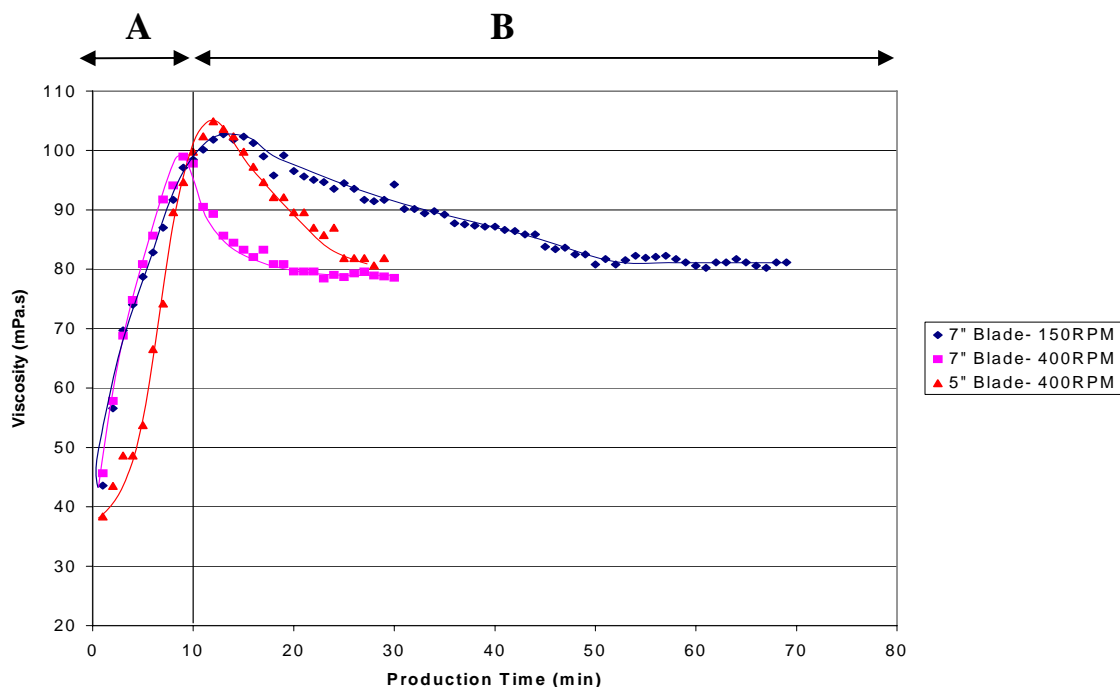


Fig.4.7 Viscosity Development During Vesicated Bead Production at Various Production Conditions in the 20% Reactor Vessel
A – Addition Period **B** – Emulsification Period

The decrease in viscosity over the emulsification period is possibly related to the reduction in average particle size, which follows a similar decline during emulsification as seen in Figure 4.2. Theoretically, more shear is necessary to generate smaller globules, whereas this requirement lessens towards the end of emulsification with the majority of globules already possessing small stable particle sizes.

4.2.2 Rheological Behaviour of Vesicated Beads After Production

As mentioned in Chapter 2, it was observed that when a completed batch of vesicated beads were left in a static state over an extended length of time after catalysis, the viscosity increased to a point where the fluid seemed to be in a gel phase. By re-dispersing the batch, the viscosity decreased, and re-thickened over time as the shear was removed. This is known as thixotropic behaviour and is the phenomena of a substance's viscosity being shear-time dependent^[15]. This might be due to the structural packing of

the solid bead granules in dispersion. When left static, the granules position themselves closely together in the stabilising colloid structure and are forced apart when exposed to agitation, resulting in a decrease in viscosity. After agitation is removed, the particles once again slowly rearrange themselves in a compact structure and the viscosity increases again. This shear-time dependency behaviour was studied in more detail by conducting experiments using the Haake rheometer.

An unagitated sample of a standard batch is carefully measured into a cup-and-spindle mechanism and fixed onto the rheometer. The spindle applies a constant shear rate by first allowing it to rotate at a fixed speed (32 rpm) over an extended period of time. The shear stress exerted on the spindle is recorded over this time.

The experiment was repeated using a sample of the same batch, but with a higher rotation speed (64 rpm). The change in shear stress measured in each case appears in Figure 4.8.

In both cases the shear stress drops logarithmically over time and approaches a minimum. If agitation is removed and the sample left to rest, the zero shear viscosity is recovered after some time (thixotropic behaviour).

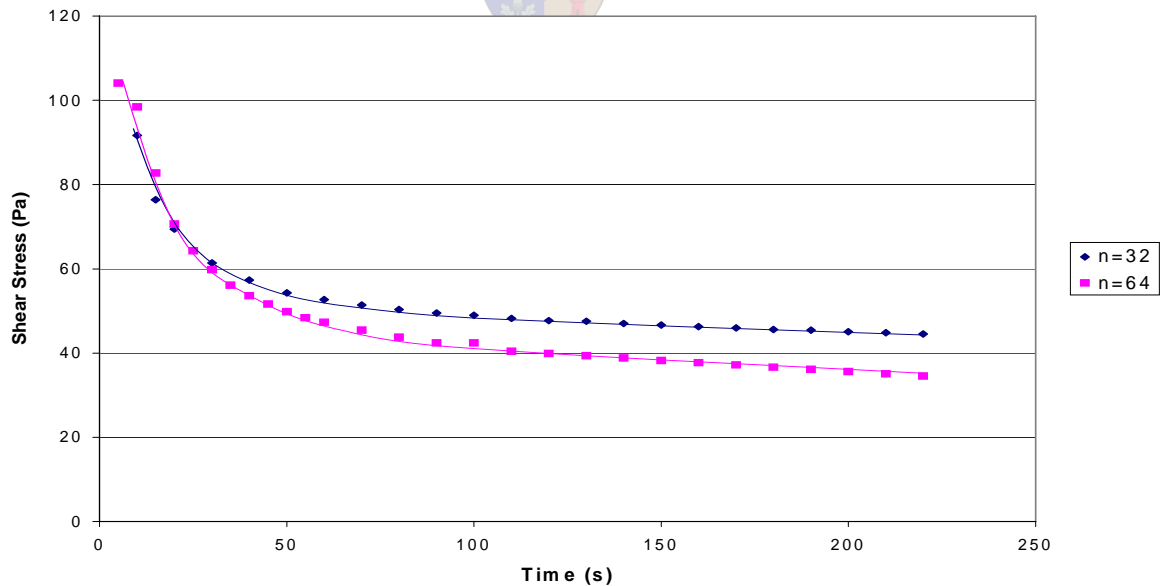


Fig.4.8 Shear-time Dependence of Vesiculated Beads' Viscosity Observed at Constant Shear Rate

From Figure 4.8 it was also observed that when the applied shear rate was changed, the final shear stress also differed. This is a characteristic of a fluid being non-Newtonian in the sense that their viscosity depends on the rate of shear. To investigate this further, experimentation was continued on the rheometer. This time shear stress exerted on the spindle was measured at various rotation speeds. Each time this speed was adjusted, a time period was allowed for the shear stress to stabilise, due to the thixotropic behaviour of the fluid, before readings were recorded.

The Haake Rheometer used for rheological measurements was incapable of automatically recording the shear stress while increasing the shear stress. It was only possible to manually adjust the spindle speed and wait for the shear stress reading to stabilise before readings could be recorded by hand. Figure 4.9 graphically presents these recordings from the analysis of two samples, the one being a reproduction of the other. The results also appear in Section B2, Appendix B.

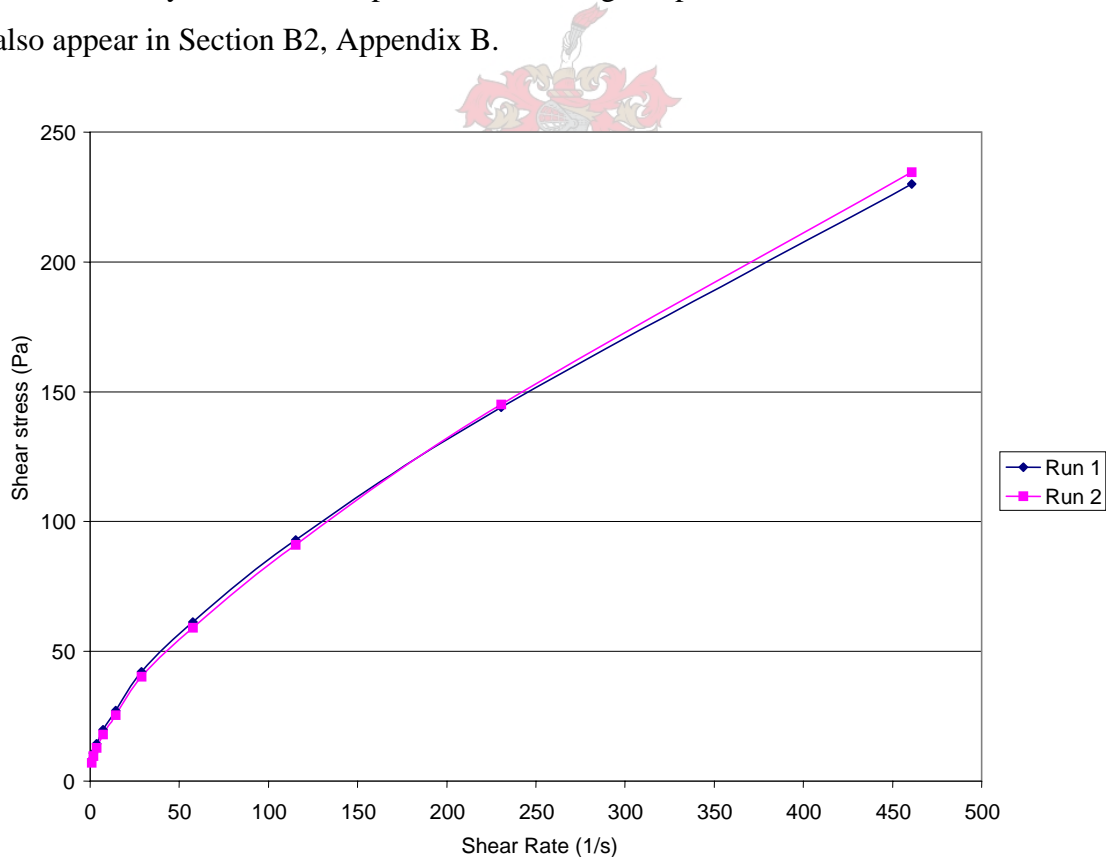


Fig.4.9 Shear-Stress Dependence on Shear-Rate of Vesiculated Beads' Viscosity

The graph confirms the shear rate dependency of viscosity, since Newtonian fluids would possess a linear increase in shear stress as the shear rate was increased. However, in this case it was only possible to determine the dynamic viscosity of the system at a specific shear rate by calculating the slope of a tangent on the shear stress-shear rate curve at that point. This non-Newtonian behaviour can be classified by using the power law equation^[15] presented by Equation 4.1.

$$\tau = K\gamma^n \quad \dots(4.1)$$

where:

τ = Shear stress (Pa)

K = Consistency index

γ = Shear rate (1/s)

n = Power law index; $n=1$ implies Newtonian behaviour

$n>1$ implies “shear thickening” behaviour

$n<1$ implies “shear thinning” behaviour

By applying logarithms, this equation can be reduced to Equations 4.2 and 4.3.

$$\ln \tau = \ln K + n \ln \gamma \quad \dots(4.2)$$

or
$$\ln \tau_1 - \ln \tau_2 = n[\ln(\gamma_1) - \ln(\gamma_2)] \quad \dots(4.3)$$

where 1 and 2 is any two points on the curves in Figure 4.9.

By performing a logarithmic plot of the data in Figure 4.9, a linear curve is obtained (Figure 4.10) where the value of n is equal to the slope of this curve, according to Equation 4.2. A typical calculation of n appears in Section B2.1, Appendix B, where the value of n is found to be 0.54. This indicates that the vesiculated beads possess pseudoplastic behaviour, in other words, when shear rate is increased, the dynamic viscosity decreases.

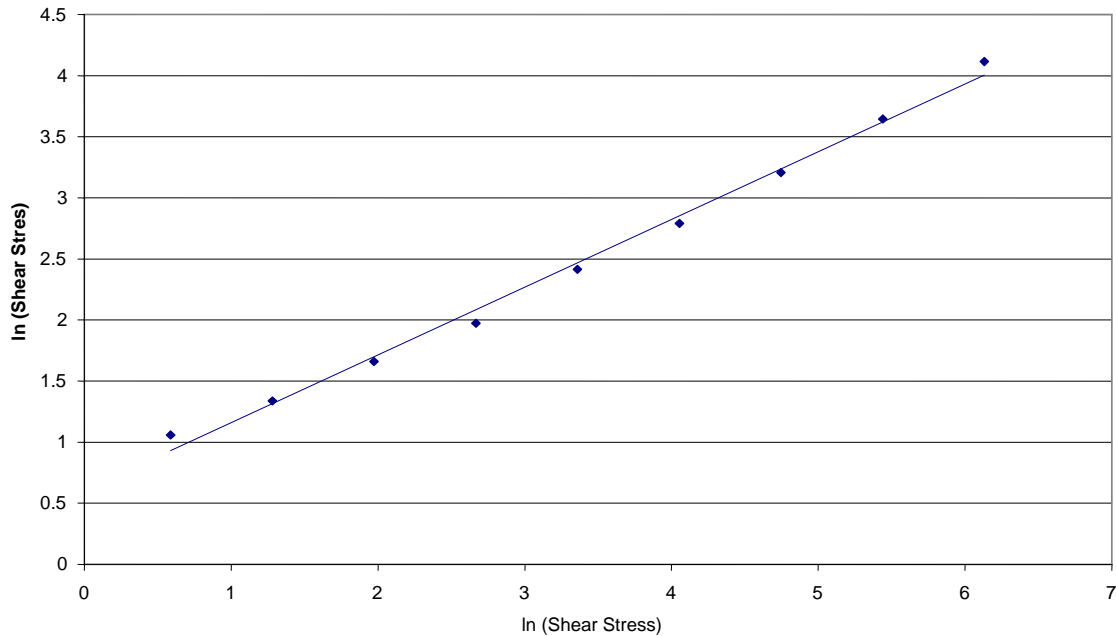


Fig.4.10 Logarithmic Plot of Strain against Shear Rate

This conclusion emphasises the importance of conducting viscosity measurements on completed batches of vesiculated beads under specified shear conditions, in other words at identical spindle speed, when the Brookfield viscometer is used, with readings taken after a predetermined period of time or alternatively to determine the flow curve with a rotoviscometer.

4.3 Temperature Development During and After Production

The fluid temperature in the primary reactor was measured using a PT100 temperature probe located in the base of the vessel and this was recorded on computer every minute and saved to a file. This allowed us to study the temperature variation during production of a vesiculated bead batch.

It is standard procedure to control the production temperature, maintaining it at a value of 24°C. However, an experiment was performed in the 5ℓ vessel where no external heating or cooling was applied, i.e. there was no water in the water jacket. Upon completion of

the final catalyst additions, the motors were switched off and measurement of temperature continued for about 70 minutes afterwards with the batch remaining static within the vessel. Figure 4.11 shows the temperature increase over the continuous period.

As soon as the addition period was started, a slight temperature increase developed which continued during the whole addition and emulsification stages (Stages A and B). The mechanism for this phenomenon was discussed in Chapter 2 where the formation of a more stable macro-molecular structure of grouped polyamine molecules with surrounding polyester chains (neutralisation) is an exothermic reaction, resulting in a temperature increase.

Almost instantly after catalyst addition (Stage C), a more pronounced increase in temperature of more than 10°C was observed, over a period of one hour (Stage D). This was caused by the exothermic polymerisation reaction that took place to form the final solid vesiculated beads.

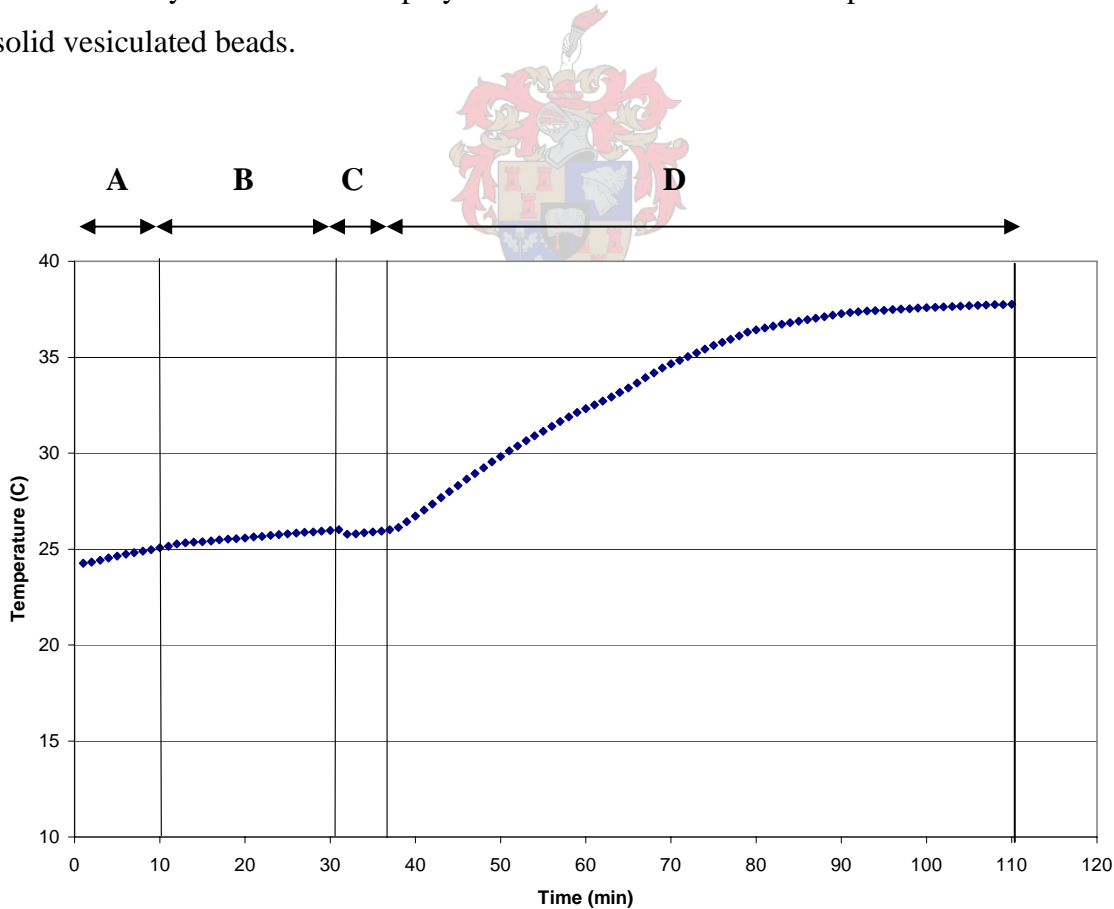


Fig.4.11 Temperature Development During and After Production
A= Addition Period, B= Emulsification Period, C= Post Treatment Period, D= Static Period

4.4 Particle Formation After Catalysis

The temperature profile in Figure 4.11 indicates that the exotherm reaches a maximum temperature about an hour after catalysis. This implies that polymerisation is nearing completion and solid beads have now been formed.

To determine if this is indeed the case, a standard batch was prepared in the 5ℓ vessel and left static after catalysis. Over a period of an hour, small 100ml samples were extracted and polymerisation immediately stopped with treatment of 2.5ml of 1 wt% potassium permanganate (KMnO₄)-solution to stop free radical formation. The permanganate is a much stronger oxidant than the organic peroxide and while oxidation of the redox activator occurs, reduction of permanganate to manganate is more prone to happen, thus leaving the organic peroxide unreacted.

To eliminate existing free radicals, 100ml 5 wt% hydroquinone-solution was also added and the sample immediately put in ice to inhibit any further possible polymerisation.

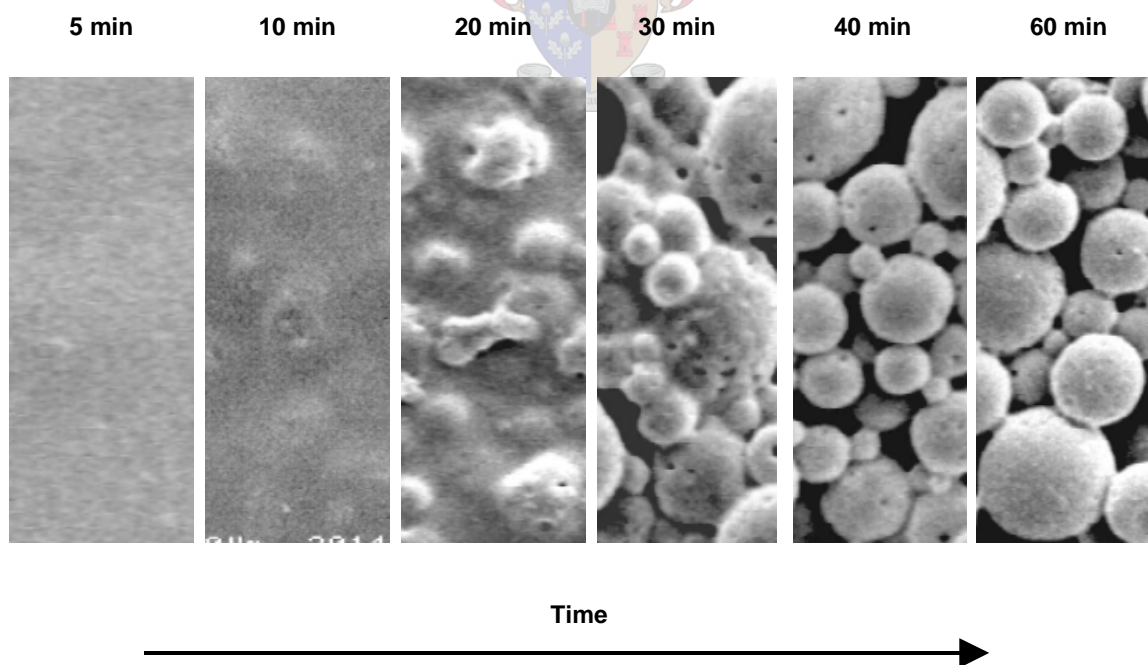


Fig.4.12 Vesiculated Bead Development over a Period of 1 Hour after Catalysis

A sample was dried and SEM photographs taken. Figure 4.12 shows the solid particle formation over time. Only 10 minutes after catalyses, a clear definition of solid development was observed and as expected it was found that almost discreet beads already formed after 1 hour.

A more analytical approach to the development of the reaction is to measure the consumption of free styrene monomer. As the reaction progresses, more styrene will participate in the polymerisation and hence less free monomer will be measured in the vesiculated beads system. Measurements of the styrene concentration in each sample were performed on a gas chromatograph (GC) and the results of each sample (in ppm) appear in Figure 4.16. A description of the analytical procedure that is followed to measure the styrene concentration on the gas chromatograph appears in Section B3, Appendix B.

We observe that even though the discreet beads already formed 60 minutes after catalysis, polymerisation still continues for at least 60 minutes afterwards.

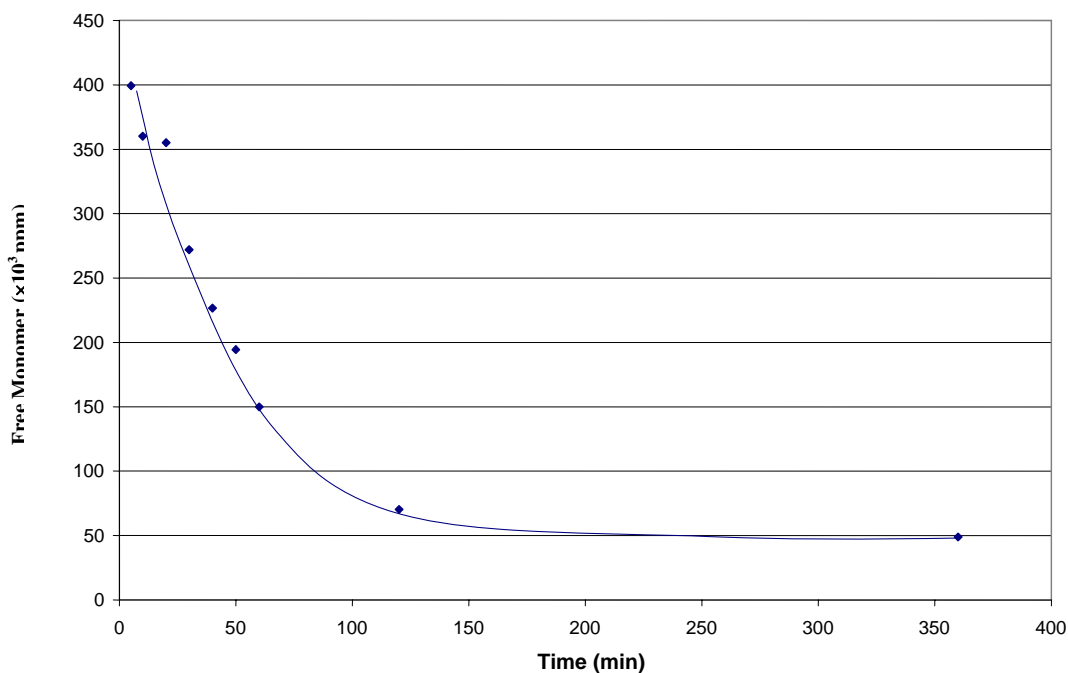
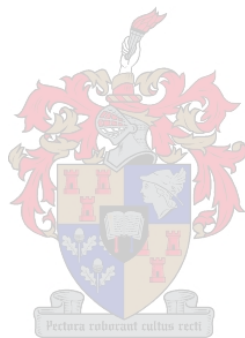


Fig 4.13 Free Monomer Analysis over Time of Vesiculated Bead Samples taken after Catalysis

The transient behaviour of the bead properties discussed in this chapter can assist us in understanding the mechanisms involved in the bead property response to production or processing variables upon completion of a run. The effect of process variables on bead properties will be discussed in the following chapter.



Chapter 5

Effect of Processing Parameters

This chapter includes a discussion of the different vesiculated bead production runs that were carried out on the 5ℓ reactor vessel, where in each set of experiments, variations of a different processing parameter were investigated. These parameters include emulsification temperature, organic phase addition rate, emulsification time, batch size and mixing speed.

5.1 Emulsification Temperature

5.1.1 Standard Formulation

It was first investigated if and how relatively low temperature conditions during production, influence properties like average particle size, pH, viscosity and opacity. In this discussion, low temperature refers to conditions within the ambient temperature range. This was done to see if it is important to take seasonal climate changes in consideration when producing vesiculated beads, since current Cowles reactor vessels found in most paint factories contain no source of temperature control. In each run, a standard 5ℓ-batch was prepared (using KZN polyester resin – refer to Appendix C5, for resin data sheet), and a 4 inch diameter impeller used at a mixing speed of 400 rpm. During the addition and emulsification period, temperatures of these batches were maintained at 5, 15, 18, 21, 24, and 27°C, respectively. At the end of the emulsification period, external heating or cooling was removed to prevent inhibition of the exotherm occurring after catalysis.

A further investigation was performed studying the influence at elevated temperatures of 35, 45, 55, and 65°C, respectively. These conditions will not normally prevail during production, but it was nevertheless considered to be useful for academic purposes. The property analysis results appear in Table 5.1.

Table 5.1 Effect of Emulsification Temperature on Properties (Standard Formulation)

Temp. (°C)	α_n (μm)	pH	η_{mf} (mPa.s)	Solids (wt/wt%)	θ_b (%)	θ_w (%)	$\theta = \theta_b/\theta_w$
5	3.11	6.80	820	23.5	92.3	95.2	0.97
15	2.96	6.83	1100	23.7	90.3	94.1	0.96
18	3.21	6.84	1214	22.9	89.5	94.2	0.95
21	3.14	6.84	1368	23.7	88.5	94.1	0.94
24	3.12	6.83	1245	23.4	86.0	93.5	0.92
27	3.34	6.83	1345	23.9	83.3	90.9	0.91
35	3.54	6.78	1482	23.9	78.4	89.1	0.88
45	4.79	6.67	1410	23.7	73.9	89.0	0.83
55	5.70	6.49	1500	23.5	72.3	89.2	0.80
65	8.59	6.23	1260	23.7	70.5	89.2	0.79

5.1.1.1 Effect on Number Average Particle Size

Figure 5.1 presents the number average particle size values for the runs performed.

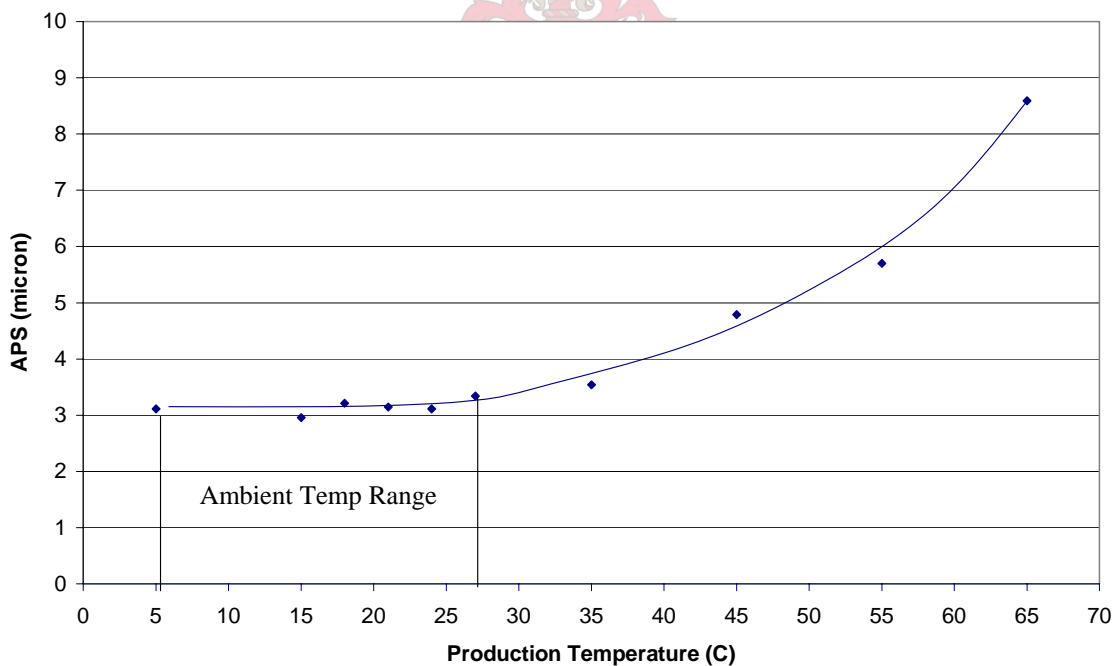


Fig. 5.1 Effect of Temperature on Number Average Particle Size (Standard Formulation)

From the graph it is clear that the average particle size remains virtually constant with an average value of 3.07 micron over the lower (ambient) temperature range and starts increasing almost exponentially after about 27°C. By performing a non-linear

regression analysis, using the statistical software package, Polymath, this exponential increase in particle size (α_n) can be described by Equation 5.1. The regression results appear in Figure C1.1, Appendix C.

$$\alpha_n(T) = \alpha_{na} + 10^{-6} T^{3.7} \quad T > 27^\circ C \quad \dots(5.1)$$

where:

α_{na} = Average Particle Size at Ambient Temperature (μm) = $3.07\mu\text{m}$

T = Temperature ($^\circ\text{C}$)

The temperature exponent is found to be very large, indicating that the effect of temperature on the average particle size starts getting increasingly significant as temperature increases above 27°C . The significance of this parameter will be investigated further in Chapter 7.

5.1.1.2 Effect on pH

If we study the pH values of each run, it appears that it remains almost constant over the ambient temperature range. After 27°C a sharp, almost exponential decline occurs with a further temperature increase (Figure 5.2).

The pH of the vesiculated beads system is predominantly influenced by the polyamine added to the aqueous and organic phases, due to fact that it is a strong base. This decline in pH might, therefore, be attributed to the fact that increasingly more polyamine molecules migrate from the aqueous phase into the organic phase as the temperature is increased.

This will be investigated further in the following section.

5.1.1.3 Effect on Final Viscosity

When the influence of temperature on viscosity measured after the batch was treated with its final post additions, was investigated, it was observed that a logarithmic

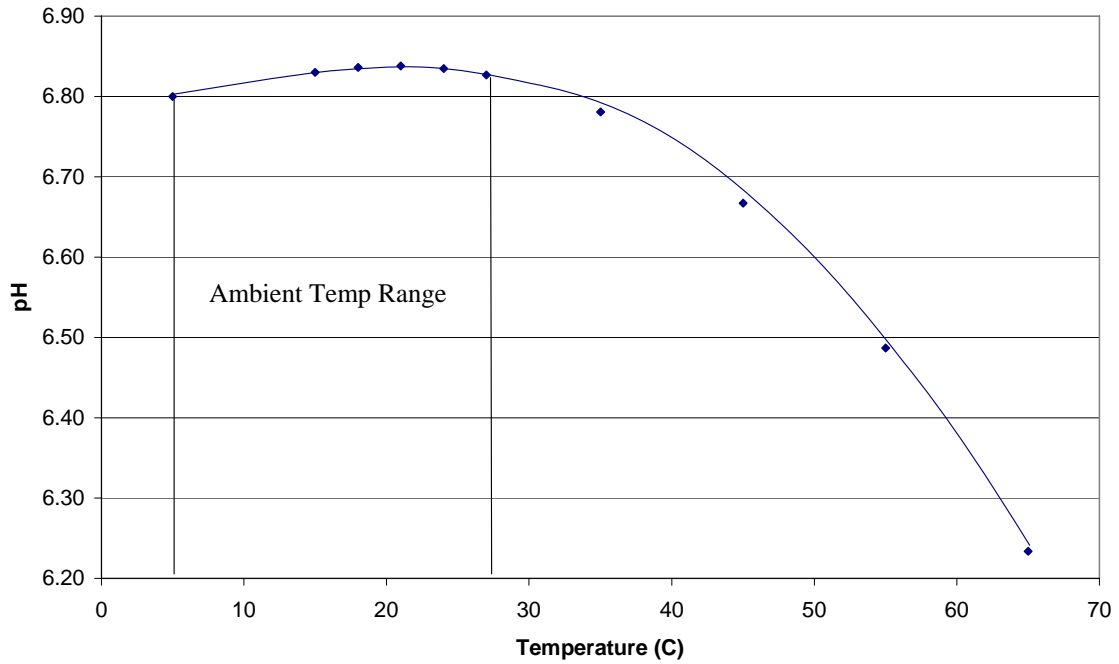


Fig. 5.2 Effect of Temperature on pH (Standard Formulation)

increase develops over the ambient temperature range to ultimately reach a maximum value. It appears that with a further increase in temperature, the viscosity starts to decrease again (Figure 5.3).

The viscosity development might be explained by looking at the system in an analogous way to the model introduced by **Souheng Wu**^[16], who studied the introduction of spherical ethylene-propylene rubber particles, with known particle size and distribution, into a nylon and polyester continuous phase during melt extrusion with a co-rotating twin screw extruder. In Wu's work, he investigated the interfacial and rheological effects on the dispersion process and found that the number average particle size (α_n) of the spherical rubber droplets is dependent on the interfacial tension (σ) between the two phases as well as the matrix viscosity (η_m). Equation 5.2 presents the proposed model.

$$\frac{\gamma\eta_m\alpha_n}{\sigma} = 4\left(\frac{\eta_d}{\eta_m}\right)^{\pm 0.84} \quad \dots(5.2)$$

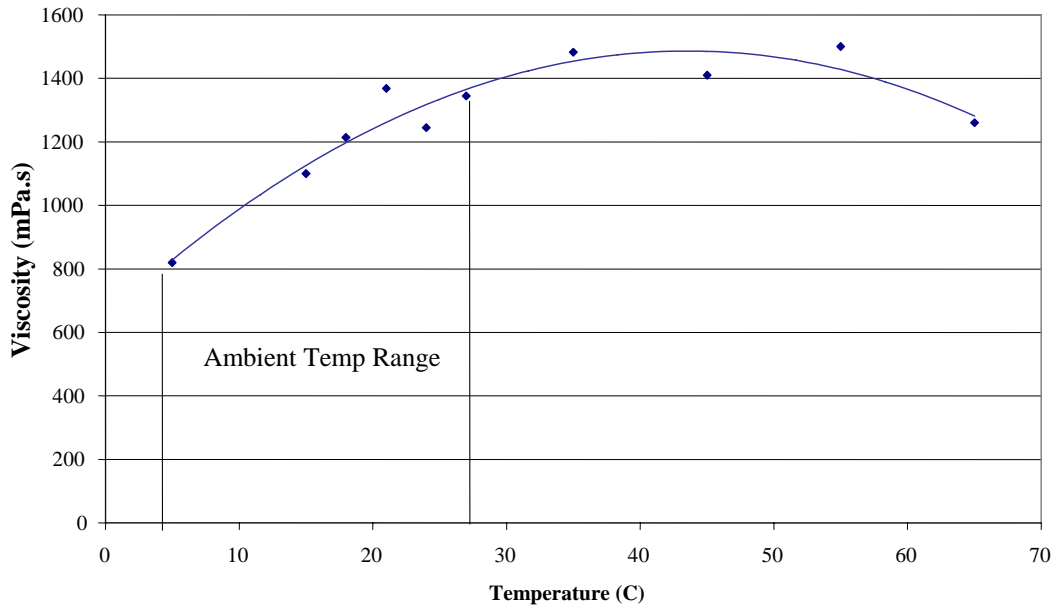
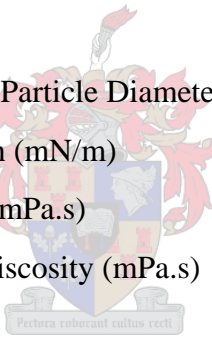


Fig. 5.3 Effect of Temperature on Final Viscosity (Standard Formulation)

where:

- γ = Shear Rate (1/s)
- α_n = Number Average Particle Diameter (m)
- σ = Interfacial Tension (mN/m)
- η_m = Matrix Viscosity (mPa.s)
- η_d = Dispersed Drop Viscosity (mPa.s)



The first term in the equation is also known as the Weber number. The plus (+) sign applies for $p > 1$ where $p = \eta_d/\eta_m$, and the minus (-) sign for $p < 1$. Since the organic phase viscosity in the vesiculated bead system is much higher than the viscosity of the dispersion, it is concluded that $p > 1$. For the set of experiments conducted above it was assumed that the droplet viscosity remained constant since the component formulation was never varied during experiments. Therefore, Equation 5.2 can be reduced to Equation 5.3.

$$\eta_m = k \left(\frac{\sigma}{\alpha_n \gamma} \right)^{0.55} \quad \text{or} \quad \eta_m \propto \left(\frac{\sigma}{\alpha_n \gamma} \right)^{0.55} \quad \dots(5.3)$$

where:

- k = Constant

Throughout this set of experiments, the production conditions remained the same, i.e. there was no changes made in mixing speed, impeller diameter or vessel size. Therefore the shear rate can be assumed to remain constant and Equation 5.3 further reduced to Equation 5.4 for each set of runs.

$$\eta_m \propto \left(\frac{\sigma}{\alpha_n}\right)^{0.55} \quad \dots(5.4)$$

The interfacial tension is proposed by Wu to be a function of temperature. Therefore, by using the production temperature and number average particle size as possible parameters for describing the final viscosity, the validity of the Souheng Wu model was tested with Equation 5.5.

$$\eta_{mf} = k\alpha_n^x T^y \quad \dots(5.5)$$

where:

η_{mf} = Final Batch Viscosity (mPa.s)

T = Production Temperature (°C)

x, y = Parameter Exponents

The viscosity, average particle size and temperature data in Table 5.1 was used in performing a non-linear regression using Polymath. Equation 5.6 presents the derived relationship and the Polymath output results appear in Figure C2.1, Appendix C. The experimental and modelled data appear in Figure 5.4, and a very good comparison is observed.

$$\eta_{mf} \propto \alpha_n^{-0.36} T^{0.34} \cong k\left(\frac{T}{\alpha_n}\right)^{-0.35} \quad \dots(5.6)$$

Equation 5.4 appears very similar to the Souheng Wu model (Equation 5.4), but by comparing the two models it appears that an increase in production temperature relates to an increase in interfacial tension.

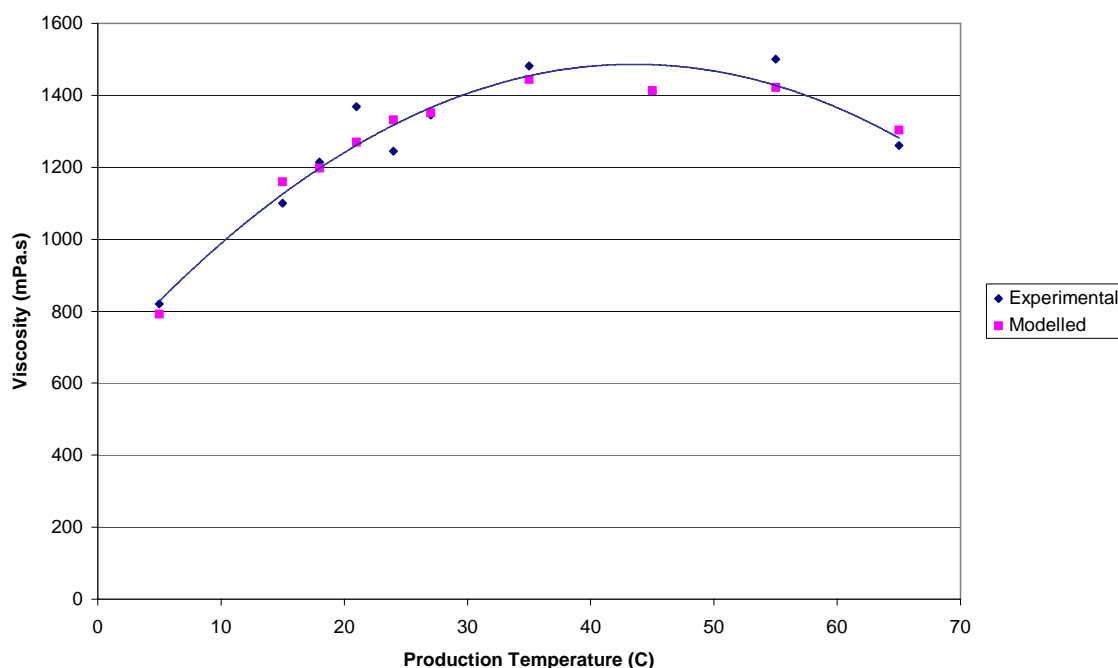
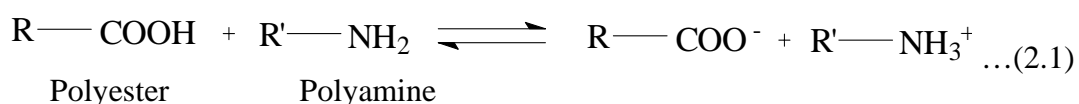


Fig. 5.4 Comparison between Experimental Viscosity Variation with Production Temperature and Modelled Values using the Souheng Wu Model

Although it is found that Equation 5.5 explains the viscosity development accurately, it should not directly be compared to the Wu model, since the latter explains the viscosity during production and Equation 5.6 explains the viscosity a day after production, in other words, the final batch temperature is not the same as the production temperature. Since the organic phase is now polymerised, the interfacial tension in the Wu model will also approach infinity. One should rather look at investigating a possible mechanism of what happens in the vesiculated bead system during production and why this model explains the final batch viscosity development so well.

It was found during experiments performed in this study that when the organic phase is separately prepared and the polyamine added to the polyester under agitation, the viscosity of the fluid increases significantly. This may be because of the neutralisation reaction occurring between the free carboxyl groups on the polyester chains and the polyamine present in the organic phase as discussed in Section 2.4.3. The reversible reaction was presented to occur as follows:



This causes polyester chains, possessing a high molecular weight, to gather in the vicinity of the amine groups. Since the polyamine molecules possess more than one amine group, more polyester chains gather around each of these groups, resulting in a more dense macro-molecular structure, possibly being the reason why the viscosity increases.

It was further observed that a distinct increase in the temperature of the organic phase developed after an agitation period of 5 minutes. This is because the neutralisation occurring is an exothermic reaction. The ionised polyamine groups formed possess hydrophilic character and more of these groups present in the organic phase will attract more water into the system, causing an increase in the water-solubility of this phase. It is, therefore, possible that at a low production temperature, the reversible neutralisation in the organic phase was suppressed, causing less ionised amine groups to be formed in the organic phase also relating to a reduction in water-solubility. This means that there is a high concentration water (relatively low viscosity) present in the aqueous phase after the beads are formed, possibly coinciding with a relatively low final batch viscosity.

As the production temperature increase, neutralisation is proposed to be favoured, causing more polyamine groups in the organic system to be ionised and the organic phase becomes increasingly water-soluble. Thus, after catalysis, there is relatively less water in the aqueous phase, which possibly causes the increase in the viscosity (Figure 5.4). The theory of a higher water-solubility relating to higher viscosity can also be seen in Table 3.5, Chapter 3, where it was shown that the higher the degree of vesiculation, and thus the solubility of the water in the organic phase, the higher the viscosity.

With an increase in neutralisation at higher temperatures, free polyamine groups, which is a strong base, present in the aqueous phase possibly also start to partake in neutralisation. This explains the drop in pH as seen in Figure 5.2. Since it was observed that the viscosity of the organic phase increases when the polyamine was added to the system, due to the more dense structural orientation of the polyester around polyamine groups associated with neutralisation, a larger viscosity difference

between the aqueous and organic phases develops. This might be related to an increase in the interfacial tension.

A two-phase liquid dispersion system possessing a high interfacial tension will be in its most stable geometrical form when the interfacial area is kept as small as possible coinciding with formation of larger spherical droplets. This could explain why the average particle size starts to increase exponentially. This is most likely also the reason why the interfacial tension dependence on temperature in Equation 5.6 contradicts Wu's model, which suggests a decrease in interfacial tension with increasing temperature.

The neutralisation of the polyamine in the aqueous phase causes the organic phase to become exceedingly water-soluble. However, the structural packing of the organic phase increases (high viscosity droplets), and it becomes increasingly difficult for the high concentration water, attracted into this phase, to migrate through the system. Consequently, it might be that a large amount of smaller vesicles are formed close to the droplet interface. Since the interfacial tension also increases, the vesicles may possibly also be released back into the continuous aqueous phase after it has formed. This suggests that the effective water-solubility after vesicle formation decreases, causing a higher concentration water in the continuous phase after the beads have formed, explaining why the final batch viscosity start to decrease again at high production temperatures.

5.1.1.4 Effect on Opacity

From Figure 5.5 we see that an increase in production temperature significantly influences opacity. The value is the highest at low temperatures and decreases almost linearly after 15°C towards 50°C. After this it appears to approach a constant value.

The decrease in opacity might also be attributed to the neutralisation occurring in the organic droplets during production. The hydrophilic ionised polyamine groups attract water into the organic phase. Due to the predominantly hydrophobic polyester chains, a tendency is created for the water molecules, in conjunction with the ionised

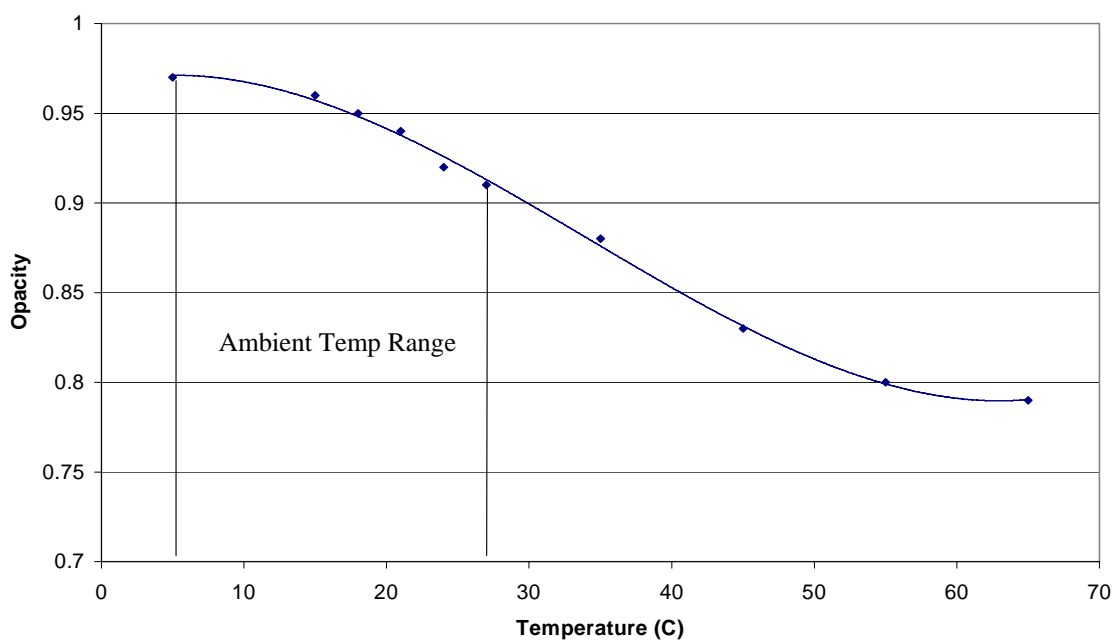


Fig. 5.5 Effect of Temperature on Opacity (Standard Formulation)

polyamine groups, to migrate toward each other to create a more thermodynamically stable macro-molecular structure. This was indicated in Chapter 2 to be a possible mechanism for the actual vesicle formation.

It would be expected that a higher water-solubility of the organic phase implies a higher degree of vesiculation and hence, a higher opacity. However, from Figure 5.5 it appears that the opposite is true.

As discussed in the previous section, lower production temperatures potentially suppresses neutralisation, thereby causing lower water-solubility of the organic phase during production. This might cause smaller vesicles (with a relatively low interfacial tension) to form, possessing a large overall interfacial area. As discussed in Section 3.3.6.2, Chapter 3, these smaller vesicles might be responsible for causing good scattering efficiency of incident light and hence, better opacity of the beads. Unfortunately at the time of the experiments there was not a reliable procedure available to determine the degree of vesiculation or the distribution of vesicles.

As the production temperature is increased, neutralisation is favoured causing higher water-solubility of the organic phase, corresponding to a higher degree of vesiculation. However, the increase in droplet viscosity is still relatively low, resulting in abundant migration of water through the system to ultimately form larger

vesicles possessing a relatively low interfacial area. The latter could be responsible for poor light-scattering efficiency and hence, lower opacity.

With a further increase in temperature, polyamine groups from the aqueous phase start migrating into the organic phase, causing a significant increase in the interfacial tension also resulting in an exponential increase in the average particle size. The water-solubility of the organic phase also increases, but it becomes increasingly difficult for water in this phase to migrate through the densely structured polyester chains, resulting in smaller vesicles to form. These vesicles once again possess a potentially larger interfacial area relative to the large particles, with a better light-scattering efficiency. This is possibly why the rate at which the opacity decreases after neutralisation with polyamine in the aqueous phase decreases, as shown in Figure 5.5.

This mechanism proposes that opacity should not just be measured against the degree of vesiculation or water-solubility, but also against the degree of neutralisation that takes place in the system.

It was also considered that the possibility exists that an increase in temperature might cause the titanium dioxide in the organic phase to migrate towards the surface of the vesiculated beads, consequently reducing the scattering efficiency and thus also in opacity. This led to the investigation discussed in the following section.

5.1.2 Formulation Excluding Titanium Dioxide

A set of experiments were performed in which the study of the effect of temperature was continued, but this time titanium dioxide was excluded from the formulation and substituted with an equal mass of polyester resin, thus maintaining the final solid content at a value of 24 wt%. Since KZN polyester resin was not available at the time of experiments, Cray Valley resin was used throughout (refer to Appendix C5 for resin data sheet).

A similar analysis was conducted as in the previous section to compare final bead properties. In particular, it was investigated if opacity would remain unaffected by

temperature variation, according to the potential titanium dioxide migration theory proposed in the previous section.

Once again, the experiments were conducted on 5kg scale under exactly the same dispersion conditions as before. In each batch the temperature was maintained at 5, 14, 20, 30, 40, 50, and 56°C, respectively. A table of the property analysis results appears in Table 5.2.

Table 5.2 Effect of Emulsification Temperature on Properties (Formulation Excluding TiO₂)

Temp (°C)	α_n (μm)	pH	η_{mf} (mPa.s)	Solids (wt/wt %)	θ_b (%)	θ_w (%)	$\theta = \theta_b/\theta_w$
5	3.70	6.81	750	23.5	82.8	92	0.9
14	3.52	6.82	1040	23.4	80.6	91.6	0.88
20	3.60	6.82	1200	23.6	79.9	91.8	0.87
30	4.42	6.83	1295	23.9	73.6	89.7	0.82
40	4.57	6.78	1268	24.0	69.9	89.6	0.78
50	6.51	6.66	1220	24.0	65.0	89.1	0.73
56	7.43	6.33	1260	24.0	63.8	88.6	0.72

5.1.2.1 Effect on Number Average Particle Size

Figure 5.6 once again show a sharp increase in the number average particle size with temperature, but if we compare the results to those obtained in the previous section, it is seen that the values appear to be somewhat larger than before and the increase starts developing at a lower temperature (25°C). Apart from the influence of titanium dioxide, the reason for this might be attributed to the different polyester resins used in each set of experiments. It has been found during the course of this study that properties are significantly influenced by variation of polyester production batches. Paint chemists are currently investigating the reason for this.

Another possibility for the increased particle size can be attributed to the increased volume polyester used in this set of experiments. Although the percentage solids remained the same, the density of titanium dioxide is much higher than that of the polyester. Therefore, higher volume polyester was needed to replace the weight of titanium dioxide removed.

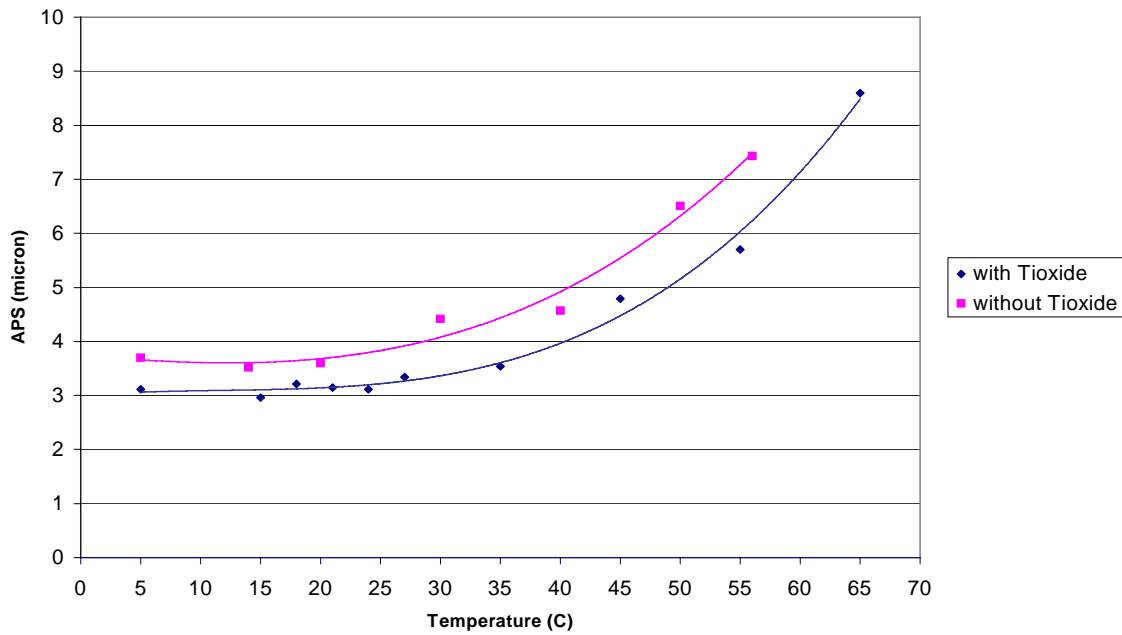


Fig. 5.6 Comparison of Temperature Effect on Average Particle Size with and without Titanium Dioxide Addition

By once again performing a regression analysis using Polymath (Figure C1.2, Appendix C), Equation 5.7 is obtained describing the average particle size dependence on temperature, with the average value over the ambient temperature range, α_a , equal to about 3.60 micrometers.

$$\alpha_n(T) = \alpha_{na} + 7.7 \times 10^{-6} T^{3.2} \quad T > 25^\circ C \quad \dots(5.7)$$

where:

α_{na} = Average Particle Size at Ambient Temperature (μm) = 3.60 μm

The temperature exponent is comparable to the value obtained where the standard formulation was used (Equation 5.1), suggesting similar dependence of average particle size on temperature.

5.1.2.2 Effect on pH

Figure 5.7 presents the pH variation with temperature and shows the same behaviour observed in the previous section (Figure 5.2). However, the exponential decrease appears to develop at an increased rate.

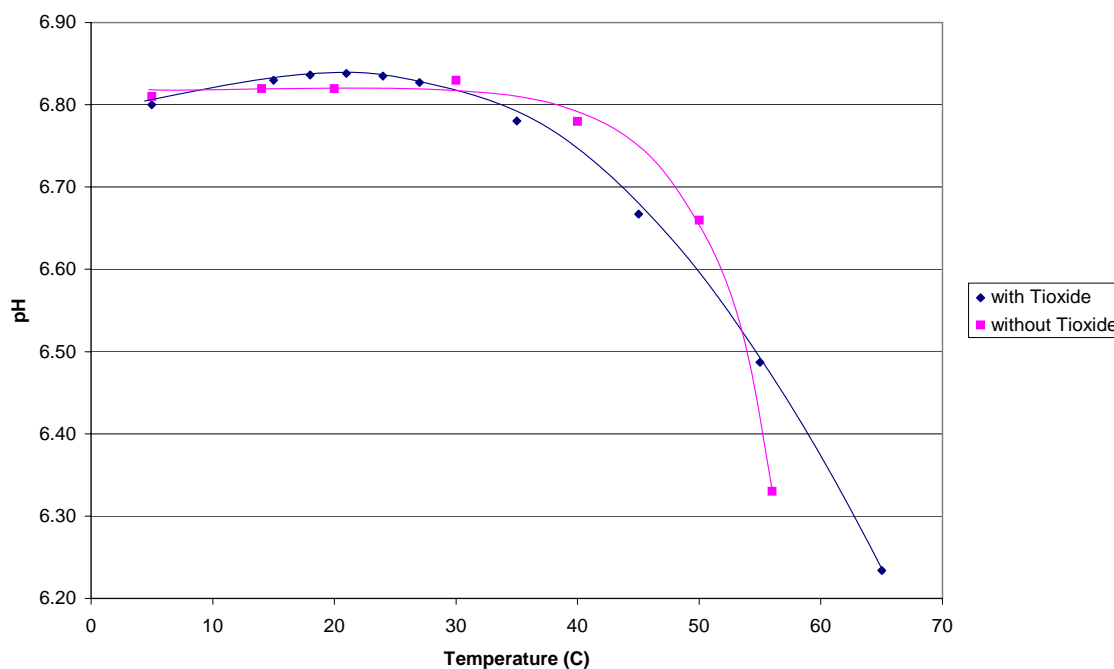


Fig. 5.7 Comparison of Temperature Effect on pH with and without Titanium Dioxide Addition

This may also be attributed to the higher volume polyester used to substitute the titanium dioxide. This implies a relatively lower concentration polyamine present in the organic phase. Less neutralisation, therefore occurs in this phase and since this reaction is favoured by temperature, the polyamine present in the aqueous phase starts partaking in neutralisation quicker and at a higher rate as the production temperature is increased, thus explaining the behaviour observed in Figure 5.7.

5.1.2.3 Effect on Viscosity

5.1.2.3(a) Final Viscosity

If we examine Figure 5.8, a viscosity increase with temperature over the ambient temperature range, is once again observed, but the values appear to be smaller than those measured in the previous section. The lower concentration polyamine relative to the polyester implies relatively less neutralisation occurring in the organic phase. Thus, the water-solubility of this phase is less. After catalysis, the lower concentration water in the organic phase relates to a higher concentration in the aqueous phase explaining why the final viscosity, is relatively less than the values measured in the previous investigation.

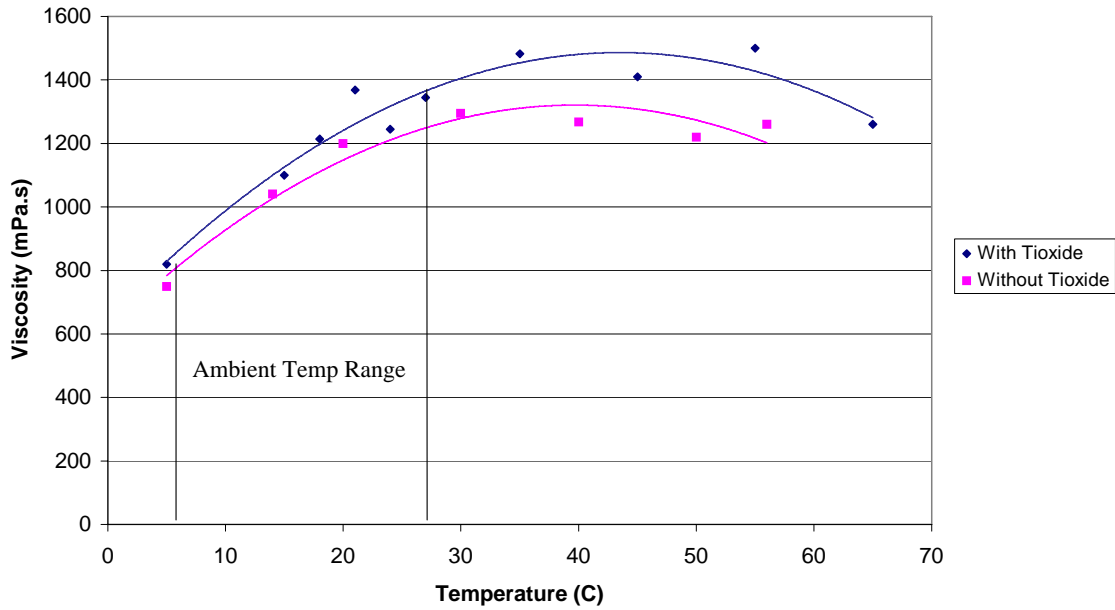


Fig. 5.8 Comparison of Temperature Effect on Viscosity with and without Titanium Dioxide Addition

By using the parameters used in Equation 5.5, it can once again be investigated if the viscosity change can be modelled as a function of average particle size and production temperature. By once again performing a non-linear regression on the data in Table 5.2 using Polymath, Equation 5.8 was derived. The output results calculated by Polymath appear in Figure C2.2, Appendix C.

$$\eta_{mf} \propto \alpha_n^{-0.36} T^{0.30} \quad \dots(5.8)$$

Figure 5.9 presents the comparison of the modelled and experimental data and a good correlation is obtained. Notice how both the average particle size and temperature exponents compare very well to those obtained where the standard formulation was used in the previous section. Thus, the final viscosity appears to have the same dependence on these parameters.

The data from both experimental runs (i.e. including and excluding titanium dioxide) was combined (Tables 5.1 and 5.2) in order to compare this to the two separate viscosity models (Equations 5.6 and 5.8). A non-linear regression was performed using Polymath and Equation 5.8 presents the combined model. The Polymath output results appear in Figure C2.3, Appendix C.

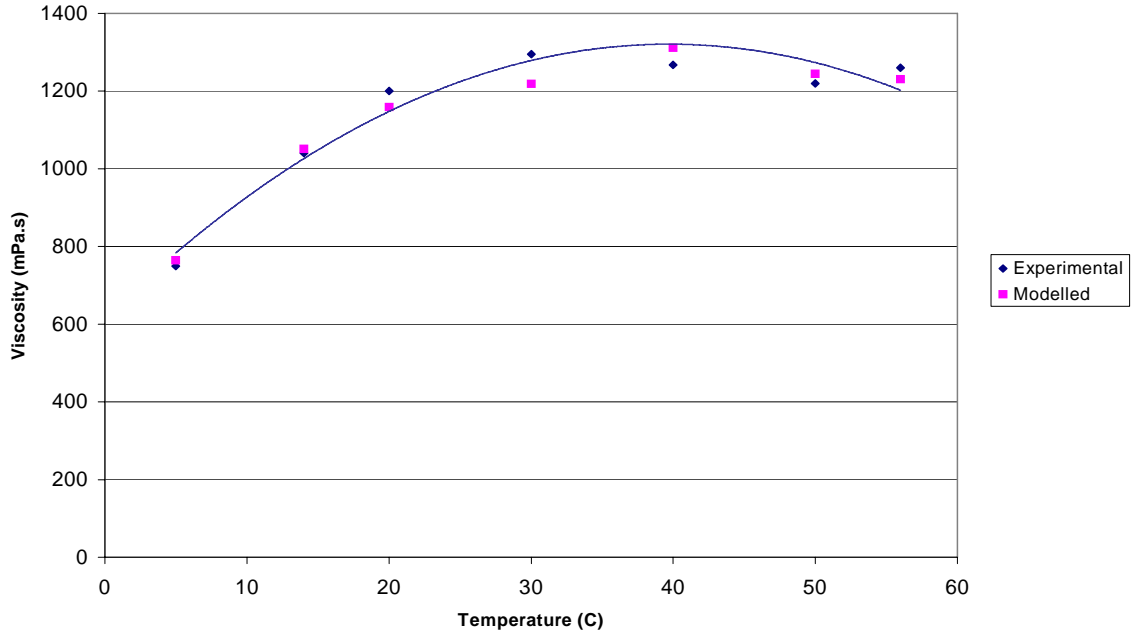


Fig. 5.9 Viscosity Comparison between Soeheng Wu Model and Experimental Data from Runs Performed Without Titanium Dioxide

$$\eta_{mf} \propto \alpha_n^{-0.38} T^{0.33} \quad \dots(5.9)$$

The average particle size and temperature exponents compare very well to the values calculated in the two separate models (Figure 5.10). The experimental and modelled viscosity values also appear in Tables C2.1 and C2.2, Appendix C.

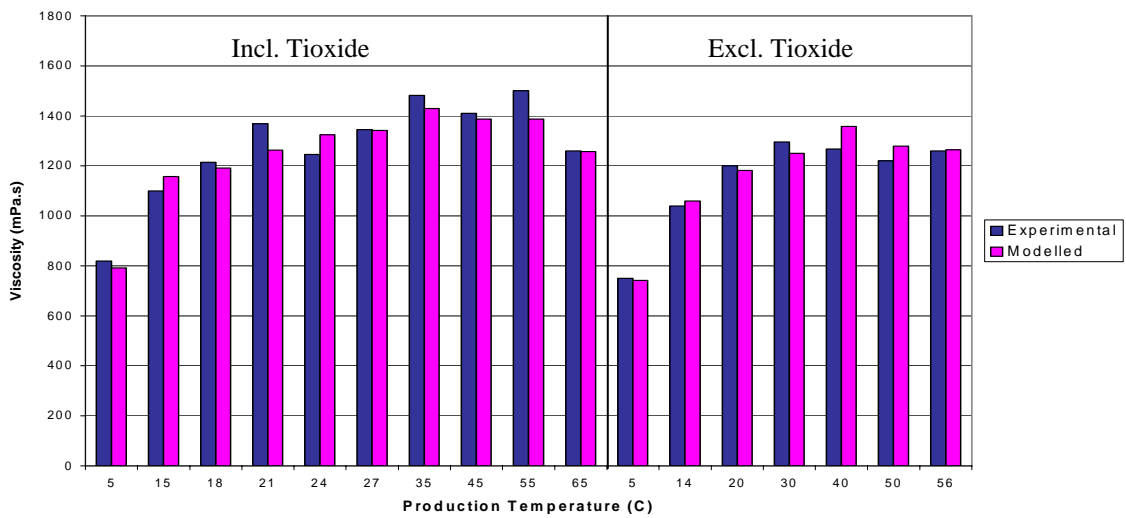


Fig. 5.10 Viscosity Comparison between Soeheng Wu Model and Experimental Data from Runs Performed with and without Titanium Dioxide

5.1.2.3(b) Production Viscosity

Figure 5.11 presents a comparison of the recorded torque data measured by the strain gauge during the emulsification period of production runs in this investigation. The exerted torque is very small using a small diameter impeller at relatively low mixing speed and due to the crude sensitivity of the strain gauge, it was difficult to obtain accurate torque measurements. This is clearly observed from the erratic data points on the graph. This made it difficult to accurately calibrate the data to viscosity units. However, it can be seen how the torque, showing very similar trends to those observed in Section 4.2.1, decreases over time. Also notice how the torque significantly drops as the production temperature is increased and it appears to stabilise after 30°C, suggesting that a further production temperature increase will not significantly affect production viscosity.

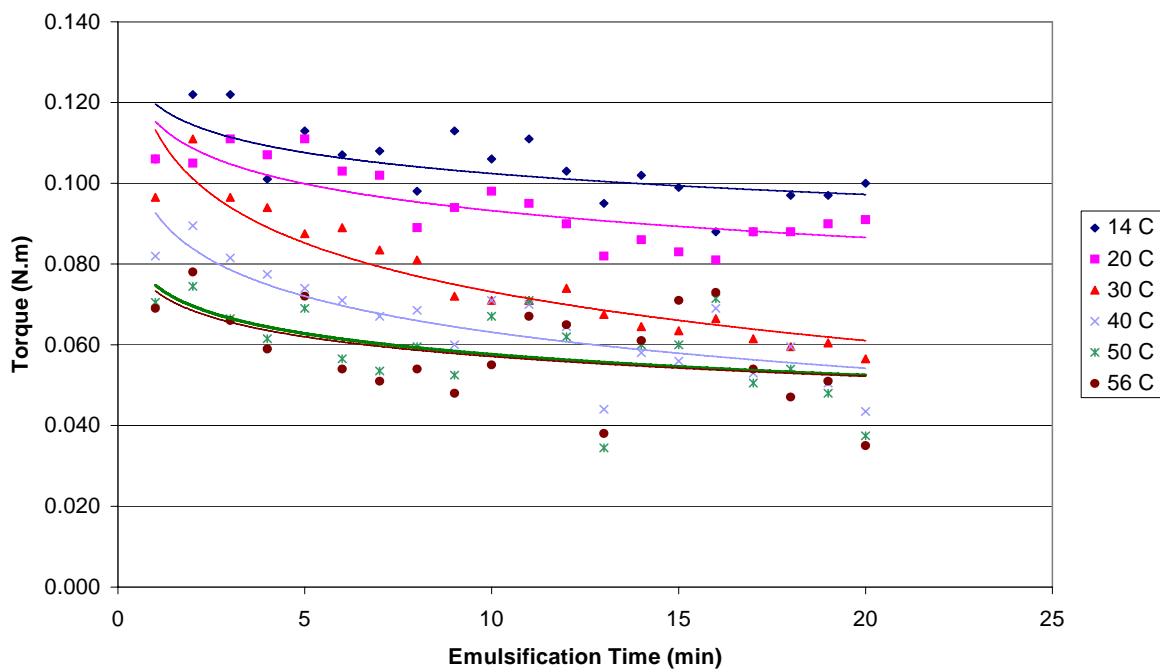


Fig. 5.11 Torque Development during the Emulsification Period as a Function of Temperature (5ℓ Vessel, 4" Diameter Impeller, Mixing Speed = 400 rpm)

The production viscosity development possibly obeys the model proposed by Wu (1987) better, suggesting that the interfacial tension decreases with increasing production temperature, causing a decrease in viscosity. This explains the fast rate of reduction in torque seen in Figure 5.11. However, as proposed in the modelling of final batch viscosity, neutralisation is favoured with increasing temperature

accompanied with an increase in droplet viscosity, accordingly causing an increase in the interfacial tension. Therefore, these two models possibly counteract each other in modelling the development of interfacial tension with temperature. From Figure 5.11 it appears that Wu's model predominates at lower production temperatures where the interfacial tension decreases with an increase in temperature. However, the interfacial tension (and average particle size) starts increasing extensively at higher temperatures as polyamine from the aqueous phase starts participating in neutralisation, presumed to be associated with temperatures in the region of 25°C, as seen on the pH graph (Figure 5.7). This might be the reason why the torque, and accordingly the production viscosity, approaches a minimum value.

5.1.2.4 Effect on Opacity

It was observed in Figure 5.12 that the removal of titanium dioxide from the formulation did not make the opacity any less temperature independent and a very similar decrease was observed as in the case where the standard formulation was used. In fact, the opacity even at ambient conditions is significantly less, substantiating the advantage of incorporating this pigment as opacifier.

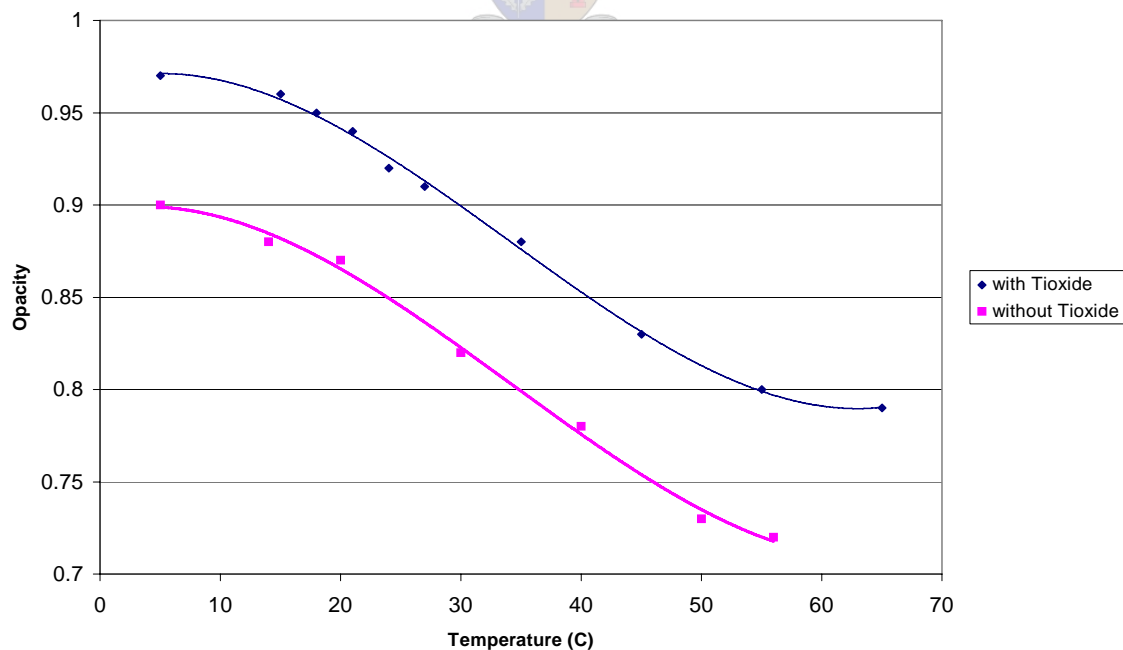


Fig. 5.12 Comparison of Temperature Effect on Opacity with and without Titanium Dioxide Addition

If we compare the SEM photographs taken from the draw-downs of the two sets of experiments at different temperatures (Section C3, Appendix C) it can also be seen that there is no visible titanium dioxide particles on the vesiculated bead's surfaces. Another factor(s) must therefore be responsible for the loss in opacity at higher temperatures. The mechanism, explained in Section 5.1.1.4, might be responsible for this behaviour.

5.2 Emulsification Time

The next parameter studied was the emulsification time allowed after completion of the addition of the organic phase to the primary aqueous phase. In the basic production procedure, a constant emulsification period of 20 minutes is maintained to allow polyester droplets to reach an average particle size with a narrow distribution, but in this set of runs this time was reduced to 2, 3.5, 5, 7.5, 10, and 15 minutes, respectively. Experiments were performed using the standard formulation and production conditions in the 5ℓ vessel (4" impeller at 400 rpm). After these periods of time, the batches were catalysed and the normal analysis procedure followed the following day. The results of the analysis appear in Table 5.3.

5.2.1 Effect on Number Average Particle Size

In Section 4.1 a similar procedure was followed under the same mixing conditions. Samples were extracted periodically during emulsification to study the development of the average particle size. If these values (Table 4.1) are compared to the ones in this investigation, a very similar reduction in average particle size is observed over time. Figure 5.13 shows that in both investigations a sharp decline in average particle size occurs during the first 5 minutes of emulsification, gradually approaching a constant minimum value. It is further observed that the average particle size in the case where sample extraction was used, is less than the values obtained in this investigation. In this set of experimental runs, polyester obtained from KZN was used, whereas in the former case, Cray Valley polyester was used. As mentioned in the Section 5.1, it was established that different polyester batches do cause variation

in certain vesiculated bead properties and this might be the reason why a difference in average particle size was observed.

Table 5.3 Effect of Emulsification Time on Properties

Emuls. Time (min)	α_n (μm)	pH	η_m (mPa.s)	Solids (wt/wt %)	θ_b (%)	θ_w (%)	$\theta = \theta_b/\theta_w$ (%/%)
2	9.83	6.98	1023	23.61	87.1	92.7	0.94
3.5	7.21	6.85	1120	23.54	88.2	91.9	0.96
5	5.26	6.97	1037	23.73	91.3	94.6	0.97
7.5	5.11	6.70	1160	24.10	88.9	92.6	0.96
10	5.09	6.93	1850	22.69	90.9	94.2	0.96
15	4.49	7.02	1396	24.05	90.9	93.8	0.97
20	4.39	7.00	1368	22.96	87.8	91.5	0.96

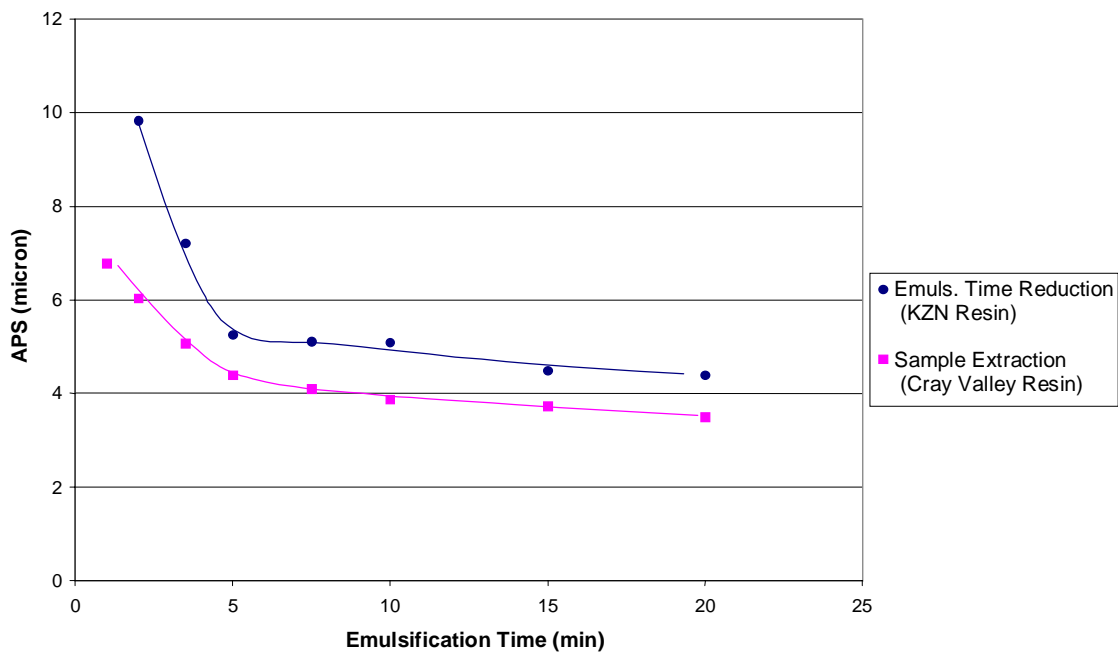


Fig. 5.13 Comparison of the Average Particle Size Development using Emulsification Time Reduction and Sample Extraction Method (4" Impeller in 5ℓ Vessel, Mixing Speed = 400 rpm)

The mutual difference in particle sizes do, however, appear to be less significant at longer emulsification periods with a difference in values of less than 1 μm . This shows that better production reproducibility is obtained if the emulsification time is longer, indicating the advantage of using a longer consistent emulsification time of 20 minutes during production.

5.2.2 Effect on Final Viscosity

Figure 5.14 presents the effect of changes in emulsification time on the final batch viscosity and it appears that a small increase in viscosity occurs as the emulsification time is increased. The value recorded at 10 minutes is very large and can possibly be due to an incorrect measurement taken.

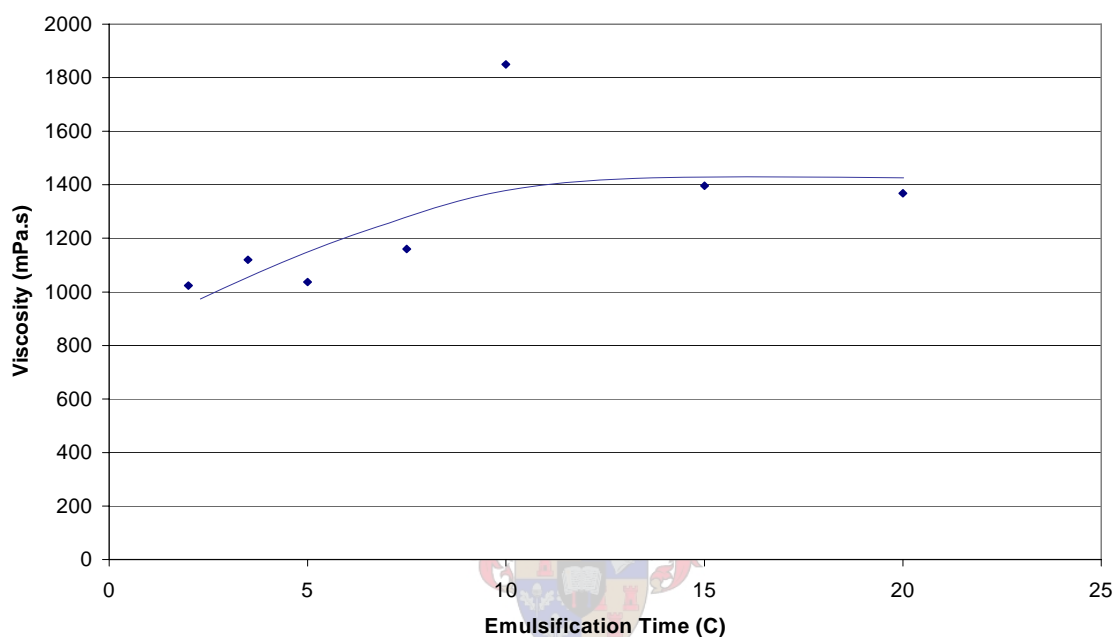


Fig. 5.14 Effect of Emulsification Time on the Final Batch Viscosity
(4" Impeller in 5ℓ Vessel, Mixing Speed = 400 rpm)

The reason for the lower viscosity at shorter emulsification times might be that at shorter emulsification times, potentially less time is allowed for water to travel into the organic phase towards the hydrophilic ionised amine groups. This means that the effective water-solubility of the organic phase is lower. After the solid beads are formed there is consequently a higher concentration of water in the continuous aqueous phase, relating to a lower viscosity than in the case where the emulsification time is longer. However, one should remember that the variation in viscosity is relatively small and it is uncertain that this small variation is really significant.

5.2.3 Effect on Opacity

It is interesting to observe that emulsification time has almost no visible effect on opacity or luminosity values measured on the black and white surfaces. It is expected that the lower final batch viscosity measured at shorter emulsification times, which relates to lower water-solubility of the polyester phase, will cause a lower degree of vesiculation and hence, a decrease in opacity. However, it was found in the previous investigation of the production temperature dependence on opacity (Section 5.1.1.4), that water-solubility does not necessarily relate to opacity. Lower solubility of the organic phase during production might result in smaller vesicles to form further away from each other, whereas at higher solubility the vesicles are closer together. The latter case creates a condition where the vesicles possibly gather forming potentially larger vesicles. The relative interfacial area in the two cases may therefore be comparable, possessing closely related light-scattering efficiencies. This could be why the opacity did not show any significant variation in this investigation.

5.3 Organic Phase Addition Rate

During the production of vesiculated beads, the organic phase is let down into the aqueous phase over a period of 10 minutes. This time period is allowed because it would not be possible to pump all the pre-dispersion at once when industrial scale production is carried out in the factories. However, a set of experiments was conducted, following standard production procedure, but reducing the addition time. This was done through manipulation of the slurry pump's discharge flowrate from the secondary to primary reactor vessel. Batches were produced with addition times of 1.5, 2.5, 5, 6, 7.5, and 10 minutes, respectively, and each succeeded by a 20-minute emulsification period. The property analysis results appear in Table 5.4.

Table 5.4 Effect of Organic Addition Time on Properties

Addition Time (min)	α_n (μm)	PSD	Skew	pH	η_{mf} (mPa.s)	Solids (wt %)	θ_b (%)	θ_w (%)	$\theta = \theta_b/\theta_w$
1.5	4.38	1.78	0.75	6.63	506	22.9	89.0	94.6	0.94
2.5	4.79	1.79	0.57	6.70	761	22.4	90.1	93.8	0.96
5.0	4.77	1.64	0.89	6.82	950	22.3	90.5	95.4	0.95
6.0	4.66	1.76	0.55	6.91	974	22.7	89.8	94.2	0.95
7.5	4.39	1.64	0.50	6.95	1039	22.0	88.8	93.8	0.95
10.0	4.60	1.56	0.36	7.00	1210	22.4	90.9	94.4	0.96

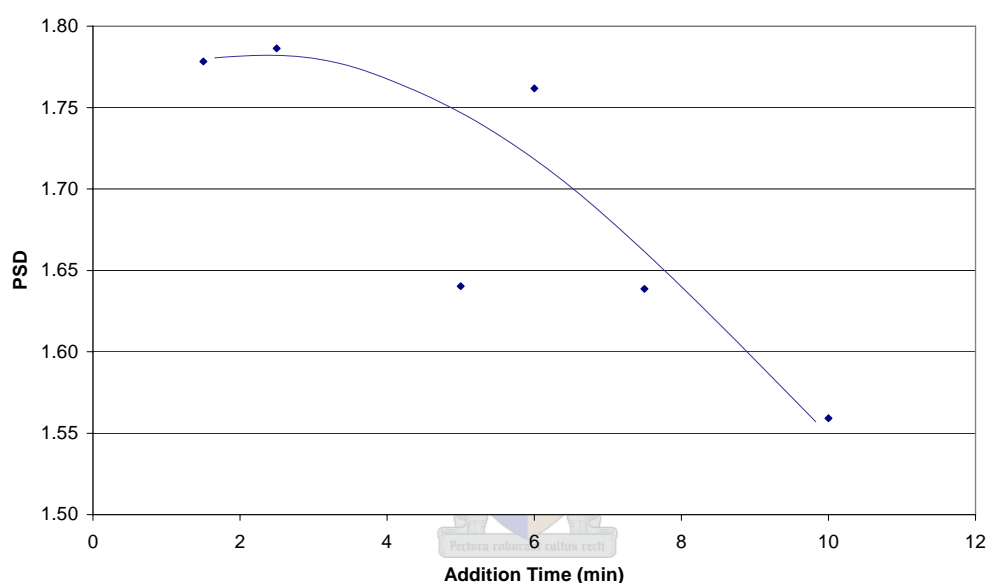


Fig. 5.15 Effect of Organic Phase Addition Time on Particle Size Distribution (5ℓ Vessel, 4" Diameter Impeller, 400 rpm)

5.3.1 Effect on Number Average Particle Size

It appears from Table 5.4 that reduction in the addition time of the organic phase has no effect on the average particle size within the variation investigated. It is expected that by increasing the addition rate, the effective time for emulsification is shorter, resulting in an increase in the average particle size as was seen in the previous investigation (Section 5.2).

However, by looking at the particle size distribution (Figure 5.15), it appears that a reduction occurs as the addition time is increased. Although the average particle size

remain unaffected by this parameter, the particle size distribution does appear to get narrower since more time is allowed for all the globules to break down to diameters closer to the average particle size.

We can further look at the skewness of the distribution. The values presented in Figure 5.16 show that higher addition rates also relate to larger skewness, which indicate that over the distribution range more particles were formed possessing diameters larger than the average particle size. This stresses the importance of taking these properties into consideration when a thorough study of the particle sizes in vesiculated bead batches are performed.

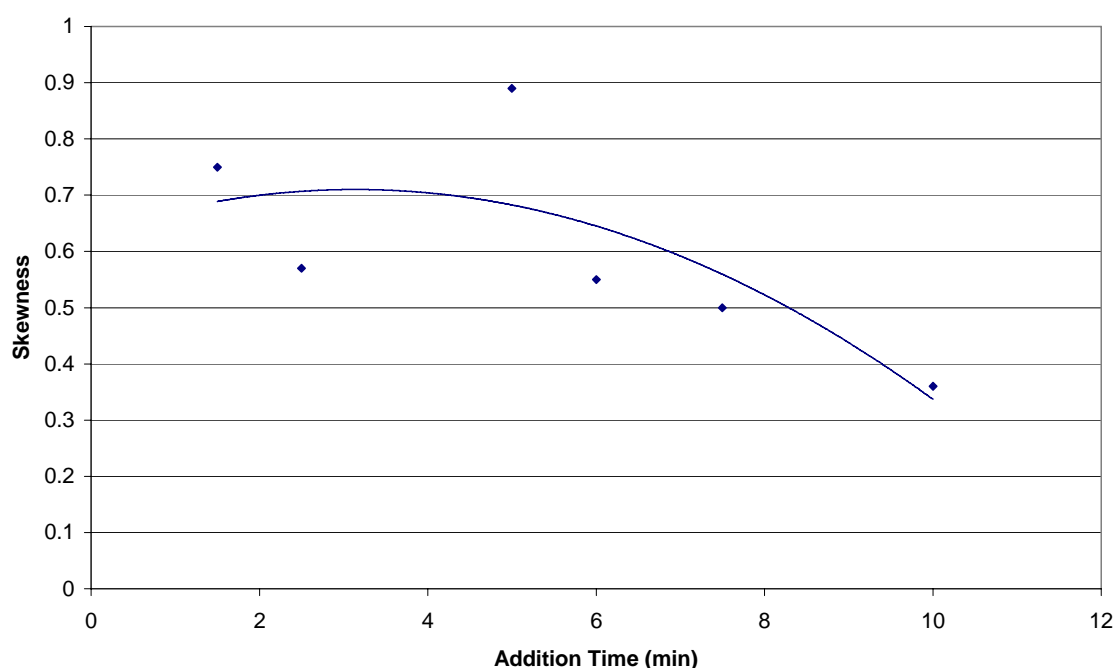


Fig. 5.16 Effect of Organic Phase Addition Rate on Skewness

5.3.2 Effect on Final Viscosity

Figure 5.17 presents the final viscosity development and a definite increase is observed as the addition period is increased. At shorter addition times the effective emulsification period in which the organic phase is in contact with the aqueous phase before catalysis, is shorter. This could imply that there is less time available for water to migrate into the organic phase. There will, therefore, be a higher concentration of water in the aqueous phase after the beads have cured, causing a lower viscosity. Longer addition times will allow more time for water-migration and with a lower

water concentration in the aqueous phase after catalysis, will cause a higher final viscosity. A very similar trend was observed in Section 5.2.2, where the emulsification time was also decreased. However, it does appear that the effect of shorter addition times have a more significant affect on the viscosity.

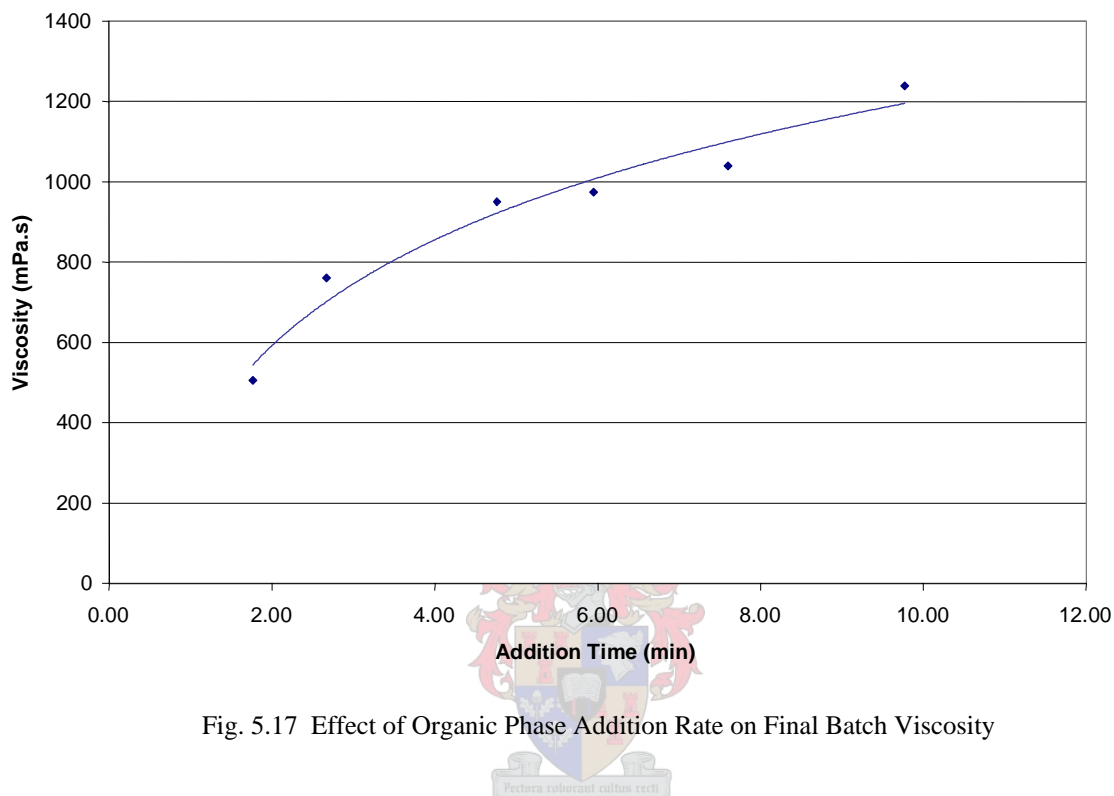


Fig. 5.17 Effect of Organic Phase Addition Rate on Final Batch Viscosity

5.3.3 Effect on pH

By investigating the change in pH with addition time (Figure 5.18), a decrease is observed with higher addition rates (i.e. shorter addition times). The pH of the aqueous solution consisting only of slightly acidic polivinyl alcohol (pH 5.81), cellulose thickener (pH 6.13) and de-ionised water (pH 6.80) without triamine present is about 6.08. With the strong basic triamine added to the aqueous phase also included the pH increases to about 10.49. From Figure 5.18 it therefore appears that there might still be a small amount of triamine present in the aqueous phase after curing since the pH range falls between 6.08 and 10.49. Furthermore it appears that, although the range may not be very wide (pH 6.63 – 7.00), more triamine migrates into the organic phase as the addition time is decreases.

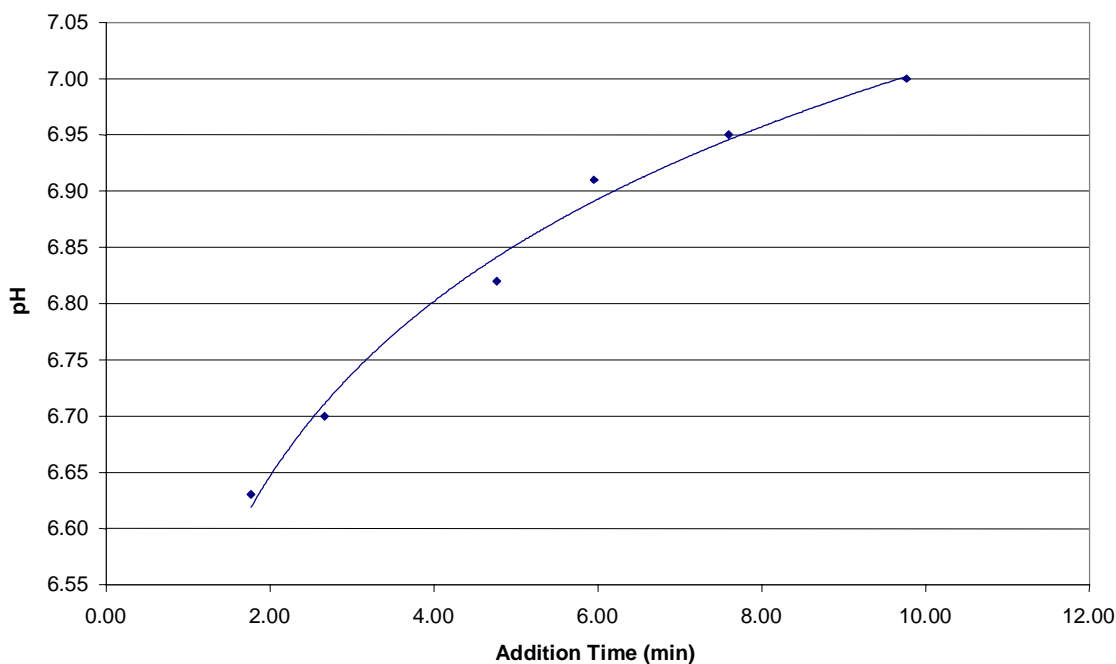


Fig. 5.18 Effect of Polyester Addition Rate on pH

5.3.4 Effect on Opacity

It was found in Section 5.2.3 that reduction in the emulsification time does not affect opacity even though the viscosity, and thus the solubility of the water in the organic phase, appear to increase with longer emulsification times. Similarly, it is found that reduction in the addition time has no visible effect on the luminosity or opacity values even though a significant variation in the product viscosity was observed.

5.4 Impeller Size

In all the experiments conducted in the previous sections, the standard 4-inch (102mm) diameter mixing blade was used in the 5ℓ reactor vessel[⊖]. In this investigation, we studied what the effect of various impeller blade sizes in the vessel has on properties. The standard formulation was used throughout using the KZN polyester and with the stirring speed remaining at 400 rpm in each run. The geometrically similar Cowles impeller blades that were used in each run were,

[⊖] Refer to Table 3.2, Chapter 3 for impeller dimensions

3 inches (76 mm), 4 inches (102 mm) and 5 inches (127mm) in diameter. The reactor vessel is only 180mm in diameter and larger impellers could not be utilised. Since it was only possible to perform three runs in this study, it was difficult to detect any conclusive variation in properties. Property analysis results of these runs appear in Table 5.5. A definite decrease in average particle and distribution can, however, be observed as the impeller diameter is increased. Other properties such as pH, viscosity and opacity appear to remain unaffected by this parameter.

Table 5.5 Effect of Impeller Size on Properties (5ℓ Vessel, 400 rpm)

Impeller Size (mm)	α_n (μm)	PSD	pH	η_{mf} (mPa.s)	Solids (wt/wt%)	θ_b (%)	θ_w (%)	$\theta = \theta_b/\theta_w$
76 (3")	4.57	2.08	6.83	995	24.11	90.0	93.6	0.96
102 (4")	3.76	1.62	6.81	1210	24.12	88.1	92.7	0.95
127 (5")	2.95	1.40	6.69	1020	23.82	90.6	94.8	0.95

5.4.1 Effect on Number Average Particle Size

Figure 5.19 shows that there is an almost linear decrease in the average particle size as a larger diameter impeller blade is used. The reason for this was discussed in Section 4.1 where it was concluded that utilisation of a larger blade causes a more effective flow pattern as a result of a higher shear area in contact with the fluid.

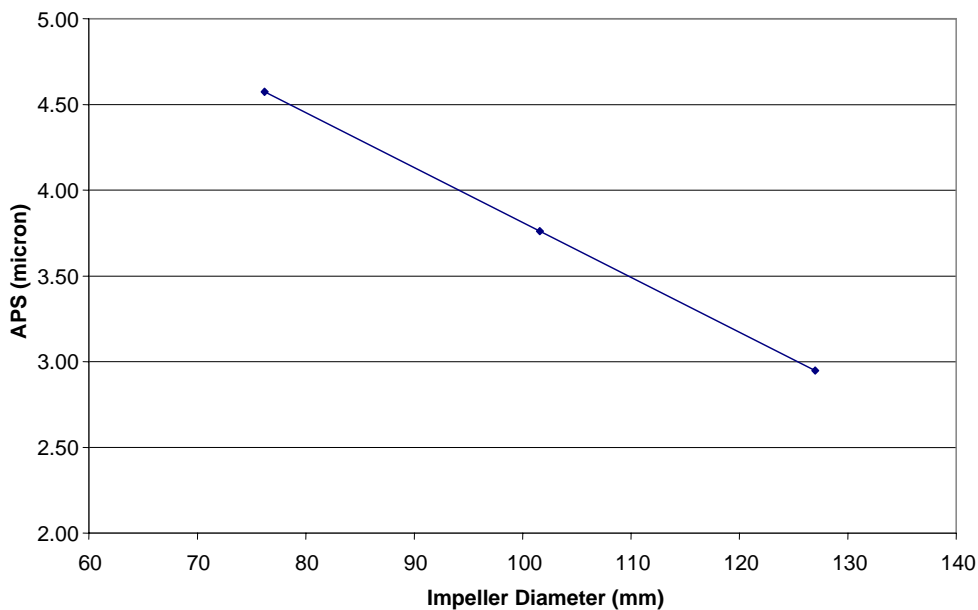


Fig. 5.19 Effect of Impeller Diameter Variation on Number Average Particle Size (5ℓ Vessel, Mixing Speed = 400 rpm)

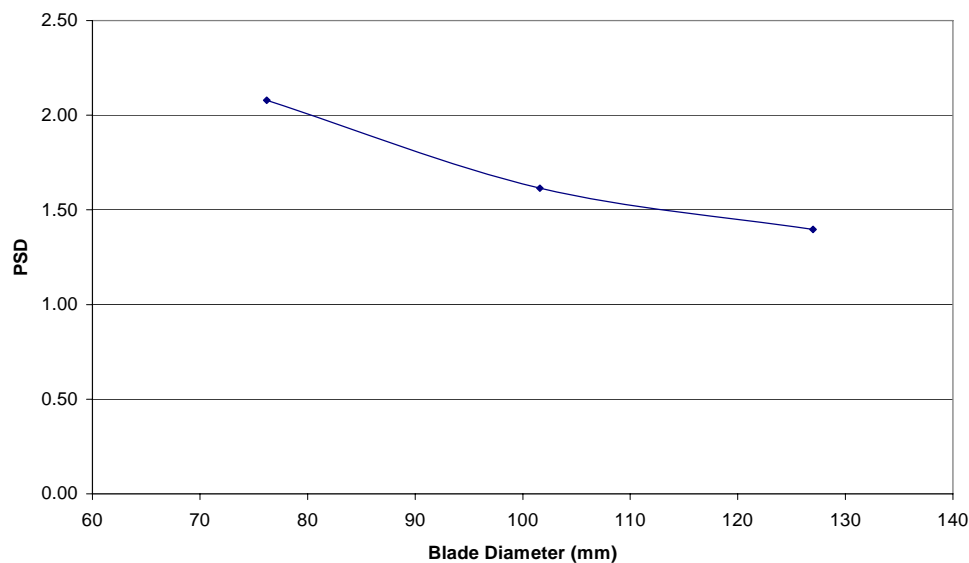
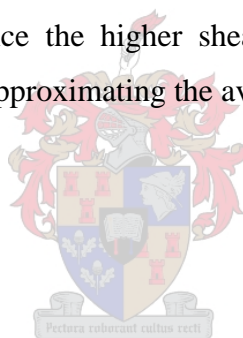


Fig. 5.20 Effect of Impeller Diameter Variation on Particle Size Distribution (5ℓ Vessel, Mixing Speed = 400 rpm)

The particle size distribution also shows a very similar decrease with increasing impeller size (Figure 5.20), since the higher shear area will cause more organic droplets to break down to sizes approximating the average particle diameter.



5.5 Mixing Speed

All the experiments performed in this discussion so far were executed using a mixing speed of 400 rpm during addition of the polyester phase and emulsification. As soon as the post treatment of de-ionised water and catalyst is started, this speed was reduced to 300 rpm. In this section variation of the dispersion speed will be studied, while maintaining the post-treatment blending speed at 300 rpm.

Experiments were performed using the standard formulation in the 5ℓ-reactor vessel and a 4-inch diameter blade. Dispersion speeds of 300, 400, 500, and 600 rpm were used, respectively. The analysis results appear in Table 5.6. From the data, it appears that pH, final batch viscosity and opacity remain unaffected by variations of this parameter within the variation investigated.

Table 5.6 Effect of Mixing Speed on Properties (5ℓ Vessel, 4” Impeller Diameter)

Mixing Speed (rpm)	α_n (μm)	PSD	pH	η_{mf} (mPa.s)	Solids (wt/wt %)	θ_b (%)	θ_w (%)	$\theta = \theta_b/\theta_w$
300	4.38	1.56	7.00	1368	23.96	90.9	94.6	0.96
400	3.50	1.82	6.94	1240	23.89	88.9	94.6	0.94
500	3.36	1.54	6.98	1154	23.47	89.3	95.0	0.94
600	2.83	1.17	6.85	1294	23.57	87.1	92.7	0.94

5.5.1 Effect on Number Average Particle Size

Figure 5.21 and 5.22 respectively presents the change in average particle size and particle size distribution with dispersion speed and a similar linear decline with elevated dispersion speed was observed as in the case where the impeller diameter was increased.

This decline is due to the higher shear rate that is being exerted on the polyester globules, causing more effective break down of smaller globules. This effect will be studied further in scale-up experiments performed on the 20ℓ-reactor vessel and discussed in Chapter 7.

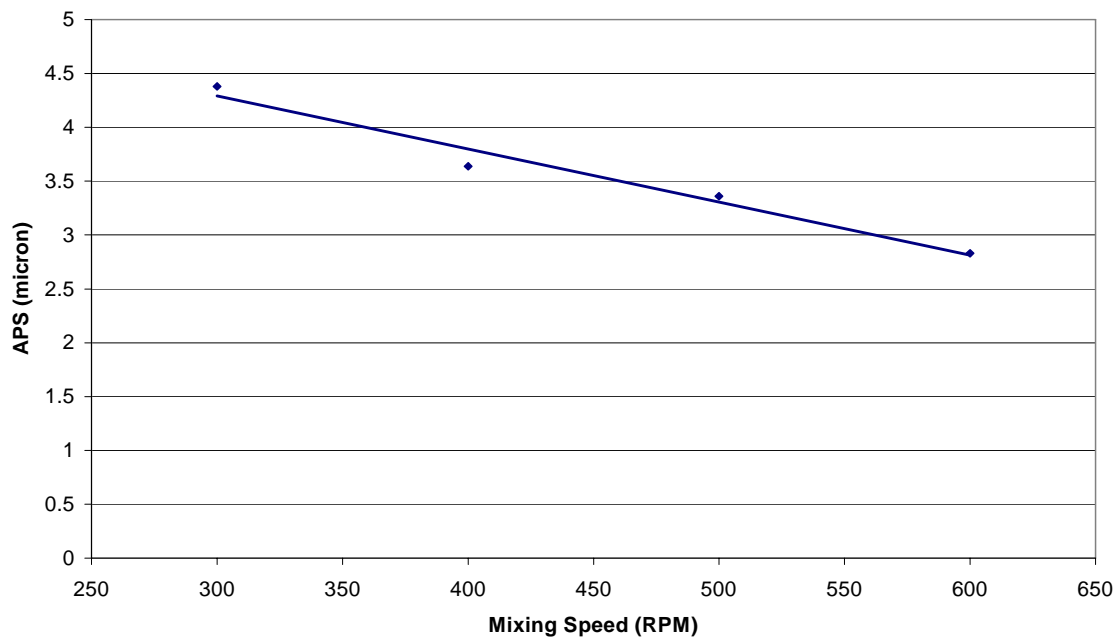


Fig. 5.21 Effect of Mixing Speed on Number Average Particle Size (5ℓ Vessel, 4” Diameter Impeller)

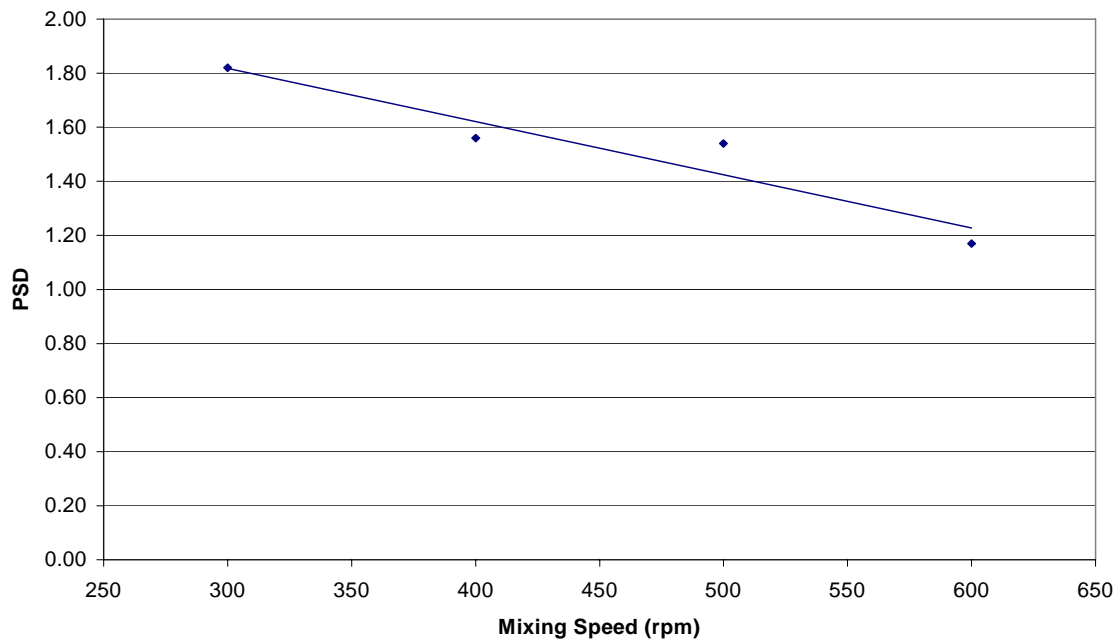
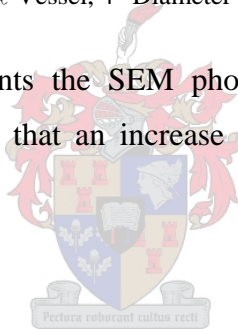


Fig. 5.22 Effect of Mixing Speed on Number Average Particle Size
(5ℓ Vessel, 4" Diameter Impeller)

Section C4, Appendix C presents the SEM photographs taken from draw-down samples of each run and shows that an increase in shear conditions do not cause damage to the vesiculated beads.



5.6 Fluid Height to Vessel Diameter Ratio

The final production parameter that was investigated, was the effect of changes in the batch volume prepared in the 5ℓ vessel. It was expected that by reducing the fluid height to vessel diameter ratio (H_f/D_t) and maintaining constant dispersion conditions, a more effective flow pattern will develop, causing better dispersion and hence smaller particle diameters. Experiments were performed following standard procedure and conditions (4-inch diameter blade dispersing at 400 rpm). Five runs were performed where the fluid height to vessel diameter was 1.1, 1.0, 0.9, 0.8 and 0.7, respectively, and the components in each formulation adjusted analogically to the final batch weight. A fluid height to vessel diameter of 1.1 corresponds to the standard 5kg batch. The analysis results appear in Table 5.7.

Table 5.7 Effect of Fluid Height to Vessel Diameter Ratio on Properties

H_f/D_t (m/m)	α_n (μm)	PSD	pH	η_{mf} (mPa.s)	Solids (wt/wt %)	θ_b (%)	θ_w (%)	$\theta = \theta_b/\theta_w$
1.1	3.56	1.49	6.90	1238	23.67	90.2	93.0	0.97
1.0	3.41	1.76	6.84	1350	23.76	87.6	94.4	0.93
0.9	4.29	1.85	6.80	1326	23.65	88.5	92.6	0.96
0.8	4.01	1.59	6.76	1468	23.41	88.2	92.8	0.95
0.7	3.91	1.66	6.75	1210	23.94	88.4	93.0	0.95

It appears that this parameter has no noticeable effect on any properties within the variations investigated and both the average particle size and distribution do not decrease as expected.

It can be concluded from the results discussed in this chapter, that the average particle size is dependent on the mixing intensity, including impeller diameter and mixing speed, as well as the emulsification temperature and time. The fluid height to vessel diameter ratio showed a negligible effect on particle size.

In Chapter 7 it will be attempted to use the data discussed in this chapter to model the average particle size as function of the important processing parameters. However, the effect of selected chemical changes in the vesiculated bead formulation will be investigated first in the following chapter.

Chapter 6

Effect of Variations in Chemical Composition

Although the focus of this study was primarily to investigate the effect of variations in processing conditions, a limited number of experiments were performed where selected constituent concentrations in the vesiculated bead formulation were altered to examine the effect on bead properties. The variations that were found to have significant effect include pre-addition of post treatment de-ionised water as well as the hydrolysed polyvinyl acetate and cellulose thickener weight ratios. The effect of an external surfactant to the polyester phase was also investigated, and finally the effect of post-treatment addition variations, which include the post-treated de-ionised water, catalyst, bactericide, and surfactant, was studied.

6.1 Pre-addition of Post Treatment Water

Experiments were conducted where it was examined what the impact would be if de-ionised water, used as post-treatment after emulsification (according to the formulation), is added directly to the primary aqueous phase before addition of the polyester resin. Different weight percentages of this water were initially added to the aqueous phase, while the rest was retained for use as post-treatment. Therefore, the total water concentration in each completed batch remained the same, thus maintaining the solid content at a constant level of 24 wt%. Six runs were performed where 0, 10, 20, 40, 60, 80, and 100 wt% of the water was used for post-treatment. The standard production procedure was followed in the 5ℓ vessel using the 4-inch diameter blade at a mixing speed of 400 rpm. The results of the property analysis are presented in Table 6.1.

6.1.1 Effect on Number Average Particle Size

A significant change in average particle size occurs as the pre-treated water added to the aqueous phase is increased. Where all the water (100 wt%) is blended into the

Table 6.1 Effect of Pre-addition of Post-treatment Water on Properties

Water used for post-addition (wt %)	α_n (μm)	pH	η_{mf} (mPa.s)	Solids (wt/wt %)	θ_b (%)	θ_w (%)	$\theta = \theta_b/\theta_w$
0	12.98	6.91	1576	23.45	86.0	92.4	0.93
20	11.28	6.82	1826	22.46	86.2	92.1	0.94
40	8.09	6.90	1503	23.28	87.9	93.1	0.94
60	7.12	6.90	2270	23.81	88.0	93.2	0.94
80	5.98	6.95	1494	22.69	92.2	94.4	0.98
100	3.81	6.94	1130	23.64	90.9	94.4	0.96

aqueous phase the particle size is extremely high and decreases almost linearly as the percentage is decreased (Figure 6.1). The last run (0 wt% water used for pre-treatment) corresponds to a standard vesiculated bead production and the particle size value is comparative to values found in past using similar standard production procedures.

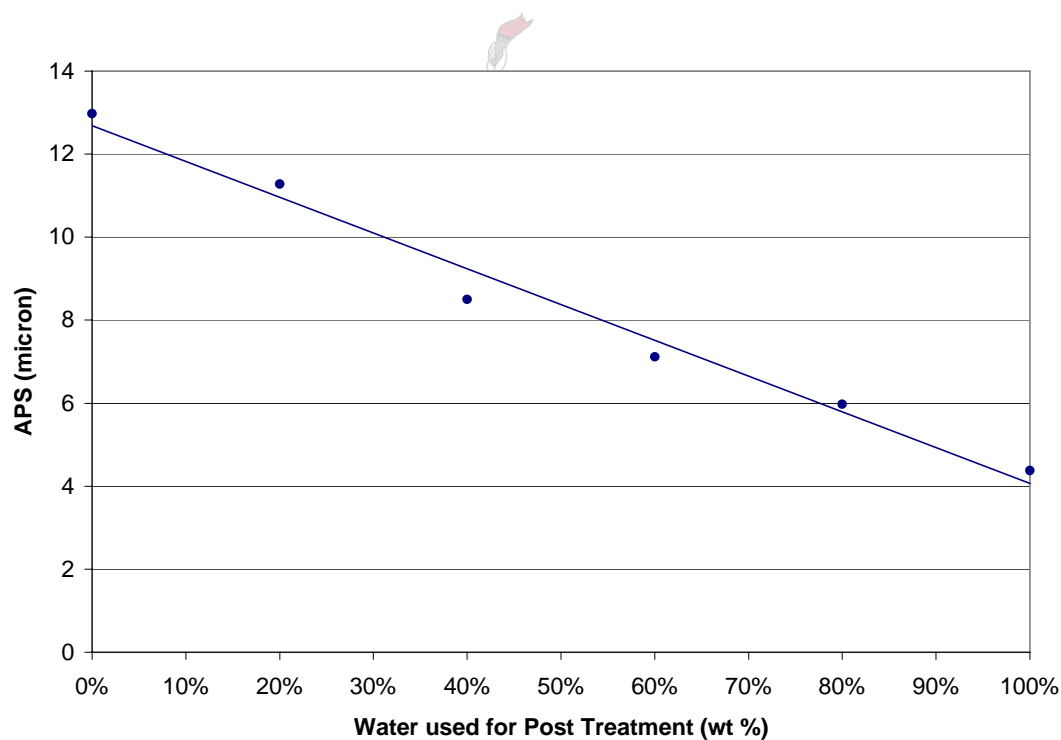


Fig. 6.1 Effect of Pre-addition of Post Treatment Water on the Number Average Particle Size (5ℓ Vessel, 4” Diameter Impeller, 400 rpm)

The reason why this occurs can possibly be explained by looking at the water-solubility of the organic phase. It was seen in Section 5.2 that by reducing the emulsification time, the water-solubility becomes lower, suggesting that water

migration into the organic droplets already occur during production. The high molecular weight colloid stabilisers (partially hydrolysed polyvinyl acetate and cellulose thickener) present in the initial aqueous phase assist in preventing formed droplets to agglomerate, effectively causing an increase in the interfacial tension. If a high water concentration is initially present in this phase, it will cause more effective migration of water (and polyamine) toward the organic droplet interface. This will make it easier for the polyamine present in the aqueous phase to perform neutralisation with the polyester. Since neutralisation is proposed to cause a more dense macro-molecular structure in the organic phase, the interfacial tension will increase, resulting in larger droplets to be formed (overall possessing a smaller interfacial area).

This possibly explains the particle size development in Figure 6.1.

6.1.2 Effect on pH

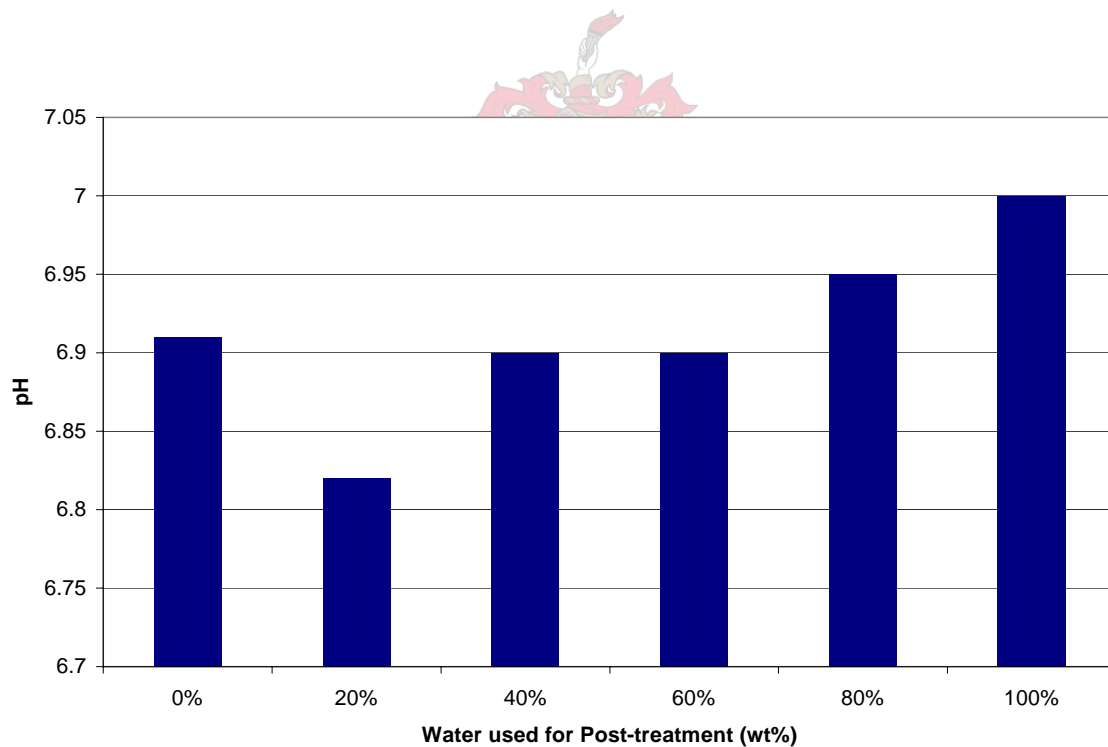


Fig. 6.2 Effect of Pre-addition of Post Treatment Water on the pH
(5ℓ Vessel, 4" Diameter Impeller, 400 rpm)

Although not evident from the values in Table 6.1, it appears from Figure 6.2 that a small decrease in pH occurs from 100% water, used for post-addition, towards 20%. This may be attributed to the ease with which the polyamine migrates through the less dense aqueous phase to perform neutralisation with the polyester. Consequently, this

will result in increasingly less polyamine base to be present after the batch is completed and explains the lower pH measured.

However, in the case where all the water was added to the initial aqueous phase, the pH shows a value larger than expected. The reason for this has not been determined.

6.1.3 Effect on Final Viscosity

If we look at the final viscosity values, presented in Figure 6.3, no distinctive variation for this set of experiments is observed and measurements appear somewhat erratic. However, the values except for the one experiment where no additional water is used for pre-addition, appear relatively larger to those measured in previous experiments. This might be attributed to the increase in the solubility as the water concentration is increased in the primary aqueous phase. This theoretically results in less water being available in the aqueous phase at the end of the production and thus causes an increase in the final batch viscosity.

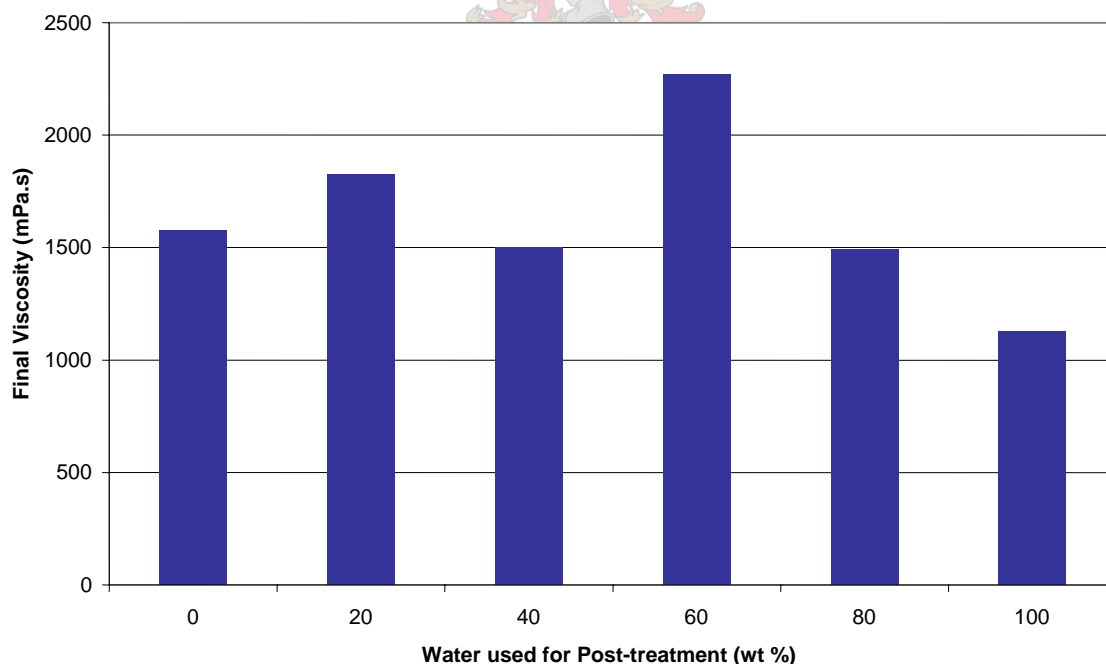


Fig. 6.3 Effect of Pre-addition of Post Treatment Water on the Final Batch Viscosity
(5l Vessel, 4" Diameter Impeller, 400 rpm)

6.1.4 Effect on Opacity

From Table 6.1 it appears that the pre-addition of water has almost no effect on the opacity. However, the effect becomes more pronounced if we look at the separate luminosity values measured on the black and white surfaces (Figure 6.4). By adding more water used for post-treatment to the primary aqueous phase it seems that the luminosity on both surfaces decreases even though it is presumed that the water-solubility increases with an increase in the water concentration.

This once again shows, similar to the case where the effect of production temperature was studied (Section 5.1), that an increase in water-solubility during production does not necessarily suggest an increase in the opacity. It is possible that with an increase in the water-solubility of the polyester, larger vesicles are formed in the organic droplets which causes a reduction in the scattering efficiency of incident light and therefore, in the luminosity as well.

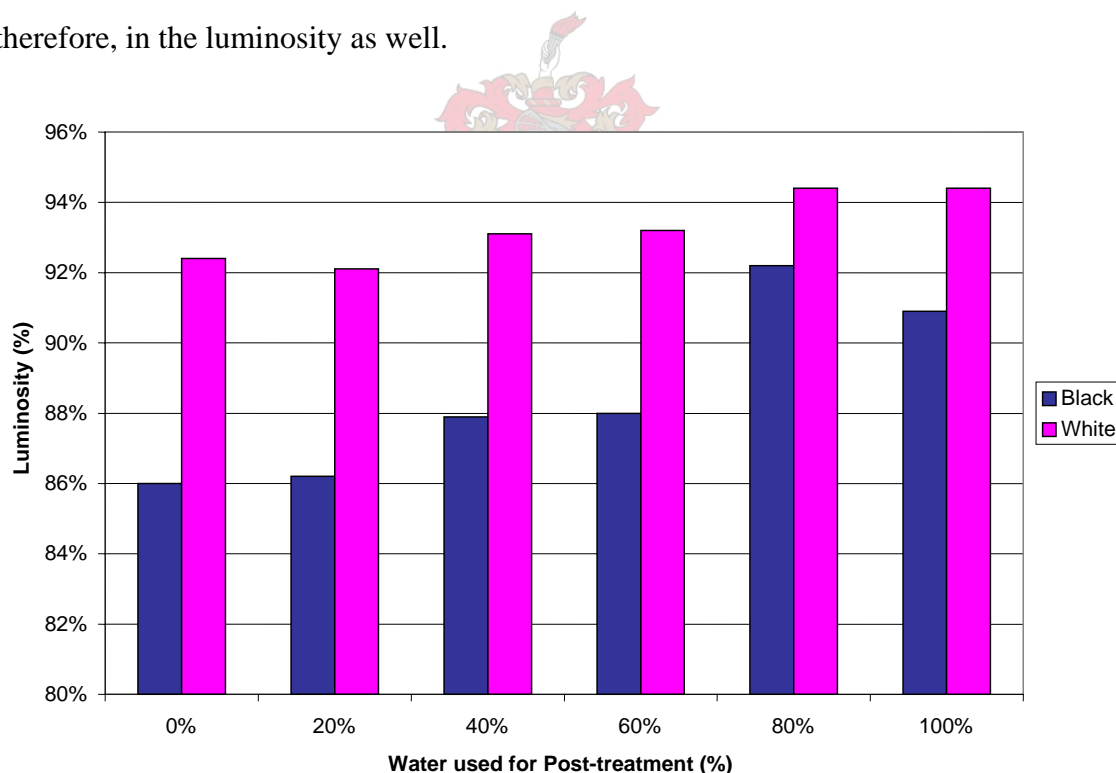


Fig. 6.4 Effect of Pre-addition of Post Treatment Water on the Luminosity on Black and White Surfaces
(5ℓ Vessel, 4" Diameter Impeller, 400 rpm)

6.2 Polyvinyl Alcohol/Cellulose Thickener Weight Ratios

In Section 6.1 it was observed that the average particle size is significantly affected by the water and colloid stabiliser concentrations in the aqueous phase. This led to an investigation into the effect of the weight ratios of polyvinyl alcohol and cellulose thickener initially loaded to the primary reactor.

Several experiments were performed in the 5ℓ-reactor vessel where this ratio was varied. Normally the aqueous phase consists of 78.5 wt% cellulose thickener solution with a concentration of 0.5 wt% and 21.5% partially hydrolysed polyvinyl acetate solution with a concentration of 10 wt%. A cellulose thickener solution weight percentage in the total primary aqueous phase of 70.0, 73.0, 76.0, 78.5 (standard), 83.0 and 86.0 wt % (respectively, consisting of 0.35, 0.37, 0.38, 0.39 (standard), 0.42 and 0.43 wt % cellulose thickener) were used individually in each run with the rest of the aqueous phase consisting of polyvinyl alcohol solution and water. The remaining components used were according to the standard formulation and prepared under normal production conditions. Results gathered from property analysis appear in Table 6.2.

Table 6.2 Effect of Polyvinyl Alcohol/ Cellulose Thickener Weight Ratios on Properties

Cellulose Thickener Conc. (wt%)	α_n (μm)	pH	η_{mf} (mPa.s)	Solids (wt/wt %)	θ_b (%)	θ_w (%)	$\theta = \theta_b/\theta_w$
0.35	4.85	6.85	1270	22.54	85.1	91.5	0.93
0.37	4.16	6.82	1150	23.12	87.0	92.5	0.94
0.38	3.15	6.87	1364	23.07	83.8	92.1	0.91
0.39	2.81	6.85	1165	22.78	85.6	93.0	0.92
0.42	2.17	6.98	996	23.15	88.5	94.2	0.94
0.43	1.80	6.95	955	23.51	88.1	93.7	0.94

6.2.1 Effect on Number Average Particle Size

Figure 6.5 indicates that as the cellulose thickener concentration in the primary aqueous phase is increased, the average particle size decreases almost linearly. A similar behaviour was observed as in the previous investigation (Section 6.1). As

before, with a lower concentration cellulose thickener in the aqueous phase, it is increasingly easier for polyamine and water to migrate through the dense cellulose chains where it is neutralised, forming large denser droplets possessing a high interfacial tension. This may once again be the reason why batches prepared using a low concentration cellulose thickener possess larger particle size.

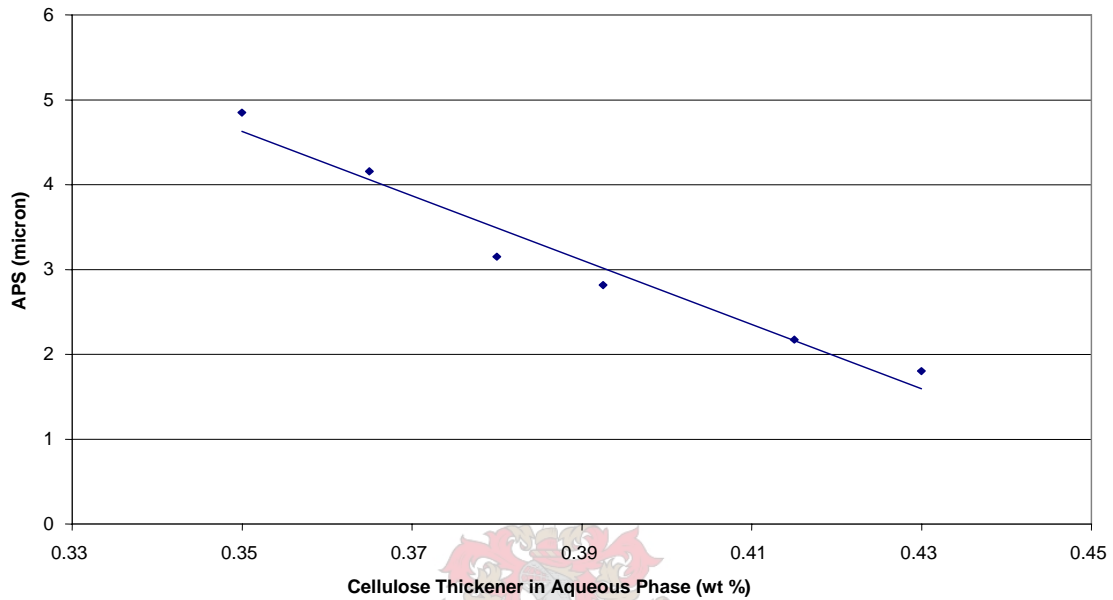
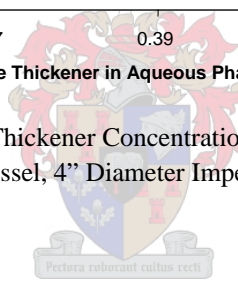


Fig.6.5 Effect of Cellulose Thickener Concentration on Number Average Particle Size (5ℓ Vessel, 4” Diameter Impeller, 400 rpm)



6.2.2 Effect on pH

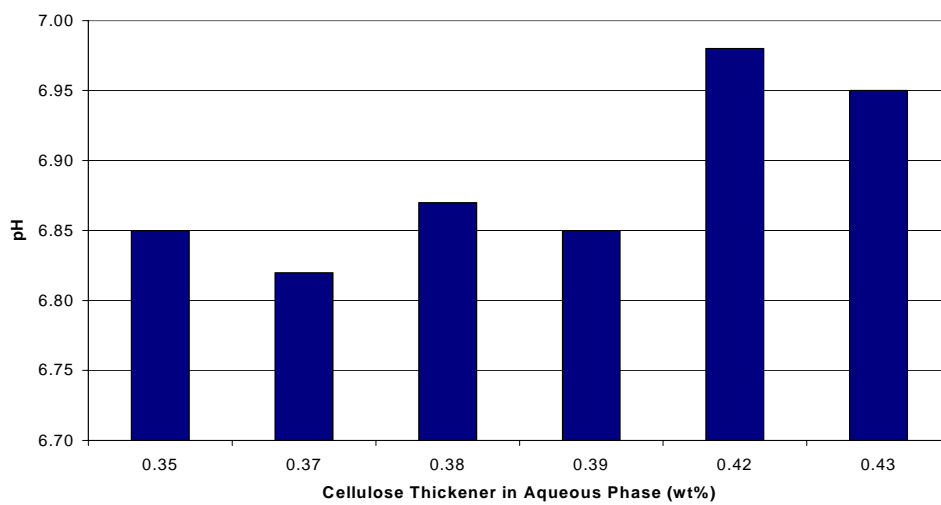


Fig.6.6 Effect of Cellulose Thickener Concentration on pH (5ℓ Vessel, 4” Diameter Impeller, 400 rpm)

Since it is proposed that the polyamine undergo increasingly more neutralisation with the polyester as the cellulose thickener concentration in the aqueous phase is lowered, it is expected that the pH will decrease accordingly. Figure 6.6 presents the measured values and although very little variation is observed, it does appear that a lower pH is found at lower concentrations.

6.2.3 Effect on Final Viscosity

Figure 6.7 presents the final viscosity values for each run and a very small increase is observed as the cellulose thickener concentration is decreased, possibly corresponding to an increasingly higher water-solubility in the organic phase during production. With a higher solubility, a lower concentration water is present in the vesiculated bead matrix after the beads have formed and hence, higher viscosity. The same behaviour was observed in Section 6.1.3. Note that at the low colloid stabiliser concentration of 0.35 wt%, a small amount of settling of the beads was observed at the bottom of the container. This indicates that the stabiliser concentration here was too low to keep the bead granules in suspension.

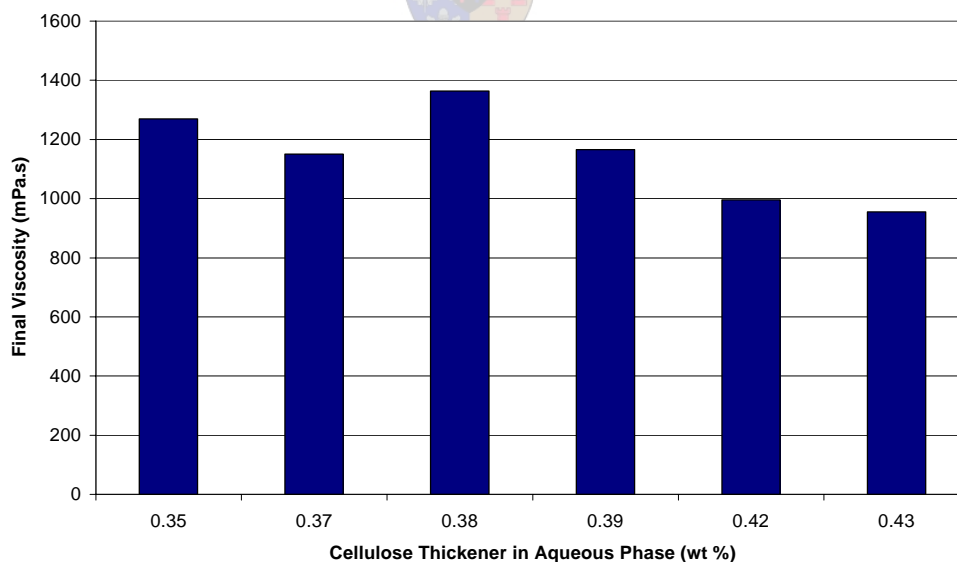


Fig.6.7 Effect of Cellulose Thickener Concentration on Final Batch Viscosity (5l Vessel, 4" Diameter Impeller, 400 rpm)

6.2.4 Effect on Opacity

Similar to the previous investigation where the effect of pre-addition of post-treatment water was investigated (Section 6.1), it was observed that very little change in the opacity occurred (Table 6.2), but Figure 6.8 indicates a small decrease in the separate luminosity measurements on the black and white surfaces as the cellulose thickener concentration was decreased. This may once again be due to potentially larger vesicles formed in the beads, causing a poorer light scattering efficiency, thus resulting in lower luminosity.

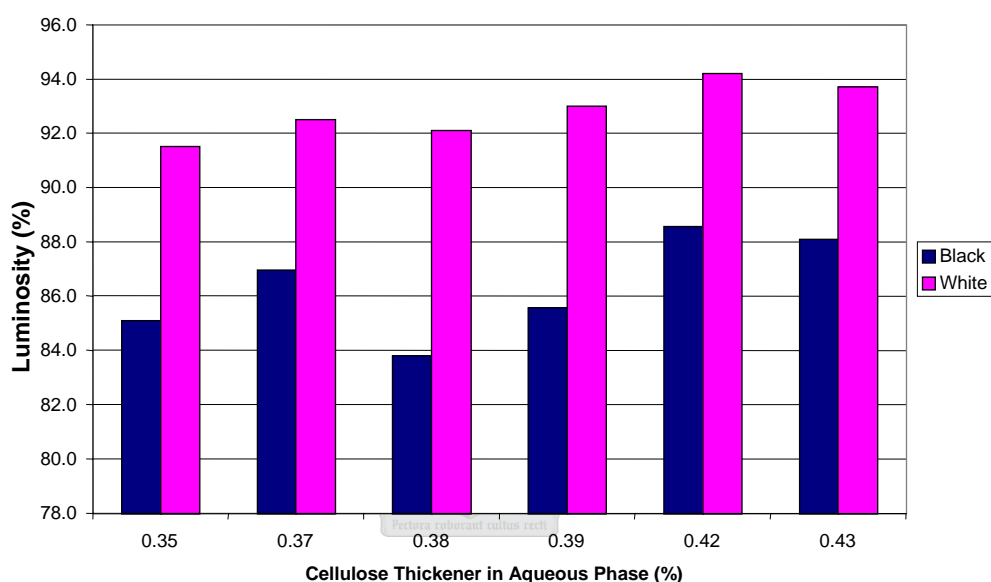


Fig.6.8 Effect of Cellulose Thickener Concentration on Luminosity
(5ℓ Vessel, 4" Diameter Impeller, 400 rpm)

6.3 Addition of Surfactant to Organic Phase

The effect of incorporating an additional surfactant into the dispersed polyester phase was also investigated. The reason for the addition of surfactant is to prevent possible migration of water vesicles, created inside the droplets during production, towards the drop surface and ultimately be released back into the continuous aqueous phase. This will increase the light scattering efficiency of the beads and hence, the opacity, resulting in a whiter bead.

Aside from the addition of 2 wt% of this surfactant into the organic pre-dispersion, the standard formulation was used under standard production procedure in the 5ℓ reactor vessel. It was, however, decided to perform three experiments where the mixing speed was maintained at 300, 400 and 500 rpm, respectively, during the addition and emulsification period, using the 4-inch diameter impeller blade. Table 6.3 contains the property analysis results.

Table 6.3 Effect of Additional Surfactant Addition on Properties at Various Mixing Speed
(5ℓ Vessel, 4" Impeller Blade)

Mixing Speed (rpm)	α_n (μm)	PSD	pH	η_{mf} (mPa.s)	Solids (wt/wt %)	θ_b (%)	θ_w (%)	$\theta = \theta_b/\theta_w$
300	3.09	1.22	6.78	1680	23.41	92.9	96.1	0.97
400	2.62	0.94	6.85	1592	23.65	91.7	96.2	0.95
500	2.18	1.00	6.73	1770	23.45	91.5	96.1	0.95

6.3.1 Effect on Number Average Particle Size

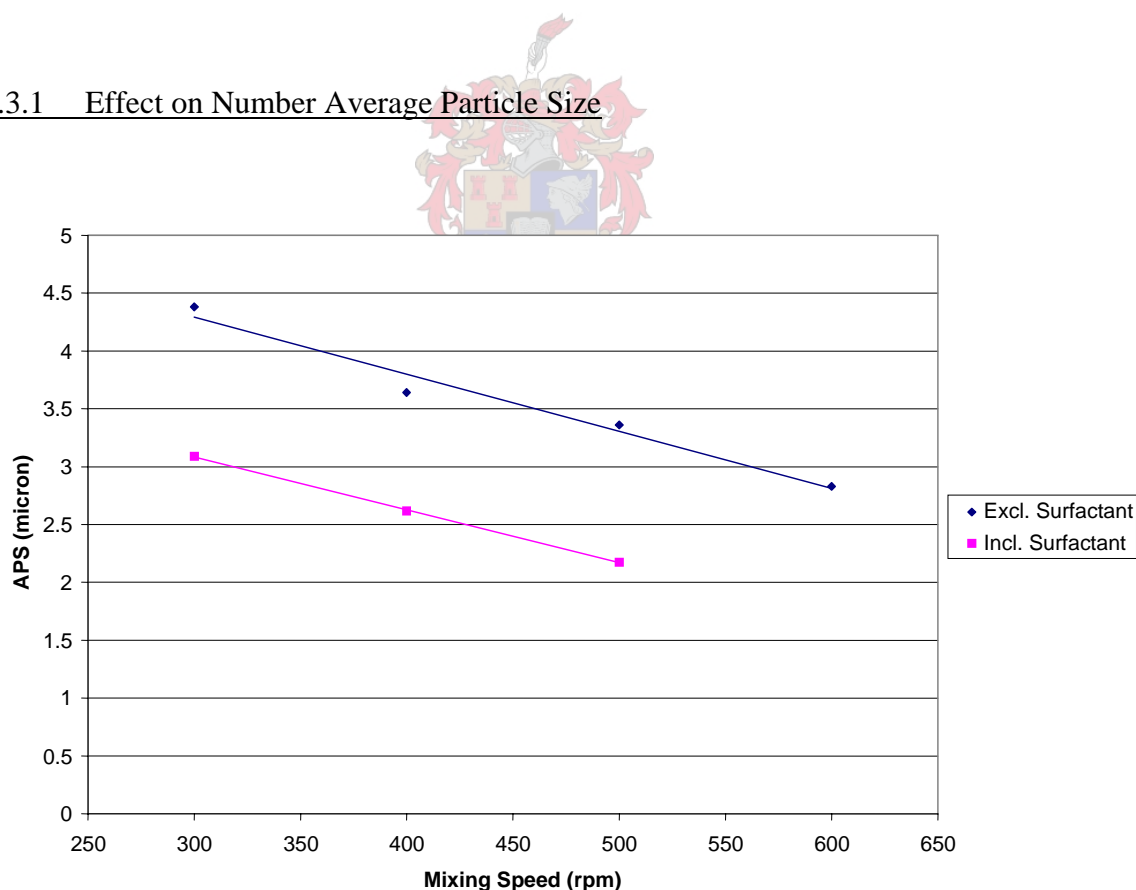


Fig.6.9 Effect of Additional Surfactant in Pre-dispersion on Number Average Particle Size at Various Mixing Speed (5ℓ Vessel, 4" Impeller Blade)

Figure 6.9 shows the comparison of the average particle size values from experiments where dispersion speed variations were investigated using the standard formulation (Section 5.5) and those where additional surfactant was included. Once again a very linear reduction in average particle is observed with an increase in mixing speed. However, the values are significantly lower than before. The reason for this might be due to the effect of the surfactant on the surface tension between the vesiculated globules and the aqueous phase. The surfactant induces a lower surface tension resulting in droplets breaking down into smaller droplets occupying a larger overall surface area.

6.3.2 Effect on Final Viscosity

Figure 6.10 presents the comparison between the final viscosity of the batches in this investigation and those obtained using the standard formulation (Table 5.6).

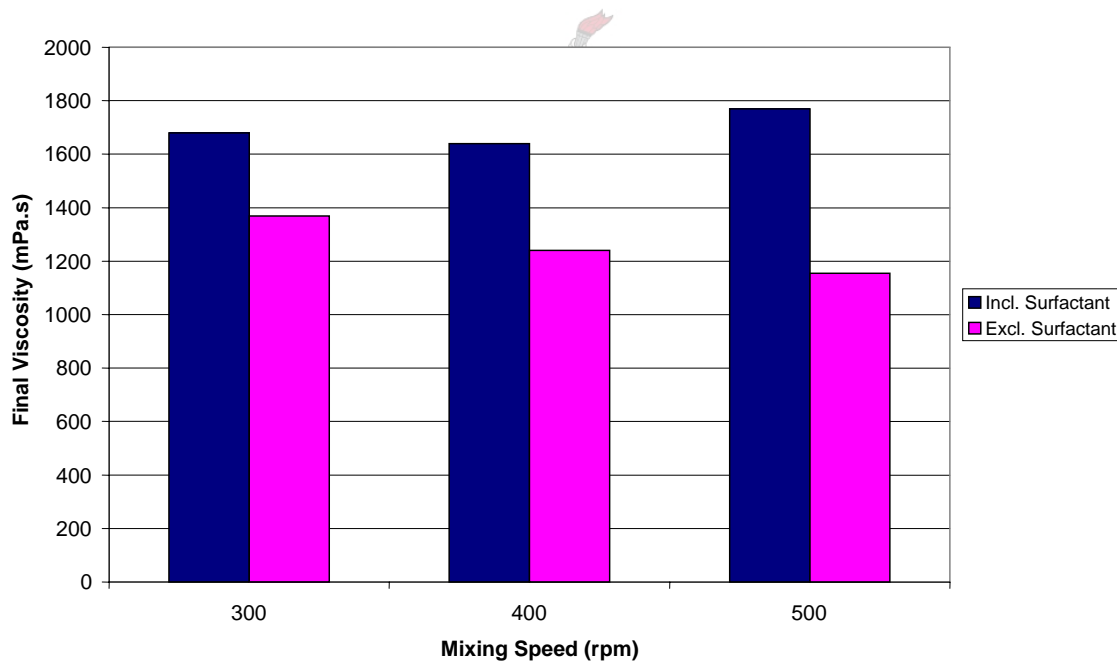


Fig.6.10 Effect of Additional Surfactant in Pre-dispersion on Final Batch Viscosity at Various Mixing Speed (5ℓ Vessel, 4” Impeller Blade)

We clearly observe a significant higher viscosity using this surfactant in the formulation. This possibly indicates that there is a significant lower concentration of water left in the aqueous phase after the solid beads have formed and more water in the beads, also implying a higher degree of vesiculation. With a lower interfacial tension, the vesicles formed during production close to the droplet interface will not

have a high tendency to migrate back into the continuous phase, thus explaining this behaviour.

The surfactant, present in the organic phase also possesses hydrophilic groups on the molecules, which will attract more water into droplets, implying it will become more water-soluble.

From all the experimental runs performed during this study, there is no decisive indication that a smaller average particle size can be related to an increase in viscosity.

6.3.3 Effect on Opacity

The opacity is higher than the values of similar runs performed without using surfactant. This can be seen more clearly by comparing the separate luminosity values for each run (Figure 6.11).

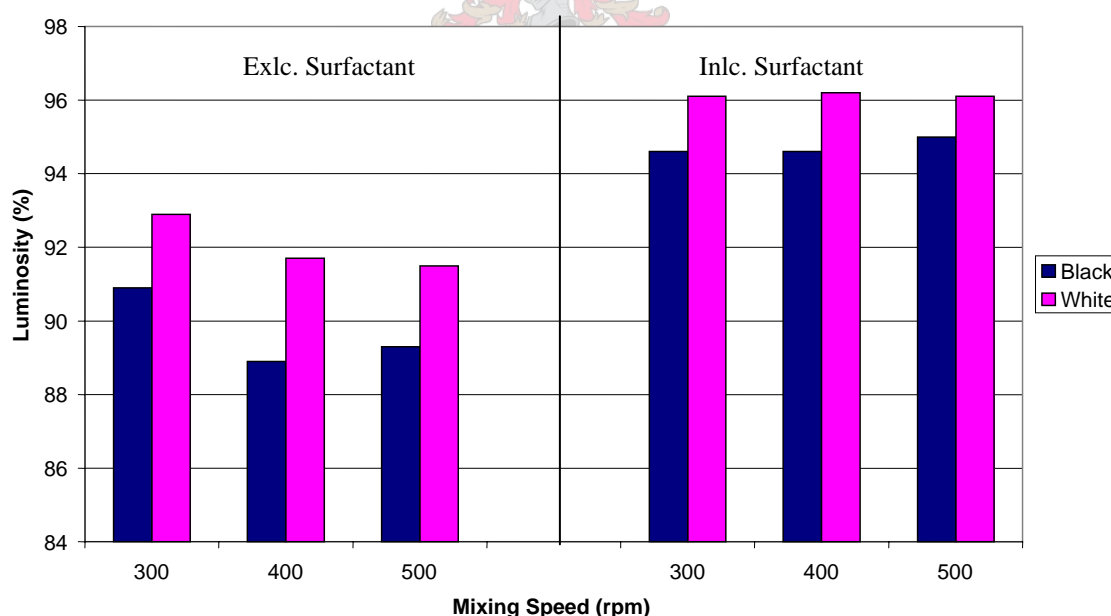


Fig.6.11 Effect of Additional Surfactant in Pre-dispersion on Luminosity at Various Mixing Speed (5ℓ Vessel, 4" Impeller Blade)

The increase in opacity can be ascribed to the higher degree of vesiculation, in other words, a higher volume vesicles found in the beads. It may also be possible that since the interfacial tension during production is lower, vesicles formed in close vicinity to

each other will not easily agglomerate. Thus, smaller vesicles are formed which may improve the scattering-efficiency of incident light and therefore improve the opacity as well. This was observed in Figure 3.14, Chapter 3, where additional surfactant was added to Sample C. Microtoming indicated the formation of very small vesicles, which corresponded to a high opacity.

6.4 Effect of Post Additions on Final Viscosity

In the course of this study it has been observed that viscosity analysis presented measurements that were extremely inconsistent and difficult to model, apart from the fact that the non-newtonian behaviour of vesiculated beads had to be taken into consideration. Since alteration of the primary constituents in the formulation, discussed in the previous sections, presented no significant variation in the viscosity, it was decided to investigate the effect of post-added components, including post-treatment water, catalyst and surfactant; the latter added 12-hours after production.

In Chapter 4 the development of average particle size over the emulsification stage was investigated where samples were extracted over the 20 minute emulsification period. During experiments conducted in the 20l reactor vessel, 250ml samples were extracted and immediately catalysed to initiate bead formation. The samples were weighed and all post treatments added proportional to the standard formulation, and recorded. Apart from using these samples for average particle size analysis, the final viscosity of each sample was also determined. This was done for two separate runs using the 4 and 5-inch diameter blades at a dispersion speed of 400 rpm, respectively.

Table 6.4 and 6.5 shows the viscosity of the samples in each run as well as the time at which it was extracted and the percentage post-treatment constituents added. The corresponding average particle size values together with the particle size distribution (PSD) and skewness of particle distribution were also calculated and presented in these tables. These parameters are assumed to be the only variables since the remainder of the constituent and production parameters are analogous for each run.

Table 6.4 Experimental Analysis and Percentage Post-Treatment Additions – Run 1
(5" Impeller, 400 rpm, 20ℓ Vessel)

Sample	η_f (mPa.s)	t_e (min)	α_n (μm)	PSD	Skew	Post-Additions (wt% of Total Batch)			
						Redox Activa- tor	F/R Init- iator	Post Treat. Water	Surfac- tant
1	545	1	5.69	2.88	1.13	0.23	0.13	14.38	1.05
2	1275	2	4.46	2.51	1.29	0.21	0.12	12.96	1.09
3	1245	3.5	3.90	1.88	1.56	0.21	0.12	12.96	1.20
4	1410	5	3.73	1.74	1.36	0.22	0.13	13.91	1.12
5	1185	7.5	3.28	1.37	1.15	0.21	0.15	13.05	0.95
6	785	10	3.34	1.40	1.10	0.22	0.16	13.40	0.93
7	1600	15	3.26	1.26	1.19	0.23	0.11	12.49	0.88
8	835	20	3.17	1.25	0.77	0.23	0.12	14.16	1.10

Table 6.5 Experimental Analysis and Percentage Post-Treatment Additions – Run 2
(4" Impeller, 400 rpm, 20ℓ Vessel)

Sample	η_f (mPa.s)	t_e (min)	α_n (μm)	PSD	Skew	Post-Additions (wt% of Total Batch)			
						Redox Activa- tor	F/R Init- iator	Post Treat. Water	Surfac- tant
1	745	1	8.81	4.82	1.38	0.25	0.12	13.61	1.02
2	1395	2	7.81	3.57	1.15	0.25	0.13	14.28	1.19
3	2120	3.5	6.29	2.80	0.65	0.25	0.14	15.06	1.17
4	755	5	5.64	2.67	1.55	0.25	0.18	16.13	1.09
5	1625	7.5	5.39	1.55	1.55	0.24	0.14	14.89	1.14
6	1585	10	5.07	1.97	0.54	0.24	0.14	15.82	1.11
7	1695	15	4.81	1.60	0.36	0.23	0.16	14.60	1.13
8	710	20	4.41	2.04	0.85	0.22	0.16	14.05	1.05

A sensitivity analysis was performed on this data to find the most influential parameter(s). This involves the execution of regression analysis to see if there exists a possible relationship between these parameters and the final batch viscosity, the latter being the dependent variable and the parameters mentioned above, the independent variables. It was investigated if a multiple linear regression model would be sufficiently accurate in accomplishing this.

In general, a multiple regression procedure will estimate a linear equation of the form:

$$Y = a + b_1 X_1 + b_2 X_2 + \dots + b_p X_p \quad \dots(6.1)$$

where:

- Y = Dependent Variable
- X = Independent Variable
- b = Regression Coefficient
- p = Number of Independent Variable

Note that in this equation, the regression coefficients represent the independent contributions of each independent variable to the prediction of the dependent variable. In other words, a large regression coefficient would signify that the independent contribution to the dependent variable is considerable, whereas small coefficients denote a less significant contribution.

The analysis was performed using Microsoft Excel's Regression Analysis Tool function, which calculates the regression coefficients using the "least-squares" method. The initial viscosity is entered as the dependent variable and percentage (w/w) post treatment water, redox activator, free radical initiator, and surfactant added to each sample as well as the average particle size (APS), particle size distribution (PSD), skewness (Skew), and emulsification time as independent variables. However, it is first necessary to standardise the data in order to convert it to values of the same order of magnitude. This is done using Equation 6.2.


$$Z' = \frac{Z - \mu}{\sigma} \quad \dots(6.2)$$

where:

- Z = Variable Value
- μ = Arithmetic Mean of the Variable Distribution
- σ = Standard Deviation of the Variable Distribution

The standardised values of each variable are presented in Tables D1.1 and D1.3, Appendix D, with the corresponding regression coefficients calculated by Excel. In both cases the coefficient of determination, or r^2 , is unity indicating a strong linear relationship between the independent variables and the viscosity. Figures 6.12 and 6.13 present a pie plot indicating the magnitude of the regression coefficients of each independent variable, respectively.

For both runs it appears that the individual final addition components show similar contributions to the final batch viscosity. The most influential components appear to be the post-treatment water and surfactant. A higher concentration post-treatment water possibly relate to more water being present in the aqueous phase after formation of the beads, effectively making the bead matrix less viscous, therefore relating to a lower viscosity.

The solid beads formed after catalysis are held stable in dispersion by the colloid stabilisers (partially hydrolysed polyvinyl acetate and cellulose stabiliser) added to the system. However, the vesiculated beads still possess a tendency to densely compact closely to each other when left static, causing a potentially higher viscosity. The surfactant added to the system after 12 hours prevents this and effectively keeps beads in a vicinity further away from each other, resulting in a lower viscosity. Therefore, more of this constituent present in the system may cause lower viscosity and explains the larger contribution.

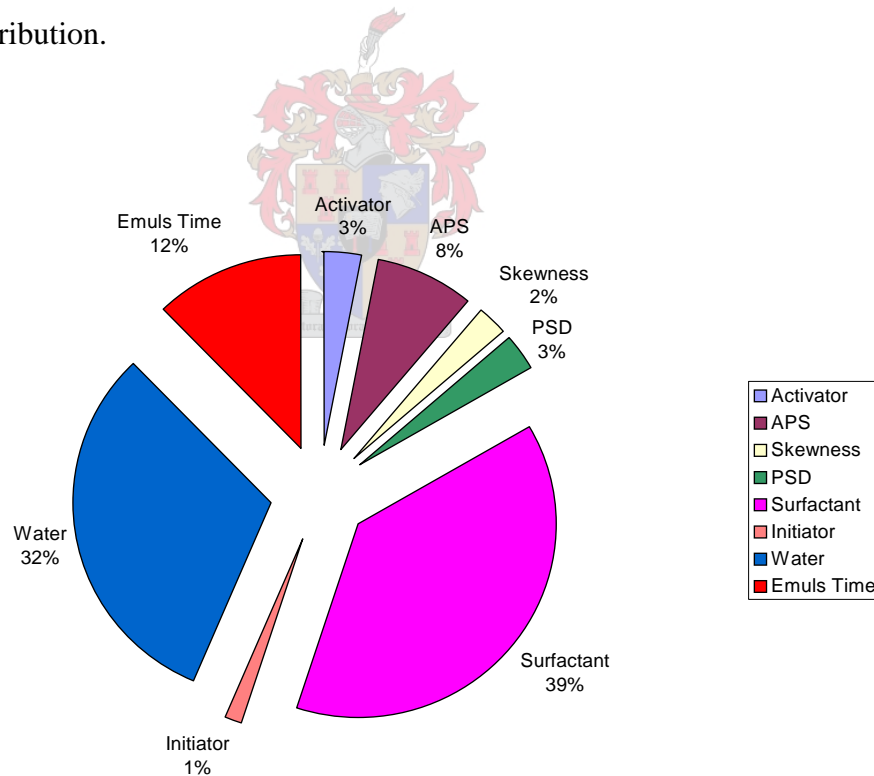


Fig.6.12 Pie Plot Indicating the Effect of Variations in Post Addition Constituents on the Final Viscosity for Run 1 (5" Impeller, 400 rpm, 20ℓ Vessel)

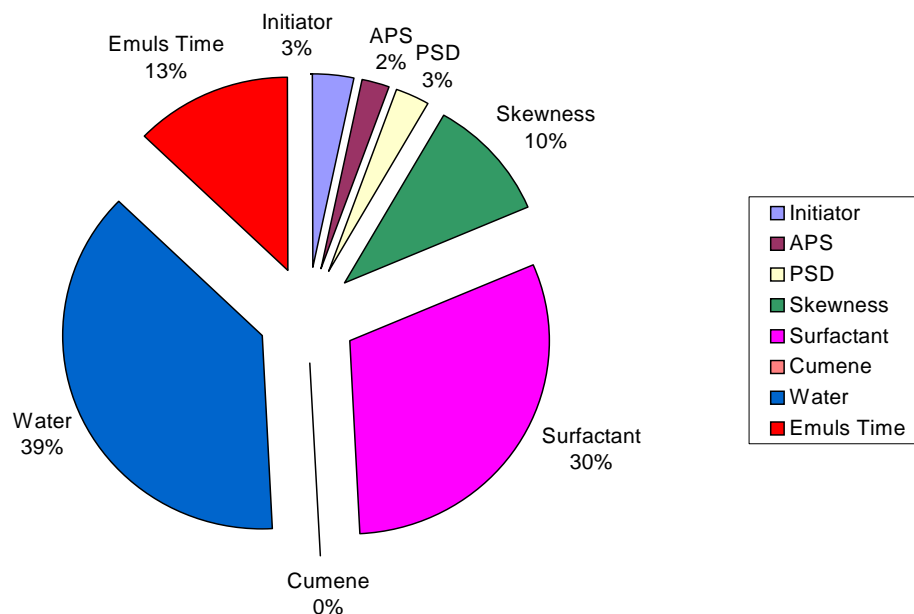


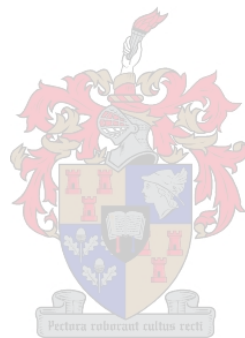
Fig.6.13 Pie Plot Indicating the Effect of Variations in Post Addition Constituents on the Final Viscosity for Run 2 (4" Impeller, 400 rpm, 20ℓ Vessel)

It was observed in the discussion of the effect on emulsification time on viscosity (Section 5.2, Chapter 5) that a shorter emulsification period presumably results in less time allowed for water to migrate into the organic phase where it forms vesicles. This was supposed to result in a higher concentration of water present in the aqueous phase after production and hence, a lower final viscosity. This might explain why this parameter, although less significant, also plays an important role in affecting the final viscosity.

It is interesting to observe that the average particle size plays a small role in influencing the final viscosity, even though it was used to model the final viscosity in the investigation of the effect of production temperature on properties (Section 5.1.1.3). However, it should be remembered that in the latter investigation, the average particle size only gave an indication of the degree of neutralisation occurring in the system at relatively higher temperatures ($T > 27^{\circ}\text{C}$) where exceedingly high neutralisation occurs, causing an increase in the interfacial tension and therefore, an increase in particle size as well. This investigation was performed at a lower temperature of 24°C and explains why this parameter showed a relatively low contribution.

The other parameters, including the particle size distribution and skewness of distribution, as well as the amount of catalyst added after production, showed very little affect on the final viscosity.

This chapter showed that bead properties, such as the average particle size, are not only sensitive to processing parameters, but also very sensitive to variations in the chemical composition of the organic and aqueous phases as well.

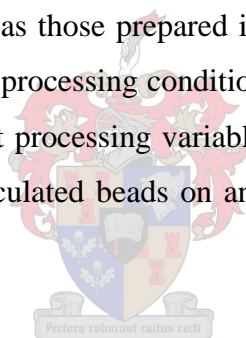


Chapter 7

Scale-up and Average Particle Size Model Development

The average particle size of vesiculated beads is a very important parameter to take into consideration when used as pigment in the coatings industry, since it significantly affects the gloss of the final paint film. If vesiculated beads possessing a relatively large average particle size are used in paint formulation, the dry film's texture is coarser, causing it to appear more matt. Smaller beads, on the other hand, cause a smoother surface with less matt appearance. Variation of this property during production will, therefore, result in coatings having different gloss levels. Consequently it is extremely important that the average particle size remain reproducible when it is used for a specific type of coating.

It has been found reasonably difficult to produce vesiculated beads on industrial scale possessing similar particle sizes as those prepared in the laboratory. This property is also very sensitive to changes in processing conditions. This is why it is important to investigate the effect of different processing variables and possibly predict how they can be changed to produce vesiculated beads on any scale possessing a prerequisite average particle size.



This chapter discusses production runs that were performed on the larger scale 20ℓ reactor vessel. The objective is to compare the properties from these runs to those obtained from similar runs conducted on the 5ℓ down-scaled version to ultimately develop accurate models describing the average particle size as a function of various processing variables. These models can then be tested on average particle size data from large industrial scale batches that have been executed for accuracy.

7.1 Scale-up Parameter Variations

Larger 20kg vesiculated bead batches were prepared in the 20ℓ reactor vessel by using the same standard formulation used in the 5kg runs. The parameters that were varied include impeller size and mixing speed.

7.1.1 Impeller Size

Similar to the experiments performed on the 5ℓ vessel, discussed in Section 5.4, where the effect of three different size diameter blades (3, 4, and 5 inches) were investigated, various runs were carried out on its scaled-up counterpart, but this time using four blades of 4, 5, 6, and 7 inch diameters, respectively. A mixing speed of 400 rpm was maintained throughout with the same production procedure followed as before. Table 7.1 presents the results from these runs.

Table 7.1 Effect of Impeller Size on Properties (20ℓ Vessel, 400 rpm)

Impeller Size (mm)	α_n (μm)	pH	η_{mf} (mPa.s)	Solids (wt/wt %)	θ_b (%)	θ_w (%)	$\theta =$ θ_b/θ_w
102 (4")	4.41	6.86	905	24.13	88.7	93.4	0.95
127 (5")	3.17	6.76	1253	23.94	85.3	90.7	0.94
153 (6")	3.13	6.64	1402	24.01	89.2	93.9	0.95
178 (7")	2.55	6.82	1150	23.63	87.3	91.9	0.95

Similar to the runs performed on the 5ℓ vessel using various diameter impellers (Table 5.5), it appears that this parameter has no apparent effect on luminosity, opacity or pH within the variation investigated. There appears to be a significant variation in viscosity values, but it is uncertain if this was caused by the effect of different impellers used.

7.1.1.1 Effect on Number Average Particle Size

From Figure 7.1 it is observed that once again a definite, almost linear decrease occurs in the average particle size as the impeller diameter is increased. By comparing this with values obtained from runs performed in the 5ℓ vessel it is seen that a similar trend is obtained, but with values appearing somewhat larger where the same size impeller is used. This indicates that not only is the particle size dependent on the size of the blade, but on the size of the vessel as well. Therefore, these parameters need to be taken in consideration when deriving a model describing average particle size.

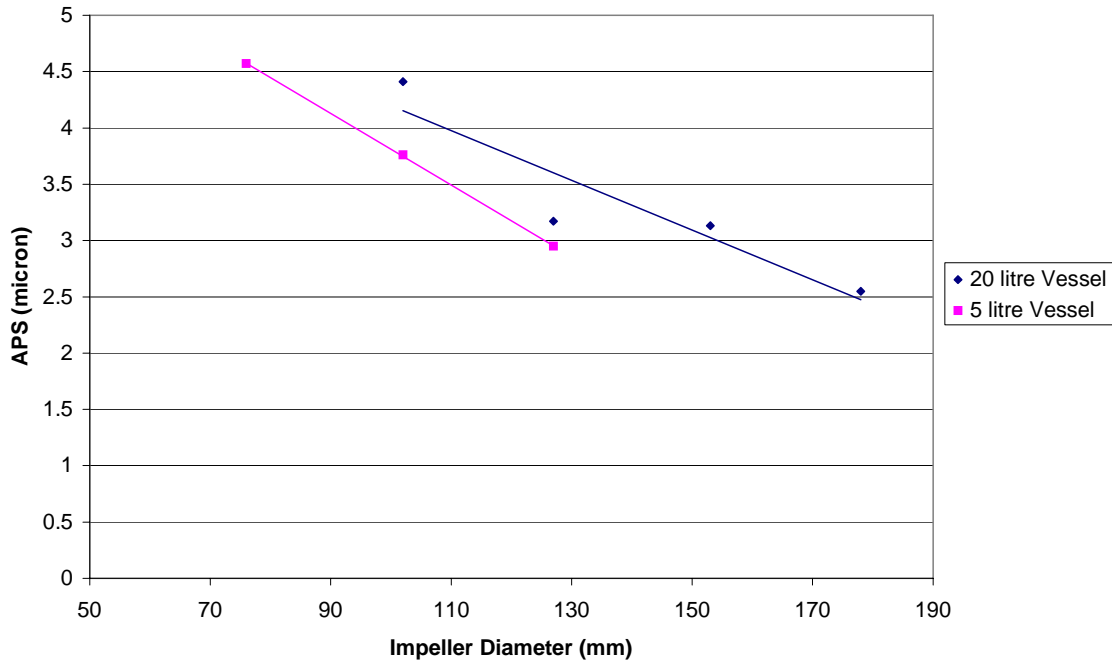


Fig. 7.1 Effect of Impeller Diameter Variation on Number Average Particle Size (20ℓ Vessel, Mixing Speed = 400rpm)

7.1.2. Mixing Speed

By using the 6 inch Cowles stirrer in the 20ℓ vessel, having the same blade to vessel diameter as the standard 4-inch stirrer used in the 5ℓ vessel, experiments were performed at various mixing speeds including 300, 400 and 500 rpm, respectively.

The results of the analysis appear in Table 7.2 and it once again appears that the pH, final viscosity and opacity is unaffected with values in the same order of magnitude as those found in Table 5.6.

Table 7.2 Effect of Mixing Speed on Properties (20ℓ Vessel, 6" Impeller Diameter)

Mixing Speed (rpm)	α_n (μm)	pH	η_{mf} (mPa.s)	Solids (wt/wt %)	θ_b (%)	θ_w (%)	$\theta = \theta_b/\theta_w$
300	3.95	6.89	816	23.56	85.7	91.2	0.94
400	3.13	7.01	1102	24.01	85.7	92.2	0.93
500	2.55	6.77	1120	23.80	85.9	90.4	0.95

7.1.2.1 Effect on Number Average Particle Size

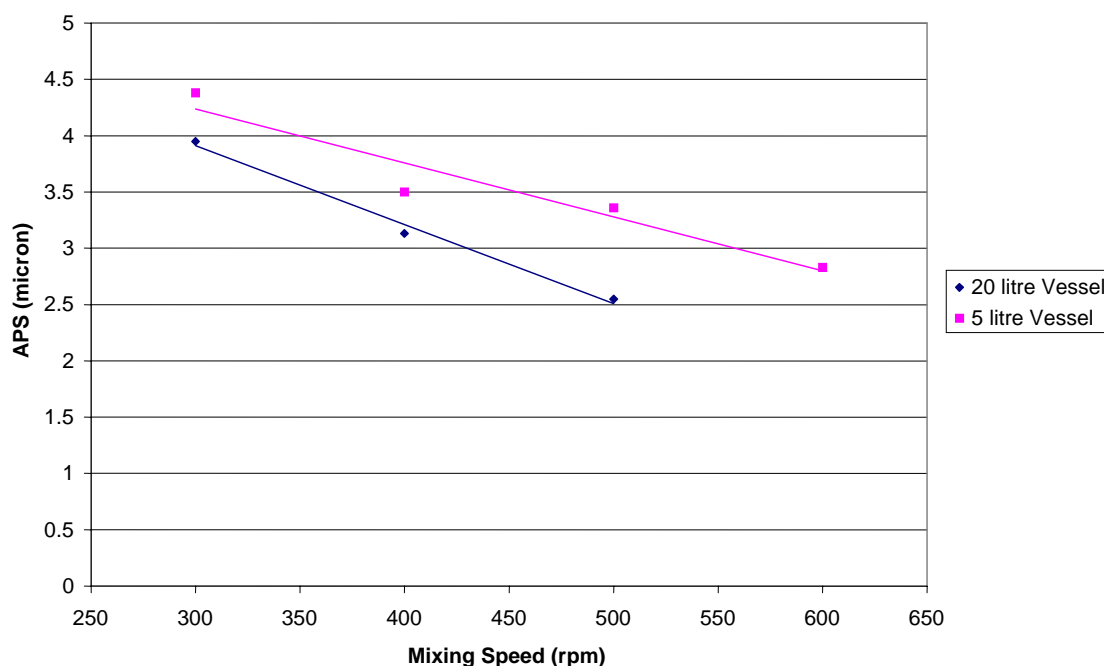


Fig.7.2 Effect of Mixing Speed on Number Average Particle Size (20ℓ Vessel, 6” Impeller Diameter)

In Section 5.5 where the effect of mixing speed on the number average particle size in the 5ℓ vessel was investigated, a definite decrease with increasing mixing speed was observed. From Figure 7.2 a very similar trend is observed, but overall the values appear somewhat higher than those obtained in the smaller vessel. This indicates that mixing speed is possibly another important parameter that needs to be considered in deriving an average particle size model for scale-up.

7.2 Average Particle Size Model

It has been established that several factors affect the average particle size. The factors include the impeller diameter, the size of the reactor vessel, and the dispersion speed. In Section 4.1 and Section 5.2 it was found that the emulsification time also influences average particle size. It will now be attempted to derive a suitable model describing this property as a function of these parameters and the model tested with

experimental values obtained in this study as well as from runs performed on industrial scale in the paint factories.

7.2.1 Average Particle Size (Standard Emulsification Time)

Using the standard production method, a time period of 20 minutes is allowed for droplets to approach their lowest obtainable particle size. This discussion focuses on modelling this average particle size value; i.e. emulsification time will first be excluded as parameter.

Andrew Klein and Vern Lowry^[17] performed an investigation into the dispersion conditions that need to be considered when performing scale-up of emulsion polymerisation in batch reactors. Several factors can cause coagulation or instability of monomer droplets dispersed in this liquid-liquid system during production. One of the important factors is insufficient agitation. Considerable emphasis was placed on determining the minimum rotational speed of an impeller (N_{\min}) to ensure sufficient emulsification, thereby evading coagulum formation.

It was found that the minimum rotational speed could be obtained by using Equation 7.1, presented by **Grossmann**^[18].

$$N_{\min} = 0.2 \left(\frac{D_t}{D_i} \right) D_i^{-0.765} \left(\frac{\Delta \rho g}{\eta_c} \right)^{0.294} \left(\frac{\gamma}{\rho_c} \right)^{0.353} (1 - \phi_d)^{1.37} (1 + 3.5)^{0.59} \left(\frac{h}{D_t} \right)^{0.4} \dots (7.1)$$

where:

N_{\min} = Minimum Rotational Speed (revolutions/s)

D_t = Vessel Diameter (m)

D_i = Impeller Diameter (m)

$\Delta \rho$ = Fluid Density Difference between Monomer and Continuous Phase (kg/m^3)

g = Gravitational Constant (m/s^2)

η_c = Viscosity of Continuous Phase (mPa.s)

γ = Interfacial Tension (mN/m)

- ρ_c = Density of Continuous Phase (kg/m³)
- ϕ_d = Volume Fraction of Dispersed Phase (m³/m³)
- h = Distance of Impeller from Bottom of Vessel (m)

This equation can be simplified to Equation 7.2, assuming constant fluid parameters and geometric similarity.

$$D_i^{0.765} N_{\min} = \text{constant} \quad \dots(7.2)$$

This model may be modified further to describe the vesiculated bead system. First assume that the constant term on the right of Equation 7.2 describes the average particle size. Since it was established that particle size is also dependent on the vessel size, another term should be included on the left-hand side of this equation, namely the impeller to vessel diameter ratio (D_i/D_t), in order to accommodate geometric non-similarities.

Equation 7.2 can therefore be rewritten as:

$$\alpha_n = kN^w D_i^x \left(\frac{D_i}{D_t}\right)^y \quad (\mu\text{m}) \quad \dots(7.3)$$

where:

- α_n = Average Particle Size using Standard Emulsification Time (μm)
- k = Constant
- w, x, y = Parameter Exponents

By using average particle size results from experiments performed in the study where the impeller diameter and mixing speed were varied in both vessels, the unknown constant and exponents in Equation 7.3 can be solved using non-linear regression analysis. This was done using the Polymath software package. By entering this non-linear equation, with (α_n) as the dependent variable and rotation speed (N), impeller diameter (D_i), and vessel diameter (D_t) as the independent variables, the program uses an algorithm for finding the unknown parameters that will minimise the sum square of the errors.

A table containing all the input data used in this analysis appears in Table E1.1, Appendix E, presenting the number average particle size values obtained from selected runs performed on both vessels (5ℓ and 20ℓ) during the course of this study. The solution obtained from Polymath appears in Figure E1, Appendix E. The regression provided the following result:

$$\alpha_n^{-1} = 0.27N^{0.71}D_i^{0.53}\left(\frac{D_i}{D_t}\right)^{0.27} \quad (1/\mu\text{m}) \quad \text{SSE}=2.03 \quad \dots(7.4)$$

The sum of squares of the errors is equal to 2.03, which is reasonably low, suggesting that the model is accurate in describing average particle size for the runs performed on laboratory scale. Table E1.1 also presents the experimental and modelled values of the runs used to perform the regression analysis.

Figure 7.3 shows the comparison between experimental data and modelled values for the runs performed on the 5ℓ and 20ℓ vessels at various mixing speed, while Figure 7.4 presents the comparison of data where the influence of impeller diameter were investigated. The model compares very well to the experimental data, and can be tested on average particle size data from industrial scale runs to see if it is applicable for scale-up to larger vessels.

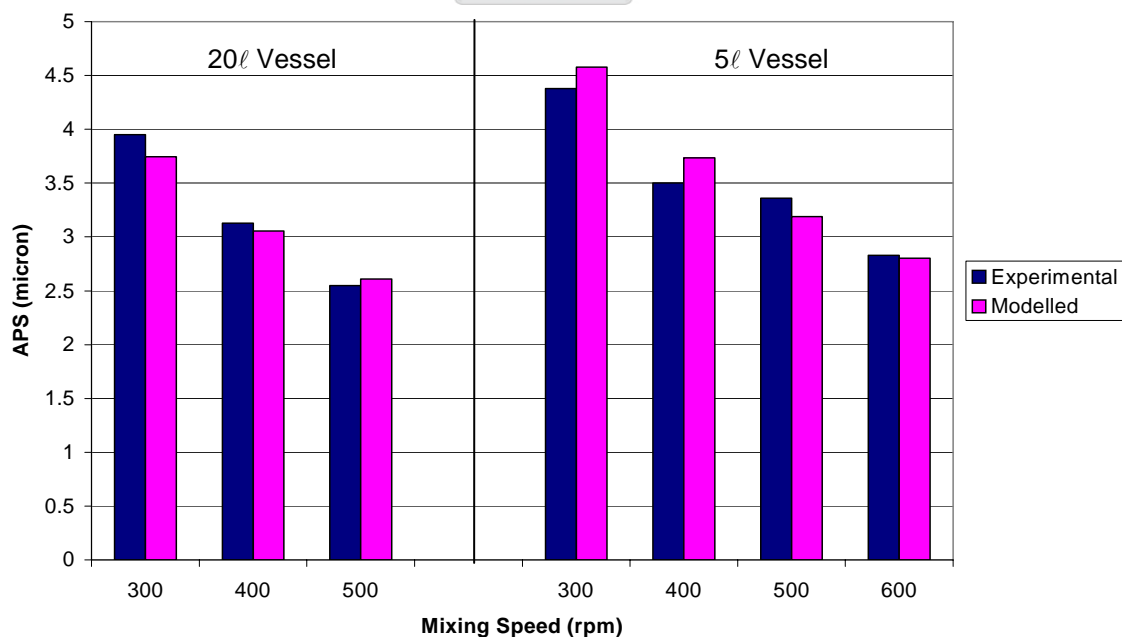


Fig.7.3 Comparison of Experimental Number Average Particle Size Data with Modelled Values at Various Mixing Speeds (Impeller Diameter Constant = 4" for 5ℓ vessel/ 6" for 20ℓ vessel)

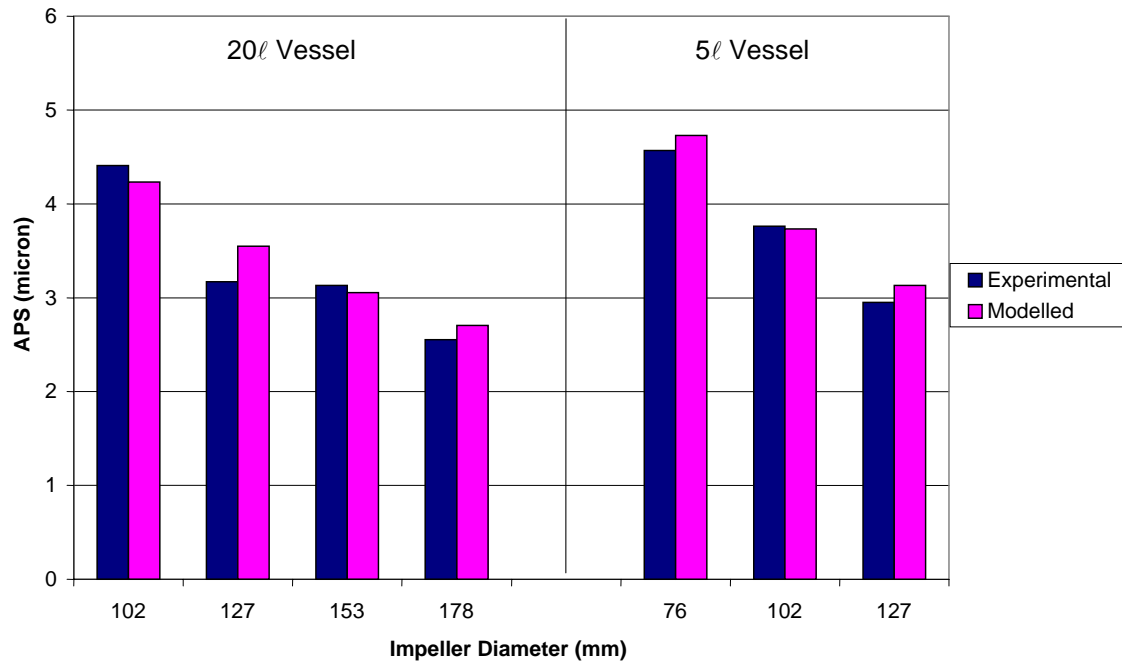


Fig.7.4 Comparison of Experimental Number Average Particle Size Data and Modelled Values at Various Impeller Diameters (Mixing Speed Constant = 400 rpm)

7.2.2 Average Particle Size Development (Reduced Emulsification Time)

After starting the emulsification period, it was found in Chapter 4 that the average particle size is very large and logarithmically declines with time to approach a minimum value after 20 minutes. This time dependency is useful when it is desired to manufacture vesiculated beads possessing a larger average particle size using existing reactor configurations. By once again applying Equation 7.3, but this time considering emulsification time as additional parameter, the following equation is investigated:

$$\alpha_{nt} = kN^w D_i^x \left(\frac{D_i}{D_t}\right)^y t_e^z \quad (\mu\text{m}) \quad \dots(7.5)$$

where:

t_e = Time after emulsification is initiated (s)

α_{nt} = Average Particle Size at time t_e (μm)

w,x,y,z= Parameter Exponents

By using the data in Table 4.1, which include the average particle size values obtained during the investigation of the effect of emulsification time carried out in both the 5ℓ and 20ℓ vessels (Section 4.1), non-linear regression is once again performed using Polymath. The estimated parameter exponents appear in Section E2, Appendix E, and graphically present the comparison between the experimental and modelled data values. Equation 7.6 presents the proposed model.

$$\alpha_t^{-1} = 0.0448 N^{0.90} D_i^{0.52} \left(\frac{D_i}{D_t}\right)^{0.44} t_e^{0.23} \quad (1/\mu\text{m}) \quad \text{SSE}= 10.3 \quad \dots(7.6)$$

The sum of the squared errors (SSE) value is reasonably small, indicating that this model is accurate enough in explaining the dependence of average particle size on these production parameters for the set of experiments conducted.

Ideally, the mixing speed (N), impeller diameter (D_i) and impeller to vessel diameter ratio (D_i/D_t) exponents should be the same as those found in Equation 7.4. However, there is a significant difference in the mixing speed and impeller/vessel diameter ratio exponents. The number of runs used to derive this model is very limited and only one run was performed on the 5ℓ vessel. Most of these runs were also performed using a consistent mixing speed of 400 rpm. This is possibly the reason why the exponents show such a significant variation from Equation 7.4. A contributing factor may also be that the same polyester batch was used in the latter investigation. The experimental data used to model Equation 7.4 includes those from runs where different batches were used. It was found in the course of this study that this possibly affects the reproducibility of the average particle size.

The accuracy of this time dependence scale-up model is under question, due to the limited number of production parameter variations performed. Therefore, it was decided to replace the mixing speed (N), impeller diameter (D_i) as well as the impeller/vessel diameter ratio (D_i/D_t) exponents with the ones obtained in Equation 7.4 and investigate if this will significantly affect the accuracy of this model. Equation 7.7 presents the new model under investigation.

$$\alpha_t^{-1} = kN^{0.71} D_i^{0.53} \left(\frac{D_i}{D_t}\right)^{0.27} t_e^z \quad (1/\mu\text{m}) \quad \dots(7.7)$$

By using Polymath, the unknown parameter values were calculated and Equation 7.8 obtained. Figure E2.2, Appendix E, contains the regression coefficients estimated by Polymath and graphically shows the comparison between the experimental and modelled average particle size values.

$$\alpha_t^{-1} = 0.0583 N^{0.71} D_i^{0.53} \left(\frac{D_i}{D_t}\right)^{0.27} t_e^{0.22} \quad (1/\mu\text{m}) \quad \text{SSE}= 15.56 \quad \dots(7.8)$$

The sum of squared errors is 15.56, which is not significantly larger than the 10.3 obtained in Equation 7.6. The emulsification time (t_e) coefficients are also very comparable. Using the standard emulsification time of 20 minutes ($t_e = 1,200$ s), Equation 7.8 reduces to the following:

$$\alpha_t^{-1} = 0.28 N^{0.71} D_i^{0.53} \left(\frac{D_i}{D_t}\right)^{0.27} \quad (1/\mu\text{m}) \quad \dots(7.9)$$


The constant value of 0.28 is comparable to Equation 7.4. As an example, Figure 7.6 graphically presents the comparison between the experimental average particle size data and the modelled values, using both Equations 7.6 and 7.9, for two runs conducted in the 5ℓ and 20ℓ vessels. The two models both appear to represent the experimental values very well. It would, therefore, be preferable to use the results from Equations 7.8 and 7.9 rather than Equation 7.6 when the effect of emulsification time is predicted.

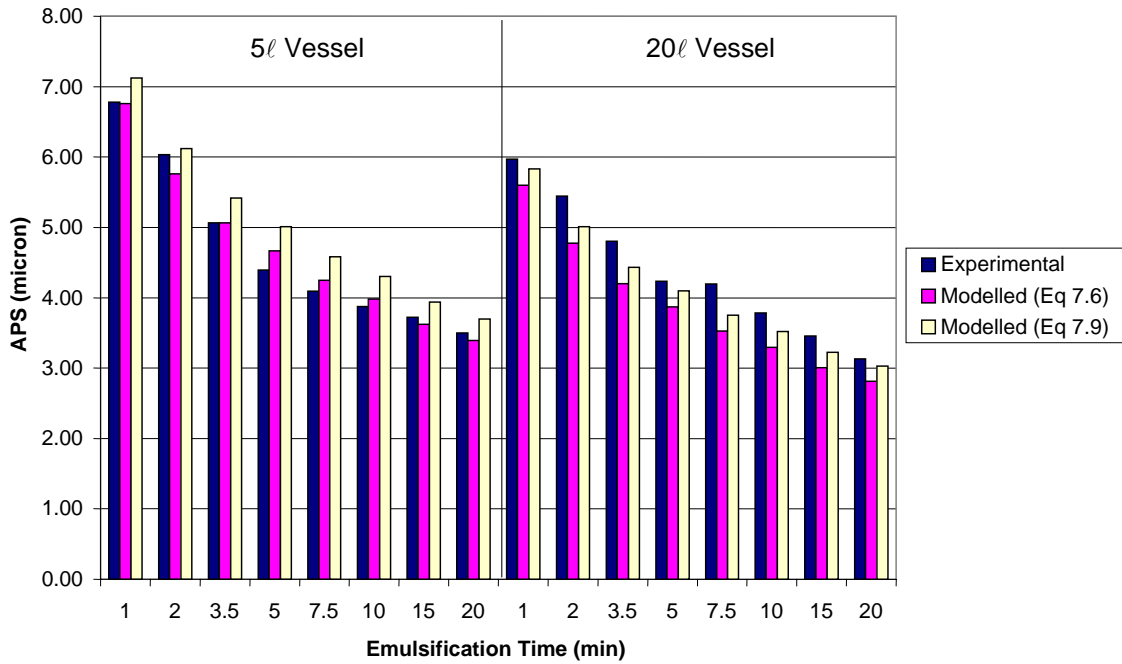


Fig.7.5 Comparison of Experimental APS and Modelled Values of Runs Performed in 5l and 20l Vessels at Various Emulsification Times (Dispersion Speed Constant = 400RPM) (Blade Diameter Constant = 4-inches for 5l Vessel/ 6-inches for 20l Vessel)

7.2.3 Average Particle Size Development (Effect of Temperature)

In Section 5.1.1.1 the effect of temperature (T) on the number average particle size was investigated. It was found that it remains approximately constant over the ambient temperature range. Higher than 27°C, however, the average particle size increases exponentially as described by Equation 5.1.

$$\alpha_n(T) = \alpha_{na} + 10^{-6} T^{3.7} \quad T > 27^\circ C \quad (\mu m) \quad T \text{ in } ^\circ C \dots(5.1)$$

The average particle size at ambient temperature (α_{na}) can be substituted by Equation 7.4) to produce Equation 7.10.

$$\alpha_n(T) = 0.27N^{-0.71} D_i^{-0.53} \left(\frac{D_i}{D_t}\right)^{-0.27} + 10^{-6} T^{3.7} \quad T > 27^\circ C \quad (\mu m) \quad \dots(7.10)$$

From the magnitude of the parameter exponents, it can be seen that temperature is the predominant parameter that affects average particle size at temperature above 27°C.

7.2.4 Average Particle Size Comparison of Industrial Scale Runs

7.2.4.1 Effect of Mixing Speed

Initial attempts were made by Plascon Paint to scale-up production volumes to 150kg in one of the existing Cowles dispersers found in their paint factories. The vessel used consisted of a large plastic container with an inside diameter of 57cm, while the impeller blade diameter was 20cm. Four runs were performed where the mixing speed was varied. The speed used in each run was 185, 220, 250 and 280 rpm, respectively. Table 7.3 shows the results of analysis. Equation 7.4 was used to model the average particle size as a function of the impeller diameter (0.20m), vessel diameter (0.57m) and the individual mixing speed (s^{-1}).

Table 7.3 Industrial Scale-up Runs Performed at Various Mixing Speed (150kg, 20cm Impeller)

Mixing Speed (rpm)	α_n (exp.) (μm)	α_n (mod) (μm)	pH	η_{mf} (mPa.s)	Solids (wt/wt %)	Opacity (θ)
185	8.0	7.92	6.47	1100	24.34	0.86
220	9.0	6.66	6.56	1100	22.60	0.88
250	5.7	5.86	6.68	850	23.89	0.90
280	7.5	5.24	6.61	1250	22.42	0.89

Similar to runs performed on lab-scale, it appears that mixing speed has little effect on the final viscosity, pH and opacity. The average particle size results appear to be very irregular and difficult to model with the values at 220 and 280rpm are much larger than expected. However, it seems that the model predicts the average particle size well in the runs performed at 185 and 250rpm. Figure 7.6 shows a graphic comparison between the experimental and modelled data. The reason why the particle size of the production runs is so erratic, may be due to the small impeller to vessel diameter ratio. Laboratory scale work has shown that erratic property results (for example average particle size and opacity) were obtained when the ratio falls

below 0.40. The smallest ratio used during this study was 0.42, but in this case the ratio was 0.35, which is significantly smaller.

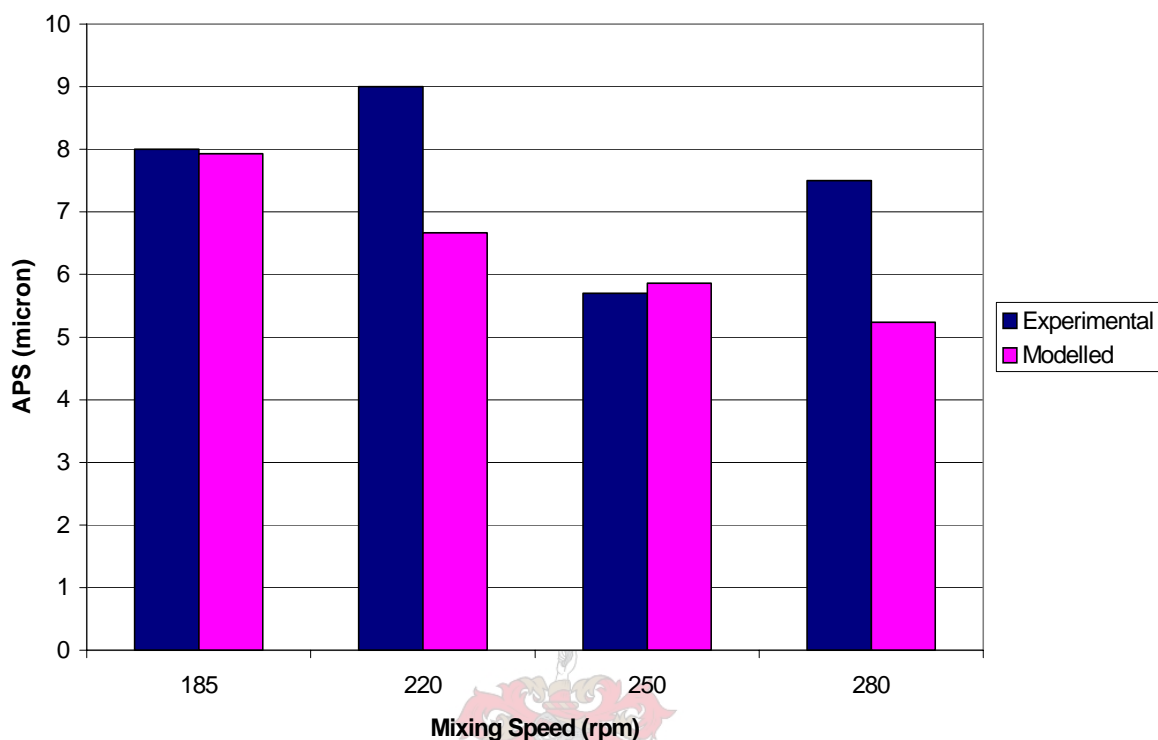


Fig.7.6 Number Average Particle Sizes of Runs Performed on 150kg Scale at Various Mixing Speed and Comparison with Modelled Values (20cm Impeller, 570cm Vessel Diameter)

7.2.4.2 Effect of Impeller Size

Since the stirring speed appeared to have little effect on the average particle size, it was decided to continue experiments using a larger diameter impeller blade. Four runs were performed using the same 57cm-diameter vessel, but with a 30cm diameter Cowles disperser blade. Two runs were performed individually using a mixing speed of 155 and 165 rpm. In the other runs the mixing speed remained the same (155 rpm), but additional surfactant was added to the organic phase, similar to the procedure discussed in Section 6.3. Table 7.4 presents the results of analysis.

The larger blade produced significantly smaller beads than in the previous set of runs where the smaller impeller was used. By once again using Equation 7.4, it was

Table 7.4 Industrial Scale-up Runs Performed using Larger Impeller (150kg, 30cm Impeller)

Including Surfactant	Speed (rpm)	α_n (exp.) (μm)	α_n (mod) (μm)	pH	η_{mf} (mPa.s)	Solids (wt %)	Opacity (θ)
No	155	4.36	4.25	6.96	7000	24.17	0.95
No	165	4.30	4.07	6.85	6200	24.36	0.96
Yes	155	3.21	4.25	6.96	3400	24.48	0.98
Yes	155	2.86	4.25	6.87	4200	24.56	0.99

attempted to predict the average particle size and these values are also presented in Table 7.4. Figure 7.7 shows a comparison between the modelled and experimental values, displaying a very accurate correlation in the case where no surfactant was included. Note that the impeller to vessel diameter ratio is 0.53, which is larger than 0.44, making Equation 7.4 applicable.

On the other hand, the experimental data where additional surfactant was included comparatively indicate a significant lower particle size than predicted. This was also observed and discussed in Section 6.3 (Figure 6.9). The derived model does not include average particle size data from runs where additional surfactant was included and can therefore not be used to accurately model the physical values. This is investigated further in the following section.

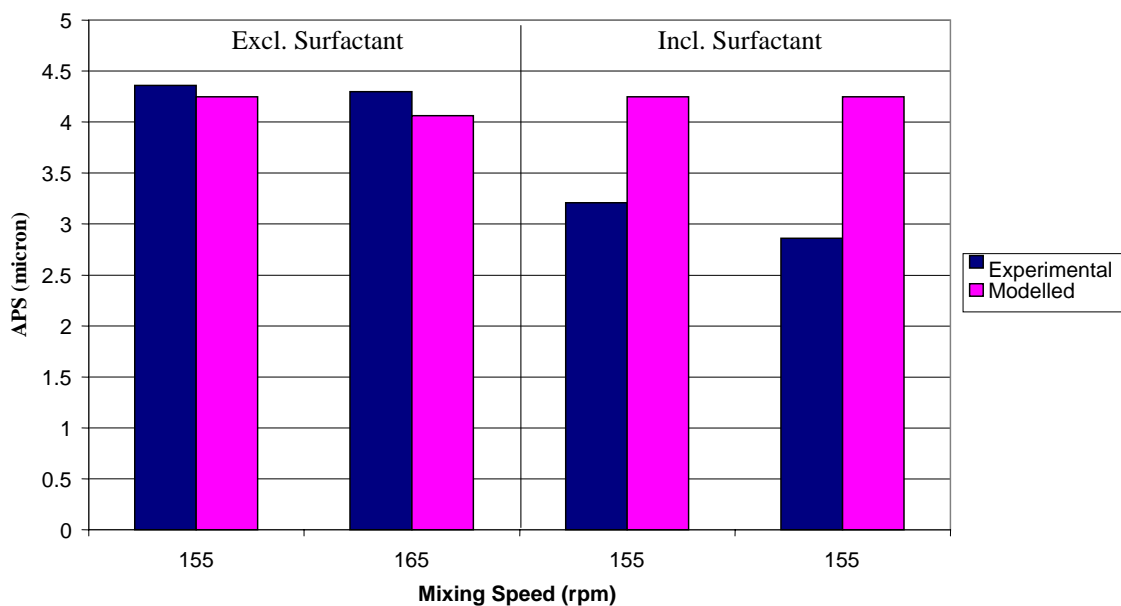


Fig.7.7 Number Average Particle Sizes of Runs Performed on 150kg Scale (Including and Excluding Surfactant) and Comparison with Modelled Values (30cm Impeller, 57cm Vessel Diameter)

Notice that the opacity in these scale-up runs is higher where surfactant was added, similar to what was found in Section 6.3. In all the runs the final viscosity is very high and the reason for this is unknown.

7.2.4.3 Effect of Additional Surfactant

A set of 3 runs was performed on even larger industrial scale using a Cowles disperser. The vessel used was approximately 100cm in diameter and a 46cm (18”) diameter impeller was used at a mixing speed of 160 rpm. All the runs were executed under similar production conditions to test reproducibility of final properties. Additional surfactant was also added to each to increase the opacity and the formulation modified to produce batches with a total solid content of 28 wt%. Using the production parameters specified above, Equation 7.4 was once again used to model the average particle size. Table 7.5 contains the property analysis results.

Table 7.5 Industrial Scale-up Runs Performed using Additional Surfactant
(630kg, 46cm Impeller, Mixing Speed = 160rpm)

Run	α_n (exp.) (μm)	α_n (mod) (μm)	pH	η_{mf} (mPa.s)	Solids (wt %)	Opacity (θ)
1	2.30	3.45	6.37	3600	28.9	0.96
2	2.70	3.45	6.44	3600	27.8	0.94
3	2.50	3.45	6.48	3000	28.1	0.94

The average particle size (and other properties) for the 3 runs remained approximately consistent, verifying reproducibility. It is once again seen that the modelled values are somewhat higher than the experimental data and Figure 7.8 shows the comparison. The overall difference is about $1\mu\text{m}$, which is not very significant, but the model should rather be refined.

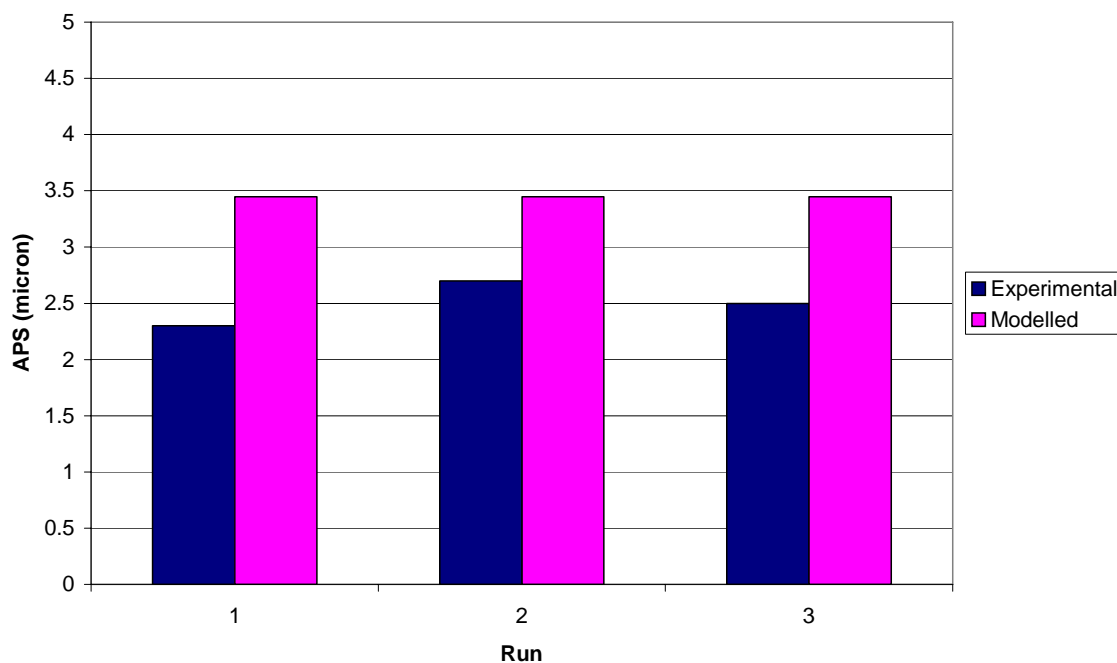


Fig.7.8 Number Average Particle Sizes of Runs Performed on 600kg Scale using Additional Surfactant and Comparison with Modelled Values (46cm Impeller, 100cm Vessel Diameter, Mixing Speed = 160rpm)



7.2.5 Average Particle Size (Effect of Additional Surfactant)

In Section 6.3, Chapter 6, as well as in the previous section (Section 7.2.4) it was established that addition of surfactant to the organic phase results in a significant reduction in the final average particle size. Hence, an attempt was made to develop an average particle size model similar to Equation 7.9, but using the data available from runs that was conducted in the past with additional surfactant included in the formulation. Since very few of these runs were performed on laboratory scale during the course of this study, data from all runs performed on industrial scale was gathered. The data used for modelling include the following sets:

Set A - 3 Laboratory scale runs (5ℓ) as discussed in Section 6.3, Chapter 6, and performed at different mixing speeds (refer to Table 6.3). The solids content of these batches were 24 wt%.

Set B - 2 Industrial scale runs (150kg) performed at 155 rpm (refer to Table 7.4, Section 7.2.4.2). The solids content of these batches were 24 wt%.

Set C - 3 Industrial scale runs (630kg) performed at 160 rpm (refer to Table 7.5, Section 7.2.4.3). The solids content of these batches were 28 wt%.

Set D - 3 Industrial scale runs (150kg) performed at different mixing speeds (160 and 180 rpm) with a solids content of 22 wt%.

Set E - 1 Industrial scale run (630 kg) performed at 140 rpm with a solids content of 28 wt%.

The mixing conditions for the runs in each set appear in Table 7.6 below. The polyester batch codes for each of the industrial scale sets are not documented, but it is known that Cray Valley resins were used in all the sets except in Set B where KZN resin was used.

Table 7.6 Data used to Model Number Average Particle Size (incl. Additional Surfactant)

Set	Run	N (rpm)	D_i (mm)	D_t (mm)	α_n (exp) (μm)	α_n (mod) (μm)
A	1	300	102	180	3.09	3.17
	2	400	102	180	2.62	2.55
	3	500	102	180	2.18	2.15
B	4	155	300	570	3.21	3.01
	5	155	300	570	2.86	3.01
C	6	160	460	990	2.30	2.60
	7	160	460	990	2.50	2.60
	8	160	460	990	2.70	2.60
D	9	160	300	570	3.09	2.93
	10	160	300	570	2.67	2.93
	11	180	300	570	2.74	2.68
E	12	140	460	990	3.13	2.87

By using the model developed and presented in Equation 7.5 ($t_e = 20\text{min}$) and the data in Table 7.6, the unknown parameter coefficients were estimated using Polymath. The regression output appear in Figure E3.1, Appendix E3 and the resulting model given by Equation 7.11.

$$\alpha_n^{-1} = 0.63 N^{0.76} D_i^{0.58} \left(\frac{D_i}{D_t}\right)^{1.01} \quad (1/\mu\text{m}) \quad \text{SSE} = 0.346 \quad \dots(7.11)$$

The modelled number average particle sizes for each set of runs also appear in Table 7.6 and a comparison with the experimental data are presented in Figure 7.9.

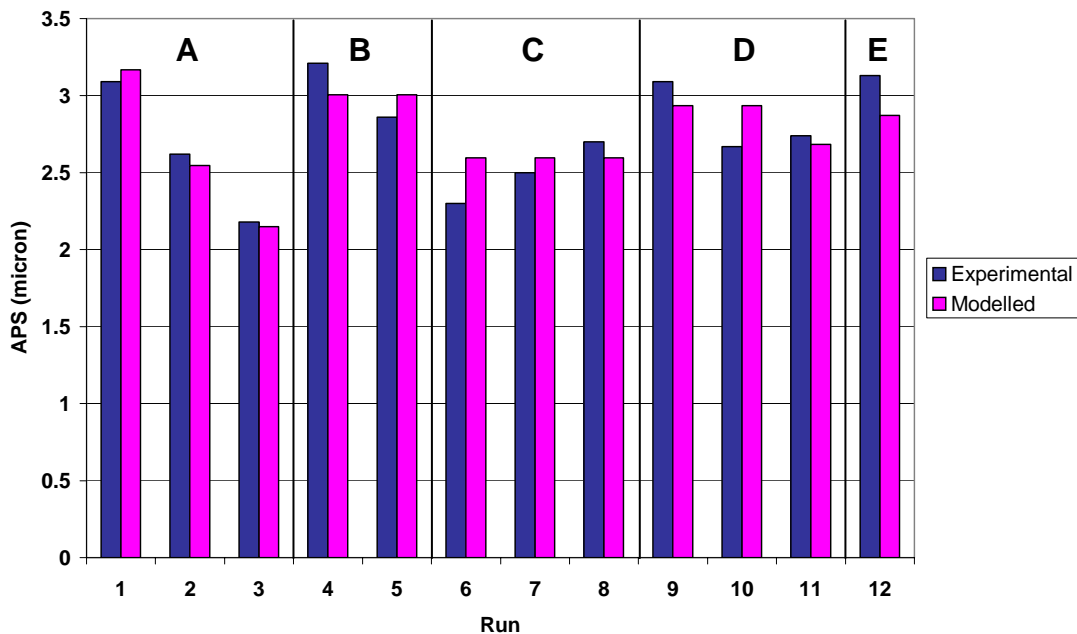


Fig. 7.9 Comparison of Experimental Number Average Particle Size Data and Modelled Values of Vesiculated Beads Produced with Additional Surfactant

It appears that this model predicts the experimental data well. Very little experimental data was available for developing this model with little variation in processing parameters. It has also been concluded further that different polyester batches do affect the average particle size. All of these factors may put the accuracy of this model under question. However, by comparing this model to the model presented by Equation 7.9, it is interesting to observe that the stirring speed (N) and impeller diameter (D_i) exponents are reasonably comparable. These exponents and in

particular the impeller to vessel diameter ratio exponent are larger than those in Equation 7.9, suggesting that the addition of surfactant to the formulation causes the average particle size to be more sensitive to processing parameters.

To test the applicability of Equation 7.11, it is suggested that more runs be performed under various processing conditions.

7.2.6 Specification Range and Limitations of Average Particle Size Models

It is important to note that the average particle size models discussed in this chapter is only valid under certain processing conditions. Manufacturing vesiculated beads outside these ranges may result in batches with inconsistent properties and average particle sizes that can not be predicted with the proposed models.

According to the patent publications of Gunning, et al.^[4], it was observed that if agitation during the emulsification stage was too violent, dispersed globules would coalesce, causing the particle diameters to grow. Depending on the type of agitation and impeller used, it was established that a critical shear rate exists, and exceeding this rate would cause coalescence.

As a general rule of thumb, Gunning proposed that the impeller tip speed should be lower than 15 metres per second where a turbine type impeller is used. For a Cowles disc-type impeller, which exerts a much higher shear than turbine impellers, the critical shear rate should be even lower. Therefore, it is advised not to perform emulsification under excessive shear conditions, since this will result in larger average particle sizes than predicted, rendering the proposed models inapplicable.

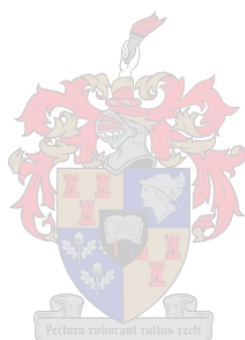
In this study, the impeller tip speed in all laboratory, as well as industrial scale runs, never exceeded 4 metres per second and the accuracy of the average particle size model was not tested at higher shear rates.

Experimentation on laboratory and industrial scale also indicated that, if the impeller to vessel diameter ratio were below 0.40, the bead properties became unstable. This was discussed in Section 7.2.4.1.

The experimental data used to develop the average particle size models in this chapter, was from runs where the impeller to vessel diameter ratio ranged between

0.42 to 0.70. It is uncertain if this model will predict values accurately outside this range.

Concluding this chapter, it must be emphasised that average particle size is extremely sensitive to chemical formulation changes. As an example it was seen in Section 7.2.4.3 to what an extent the average particle size model was affected by surfactant addition to the organic phase.



Chapter 8

Conclusions and Recommendations

8.1 Introduction

The main objective of this study was to investigate the process of producing vesiculated beads on a Cowles disperser system. This was done by first designing and constructing a 5ℓ laboratory size Cowles system, a down-scale version of the vessels found in paint companies. The system is fully integrated to measure and control temperature, addition rates and mixing speed and record the transient viscosity during production. The system was also designed to allow interchangeability with larger impellers and a 20ℓ vessel, the latter being geometrically similar to its smaller counterpart. This was done to study the effect of scale-up on properties, in particular average particle size.

It was predominantly focussed on the effect of process parameter variation on properties, which include average particle size, pH, viscosity and opacity. To a lesser extent, production runs were performed where changes were made in the vesiculated beads formulation.

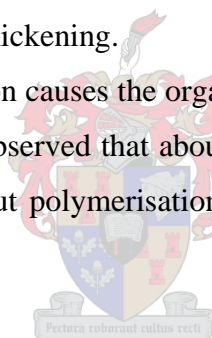
The main conclusions made from these runs will be discussed further in this chapter.

8.2 Transient Properties during Production of Vesiculated Beads

- The number average particle size reduces logarithmically over the emulsification period after the organic phase is completely added to the aqueous phase and approaches a constant average value after 20 minutes. The rate with which it approaches this constant value can be increased by either using a larger diameter Cowles impeller or increasing the mixing speed. This also causes the final average particle size to be smaller if $t_e = 20\text{min}$.
- By reducing the emulsification time ($t_e < 20\text{min}$), a larger average particle size was obtained, but with a very wide particle size distribution range. It was

attempted to increase the emulsification period by using a low mixing speed to investigate if it is possible to obtain a large average particle size with narrow particle size distribution. The distribution was, however, still wide, but comparable to runs performed using a higher mixing speed, indicating that with an appropriate selection of production conditions (mixing speed and impeller diameter), it is possible to produce vesiculated beads possessing a large average particle size and relatively narrow distribution range.

- The production viscosity increases significantly during the organic phase addition period after which it reduces almost logarithmically during the emulsification stage to approach a constant value. After catalysis the batches are left static overnight. Normally it is observed that the final viscosity is much higher after this time and possesses “shear-thinning” behaviour. Re-dispersion causes the final viscosity to reduce, but increases again after agitation is removed. This is also known as thixotropic behaviour. Post-addition of surfactant can effectively be used to partially prevent re-thickening.
- After catalysis, polymerisation causes the organic droplets to form solid thermoset polyester granules. It was observed that about 40 minutes after catalysis discrete beads are already formed, but polymerisation still continues for at least 3 hours afterwards.



8.3 Effect of Processing Parameters

8.3.1 Production Temperature

- It was observed that higher production temperatures had very little effect on average particle size over the ambient temperature range, but began to increase almost exponentially after about 27°C.
- An increase in temperature further causes an increase in the final batch viscosity, approaching a maximum after which it appears to start decreasing again. A model, proposed by Souheng Wu, was applied and it was found that the following relationship explains the final viscosity behaviour well:

$$\eta_{mf} \propto \alpha_n^{-0.38} T^{0.33} \quad \dots(5.9)$$

This implies that both the average particle size and emulsification temperature influence final viscosity.

- Lower emulsification temperatures were found to be associated with higher opacity. Experimentation indicated that variations in ambient temperatures could have a significant effect on opacity.
- The decrease in opacity with temperature cannot be attributed to titanium dioxide pigment migration to the bead surface. The same dependence on temperature was observed when the pigment was removed from the formulation and relatively lower opacity values were obtained, substantiating the advantage of using pigment in the formulation.

8.3.2 Emulsification Time

- Similar to the sample extraction method over the emulsification period, it was found that increasing the emulsification time causes a logarithmic decrease in average particle size and particle size distribution. However, comparatively there appears to be a difference in the respective values at specific emulsification times, which may be attributed to the different polyester batches used. During the course of this study it was found that various polyester batches do cause differences in the final properties of the vesiculated beads.
- A reduction of the emulsification time appears to cause a small decrease in the final batch viscosity, but shows no visible effect on the luminosity or opacity values.

8.3.3 Organic Phase Addition Rate

- An increase in the organic phase addition rate showed very little effect on the average particle size, but did show an increase in the particle size distribution skewness, which implies that more particles were formed with diameters larger than the average value.
- A significant decrease in the pH occurred as the addition rate was increased. This might be attributed to a condition that was created where neutralisation was

favoured between the polyester and polyamine present in the aqueous phase, possibly relating to an increase in the water-solubility of the organic phase and degree of vesiculation. There was, however, no visible variation in the luminosity or opacity values. It is, therefore, possible that an increase in the degree of vesiculation does not necessarily coincide with an increase in opacity.

8.3.4 Impeller Size and Mixing Speed

- By increasing the impeller diameter or mixing speed, the final average particle size and particle size distribution after an emulsification period of 20 minutes decrease almost linearly. This was observed in both the 5ℓ and 20ℓ vessels.
- These parameters showed no variation in other properties, including pH, final viscosity or opacity for the variations investigated.

8.4 Effect of Variations in Chemical Composition

- By adding more water, normally used for post-treatment after emulsification, to the initial aqueous phase, the average particle size increased almost linearly. The same behaviour was observed when the cellulose thickener concentration was reduced. This implies that the average particle size is very sensitive to the colloid stabiliser concentration present in the initial aqueous phase.
- The addition of surfactant to the organic phase during production causes a lower interfacial tension between the two phases, resulting in relatively smaller granules to be formed (smaller average particle size). This also causes a significant increase in the luminosity and opacity values. The final bead viscosity is also much higher than in the case where no surfactant is added.
- The final batch viscosity measurements taken during the course of this study showed very erratic and inconsistent behaviour. A sensitivity analysis was performed where the effect of emulsification time, particle morphology and post-additions (post-treatment water, free radical initiator, redox activator and surfactant) on viscosity was investigated. Using multiple linear regression, it was concluded that the most influential components that effect this property were the

amount of surfactant and post-treatment water added. Other properties showed very little contribution.

8.5 Average Particle Size Model

Runs performed on the 5ℓ Cowles vessel where the effect of production parameters such as impeller diameter and mixing speed on average particle size was investigated, were repeated on the larger 20ℓ vessel. A model developed by Klein et al.^[17] was used as basis for describing the average particle size as a function of mixing speed (N), impeller diameter (D_i), vessel diameter (D_t) and emulsification time (t_e). The following model was found to explain variations in this parameter very well:

$$\alpha_t^{-1} = 0.0583 N^{0.71} D_i^{0.53} \left(\frac{D_i}{D_t}\right)^{0.27} t_e^{0.22} \quad (1/\mu\text{m}) \quad \dots(7.8)$$

Note that this model is only applicable where the impeller to vessel diameter ratio is larger than 0.44.

By taking t_e = 20min, the applicability of this model to average particle size data from larger industrial scale runs performed in the past was tested. It was found that this model describes the data reasonably well. However, where additional surfactant was used in the organic phase, the average particle size was relatively smaller and since this model was not developed for the latter case, it can not be accurately applied for these conditions.

Particle size data from vesiculated bead runs with additional surfactant added to the formulation and performed on laboratory as well as industrial scale, were gathered and it was found that the following model predicts the average particle size well:

$$\alpha_n^{-1} = 0.63 N^{0.76} D_i^{0.58} \left(\frac{D_i}{D_t}\right)^{1.01} \quad (1/\mu\text{m}) \quad \text{SSE} = 0.346 \quad \dots(7.11)$$

More data is needed to establish the accuracy of this model, but comparison with Equation 7.8 shows that the process parameter exponents overall possess larger

values, indicating that the system is more sensitive to processing parameters when surfactant is included in the formulation.

In conclusion, this study has contributed to a better understanding of the complex nature of vesiculated beads and the production thereof. It further allowed manufacturers to develop a sense of possible processing limitations and an awareness of the parameters that affect bead property behaviour.

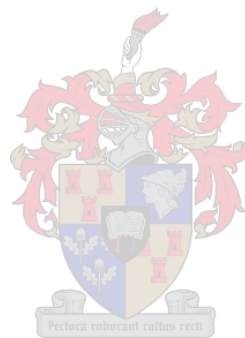
The proposed average size model has also been successfully applied in the industrialisation of vesiculated beads on the Cowles disperser and has been used in the production of 25 – 30 micrometer vesiculated beads with improved properties.

8.6 Recommendations and Future Work

The following recommendations can be made upon completion of this study:

- Production properties appear to be sensitive to various polyester batches used. It should be attempted to investigate if this is indeed the case and why. It should be established what are the critical properties of the polyester (e.g. acid value, curing or gel time, etc.) that influences these variations. If necessary, the production process of polyester in the supplier factories should be studied to establish if it is reproducible.
- Since it was found that lower production temperatures favour higher opacity, the feasibility of installing jacketed vessels in paint factories with chillers should be investigated. This will also prevent variation of opacity levels at different ambient production temperatures.
- A more detailed study should be performed on the effects of producing vesiculated beads on other vessels, like emulsion reactors, found in paint companies. Currently industrial scale (10 ton) production on emulsion reactors are being performed in one of the local paint factories. However, further optimisation of the process should prove to be advantageous.
- A more detailed study should be conducted where the effect of processing parameters on properties is investigated with surfactant added to the organic phase and a model derived that can be used to describe the average particle size as a function of scale-up parameters.

- It is currently planned to design and construct a fully integrated 200kg pilot plant Cowles reactor system, which can also be adapted to allow conversion to an emulsion reactor. This will allow a more in-depth study into the effects of production parameters on properties during scale-up.



References

1. Chapman & Hall; *Surface Coatings Volume 1, Raw Materials and their Usage*; Third Edition, London, **1993**, Chapter 23, pp. 343 – 355.
2. Powerpoint presentation – *Vesiculated Particles Project*, presented by J.F Engelbrecht, Plascon Research Centre, Stellenbosch, July **1999**.
3. *Roskill Reports on Metals and Minerals*; Titanium Minerals and Pigments; <http://www.roskill.co.uk>, **2001**.
4. Gunning, R.H.; Henshaw, B.C.; Lubbock, F.J.; *Polyester Granules and Process*; Appl. Number: 73/8448 (Australia); Dulux Australia Ltd., **1972**.
5. Goldsbrough, K.; Hodge, J.C.W.; *Production of Vesiculated Polymer Beads*; Appl. Number: 82/7714 (European); Tioxide Group PLC, **1982**.
6. Karickhoff, M.; *Vesiculated Beads*; Appl. Number: 517/491 (United States); The Sherwin Company, Ohio, **1983**.
7. Adam; Herve; Riess; Henri, G.; Nicaud; Claude, G.S.; *Particles of Hydrophobic Polymers Containing Voids*; Appl. Number: 939426 (United States); Imperial Chemical Industries, France, **1992**.
8. Kirk Othmer's Encyclopaedia of Chemical Technology, Volume 8; John Wiley of New York, **1979**, pp. 910 – 916.
9. Taylor, B.A.; Wade, W.G.; *Micronised Pigments in the Cowles Dissolver*; Golden Valley Colours Ltd., England.
10. Kirk Othmer's Encyclopaedia of Chemical Technology, Volume 15; John Wiley of New York, **1979**, pp. 604 – 616.

11. Engelbrecht, J.; Internal Report: *Vesiculated Beads – A Range of Novel Synthetic Opacifiers*; Plascon Research Centre, Stellenbosch, **2001**.
12. Technique for Determining the Degree of Vesiculation explained by Mnr. A.C. Smit, Plascon Research Centre, Stellenbosch, **2001**.
13. Microtomed Samples prepared and photographed by Ms. Y. Koen, Plascon Research Centre, Stellenbosch, **2002**.
14. Harding, S.E, et al; *Analytical Ultracentrifugation in Biochemistry and Polymer Science*; Royal Society of Chemistry, Cambridge, England **1992**, Chapter 10.
15. Larson, R.G; *The Structure and Rheology of Complex Fluids*; Oxford University Press, Oxford **1999**, Chapter 6, pp. 309 – 312.
16. Wu, S; *Formation of Dispersed Phase in Incompatible Polymer Blends: Interfacial and Rheological Effects*; Polymer Engineering and Science, Mid-March, **1987**, Vol. 27, No. 5.
17. Klein, A.; Lowry, V.; *Some Mixing Scale-Up Considerations for Emulsion Polymerisation*, Advances in Emulsion Polymerization and Latex Technology, Short Course, Lehigh University, Bethlehem, Pennsylvania, **1996**.
18. Grossman, H.; *Phase Inversion and Minimum Impeller Speed for Complete Dispersion in Agitated Liquid-Liquid Systems*; Meeting of the Working Party on Mixing, Vortrag **1980**.

